AGSO

Continuous multi-spectral fluorescence and absorption spectroscopy for hydrocarbon detection in ocean waters: Fairway Basin, Lord Howe Rise

D. HOLDWAY, A.RADLINSKI, N. EXON,
J-M. AUZENDE & S. VAN DE BEUQUE

RECORD 2000/35

AGSO
AUSTRALIAN
GEOLOGICAL SURVEY
ORGANISATION

AUSTRALIAN GEOLOGICAL SURVEY ORGANISATION

AGSO RECORD 2000/35

Continuous multi-spectral fluorescence and absorption spectroscopy for petroleum hydrocarbon detection in near-surface ocean waters: ZoNéCo5 Survey, Fairway Basin area, Lord Howe Rise

D. HOLDWAY[1], A. RADLINSKI[1], N. EXON[1], J-M. AUZENDE[2] & S. VAN DE BEUQUE[1]

[1]*Petroleum and Marine Division, Australian Geological Survey Organisation, GPO Box 378, Canberra, ACT 2601*
[2] *Ifremer, BP 2059, Nouméa, Nouvelle-Calédonie*

CANBERRA 2000

Australian Geological Survey Organisation

Chief Executive Officer: Neil Williams

Department of Industry, Science & Resources

Minister for Industry, Science & Resources: Senator The Hon. Nick Minchin
Parliamentary Secretary: The Hon Warren Entsch, MP

ISSN: 1039-0073
ISBN: 0 642 39852 6

Bibliographic reference: Holdway, D., Radlinski, A., Exon, N., Auzende, J-M. & Van de Beuque, S., 2000. Continuous multi-spectral fluorescence and absorption for petroleum hydrocarbon detection in near-surface ocean waters: ZoNéCO5 Survey, Fairway Basin area, Lord Howe Rise. Australian Geological Survey Organisation, Record 2000/35.

Contents

Figures, Tables and Appendix

Abstract

In conjunction with the French ZoNéCo5 swath mapping and geophysical profiling program, AGSO undertook a continuous analysis of near-surface waters in the Fairway Basin, north Lord Howe Rise region of the South Pacific, in order to detect petroleum hydrocarbons. A Wet Labs SAFire multi-spectral fluorescence and absorption instrument was used to directly measure dissolved poly-aromatic hydrocarbons or detect anomalous biological activity in the water column that might be the result of sea-floor petroleum seepage or the venting of natural gas from the sub-surface.

The method uses UV and visible light multi-spectral fluorescence and absorption spectroscopy to identify and quantify organic compounds dissolved in seawater. Approximately 6000 kilometres of multi-channel fluorimeter and absorption data were collected; at a sampling interval of five seconds and a ship speed of 10 knots (approximately every 25 metres). Typical background fluorescence levels at 326 - 685 nm emission wavelengths and 265 nm excitation were < 5 counts (emission). Only minor elevated fluorescence levels (2 to 3 times background) were measured throughout the survey. The most extensive of these was on the transit line from Noumea to the survey area in the shallow shelf waters of the Norfolk Ridge. This was accompanied by an absorption high that is probably the result of the presence of planktonic algae and non-organic suspended shelf derived detritus. Other minor 540 nm fluorescence anomalies on Line 2 to the south and on Line 26 to the north-west are the likely result of fish oils or gelbstoff; the former corresponding with a cool surface water front encountered on the southern end of Lines 2 to 4.

A minor absorption anomaly (α = 0.45 m^{-1}) was detected on Line 5 in the central survey area and a high intensity (α = 3.5 m^{-1}), but narrow (1 km wide) absorption event was intersected to the north-west on survey Lines 26 and 27. These events were not accompanied by any significant fluorescence on the 265 nm emission spectrum but fluoresced to a level of 75 counts at 600 nm and 685-810 nm on the 440 nm spectrum. On the return transit to Nouméa an extensive but low intensity absorption anomaly was again detected in the shallow Norfolk Ridge waters.

The low level, near background (20 counts; less than 1 ppb), fluorescence events encountered, appear to be too low in concentration to indicate anything other than normal shelf and oceanic variations caused by biological activity. There is no evidence to suggest that there are any petroleum hydrocarbon related occurrences.

The absorption anomaly in the northwest of the survey area is of unknown origin. Possible natural causes include atmospheric sourced surface-entrained dust, near-surface biologically derived material, or a seafloor derived sediment plume from a dynamic event, eg. volcano, turbidity current or mud volcano. The most likely cause is a *Trichodesmium* phytoplankton bloom. These and other minor blue-green algae have recently been detected in the area, sometimes as dense surface slicks, by both shipboard and satellite sensor systems.

Acknowledgements

We wish to thank IFREMER for the opportunity of participating in the ZoNéCo5 survey and the support of their scientists and crew. Thanks also to AGSO Marine Operations Group and ESU staff for making the freight arrangements and engineering preparations and to Natalie Crawford for instruction with laboratory calibration using the Perkin-Elmer spectrophotometer. We very much appreciate the advice and support of colleagues in PMD throughout, and the efforts of our reviewers, Ian Lavering and Melissa Fellows, who helped make this work as thorough and presentable as possible.

Introduction

During the ZoNéCo5 swath mapping and geophysical profiling survey, AGSO undertook a continuous geochemical analysis of near surface waters in the Fairway Basin region. This basin lies on the eastern flank of the north Lord Howe Rise in the South Pacific, south-west of Nouméa, New Calédonia, approximately a thousand kilometres east of Brisbane.

The Lord Howe Rise is a fragment of the Australian Plate, bounded to the east by the New Calédonia Basin and to the west by the Tasman Basin. It became detached from the Gondwana super-continent during the opening of the Tasman Sea sometime between the Lower and Late Cretaceous (chron 33 to 24 ; Hayes and Ringis, 1973 ; Weissel and Hayes, 1977 ; Shaw, 1978 ; Jongsma and Mutter, 1978 ; Symonds et al., 1996 ; Gaina et al.,1998). Taking into account its location, the Lord Howe Rise has registered all the geological events since the Cretaceous rifting phase up to the Neogene volcanic episode (Auzende et al., 2000). The Fairway Basin, which formed during the rifting, is a complex, faulted, largely north-south sedimentary basin about 100 kilometres wide and 800 kilometres long and lies in water depths of 2000 to 3000 metres. Previous studies have shown that the northern Lord Howe Rise underwent uplift and sub-aerial erosion during the Eocene, associated with compressional tectonics emphasized by a series of reverse faults at the eastern flank of the Lord Howe Rise (Lafoy et al., 1994 ; Van de Beuque et al., 1998). The summit of the ridge also shows a series of approximately north-south trending volcanoes presumed of Oligo-Miocene age (Van de Beuque et al., 1998).

Because of the early geo-history of the region, it was thought that there might be organic-rich petroleum source rocks deep within the basin (Willcox et al, 1980). Bottom simulating reflectors (BSR's), were discovered on a recent AGSO seismic survey in the area, (Exon et al, 1998). The location on this survey of many diapirs, (possibly salt domes) with implications for gas hydrate, free gas and petroleum hydrocarbon potential, have renewed interest in this deep water frontier area, (Auzende et al, 2000). The location of the survey, the regional bathymetry and relevant core sites are shown in Figure 1.

The geochemical profiling program was conducted aboard the French research vessel 'L'Atalante', from the 14/10/1999 to 7/11/1999 using a WET Labs SAFire multi-spectral fluorescence and absorption instrument especially designed for detecting polyaromatic hydrocarbons in ocean waters.

Objectives

The aim was to directly measure polyaromatic hydrocarbons and/or anomalous biological activity in the water column that might be the result of sea-floor petroleum seepage or the venting of natural gas from the sub-surface. It was recognised from the outset that the deep water and open ocean environment would ensure that any effluent associated with seep activity would be subject to extreme dilution and therefore exceptionally difficult to detect. However low level, Class 3, remotely sensed SAR anomalies in the area, obtained from RADARSAT, indicated the possibility of oil slicks. The relatively low deployment costs associated with the instrument and the desirability of obtaining data to develop rigorous processing methods, also contributed to making the survey effort desirable.

Methods

Equipment configuration

The method uses UV and visible light multi-spectral fluorescence and absorption spectroscopy to identify and quantify organic compounds dissolved in seawater.

Seawater was pumped at about 2.0 litres per minute through the ship's clean ocean-water delivery system, which continuously supplied

the ship's thermo-salinograph. The estimated pumping time to the fluorometer system was less than 1 minute. The water was passed through a venturi driven de-bubbler to remove bubbles that would otherwise introduce an unacceptable number of noise spikes into the data, and then passed to the fluorometer multi-spectral filter assembly and onto a YSI 6000UPG CTD. This latter instrument continuously recorded temperature, salinity, dissolved oxygen and pH. A system diagram is shown in Figure 2(a).

Fluorimeter characteristics

The SAFire uses UV and visible light multi-spectral fluorescence and absorption spectroscopy to identify and quantify hydrocarbons and organic compounds dissolved in seawater. These include fluorescing hydrocarbons, particularly the polycyclic aromatic hydrocarbons (PAH's), such as napthalene, anthracene and pyrene.

The instrument employs a xenon flash lamp source powered by a high voltage power supply. The light from the lamp is directed through an excitation filter, one of 6 embedded in a filter wheel assembly, rotating at 5 Hz, that allows the transmission of light to a quartz flow tube at 6 excitation wavelengths: 228 nm, 265 nm, 307 nm, 375 nm, 440 nm and 487 nm. These wavelengths extend from the UV portion of the spectrum through the visible range. The water to be analysed flows continuously through a flow tube from bottom to top under pump pressure. The incident light passes through the water and is detected by (a) an absorption detector at the top of the column and (b) 16 fluorescence emission detectors embedded in the walls of the quartz flow tube Fig. 2(b). These are referenced by a beam splitter / detector at the base of the tube which corrects for lamp aging and fluctuations in light intensity. Thus for each excitation wavelength, an absorption measurement and 16 separate fluorescence emission measurements are made. The latter can then be used to graph emission spectra from 245 to 810 nm for each excitation wavelength. The absorption measurements (at 6 wavelengths) also allow an absorption spectrum to be plotted at any selected site.

The absorption and fluorescence determinations are an average of up to 40 (over-sampled) measurements. These are output at 5 times per second. This output can then be selectively binned (further averaged) in SAFview software to provide a signal with better signal-to-noise characteristics, but with an obvious trade-off in along-line resolution.

Hydrocarbons respond most sensitively to the 228 and 265 nm range of excitation frequencies. In this study some of the emission spectra (328 to 375 nm) of these excitation wavelengths were summed to provide a bulk hydrocarbon channel for real-time monitoring. In a similar fashion, a selection of emission wavelengths in the 400 to 685 nm spectral range were summed to allow the on-line detection of biologically derived hydrocarbon compounds and help distinguish these from the hydrocarbons. A binning rate of 5 seconds (average of 25 samples) was selected for the majority of the survey. The SAFire data together with the YSI hydrographic data and GPS navigation input from the ship's navigation system were collected simultaneously. The fluorometer data were recorded on one computer while another computer ran in parallel with navigation and environmental software. The second computer was also used for on-line data processing to provide monitor records, Fig. 2(a).

It became obvious that in order to discriminate between oceanic background and the near-background level hydrocarbon anomalies expected in a deep open ocean environment (a few ng/L for typical petroleum seeps), careful attention would have to be paid to operational methodology and data processing. Essentially the instrument would have to be operated at its most sensitive and an appropriate processing protocol implemented.

Calibration

Basic calibration data for the SAFire were supplied by the manufacturer in the WET Labs SAFire User's Guide. The instrument is initialised using a device file (SAF0116) with workshop calibrated scale factors and offsets. However experience showed that in pristine oceanic conditions it was possible to observe negative values, in both absorption and fluorescence spectra using the SAF0116 offsets. This indicated that the laboratory water blanks used for the calibration file contained slight impurities, and the field results needed to be adjusted accordingly.

In this study, the approach taken to compute the absorption value (m^{-1}) was

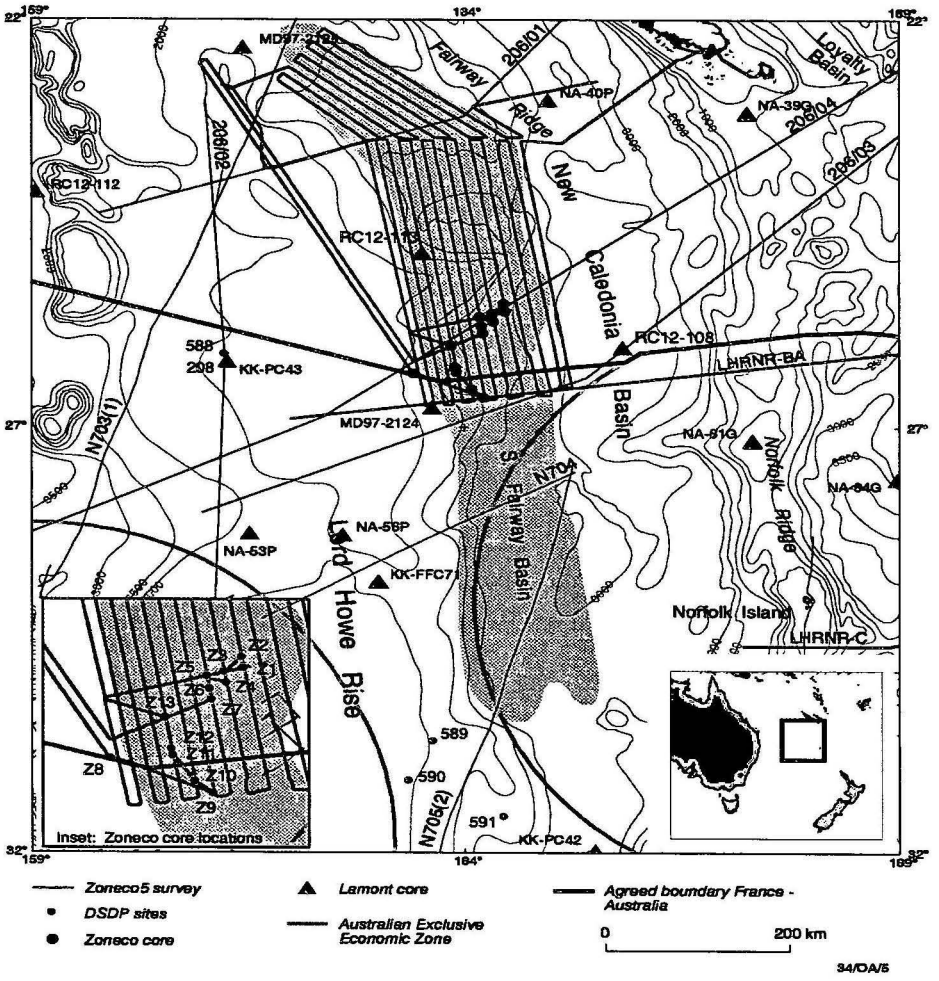

Figure 1. Survey location and bathymetric map

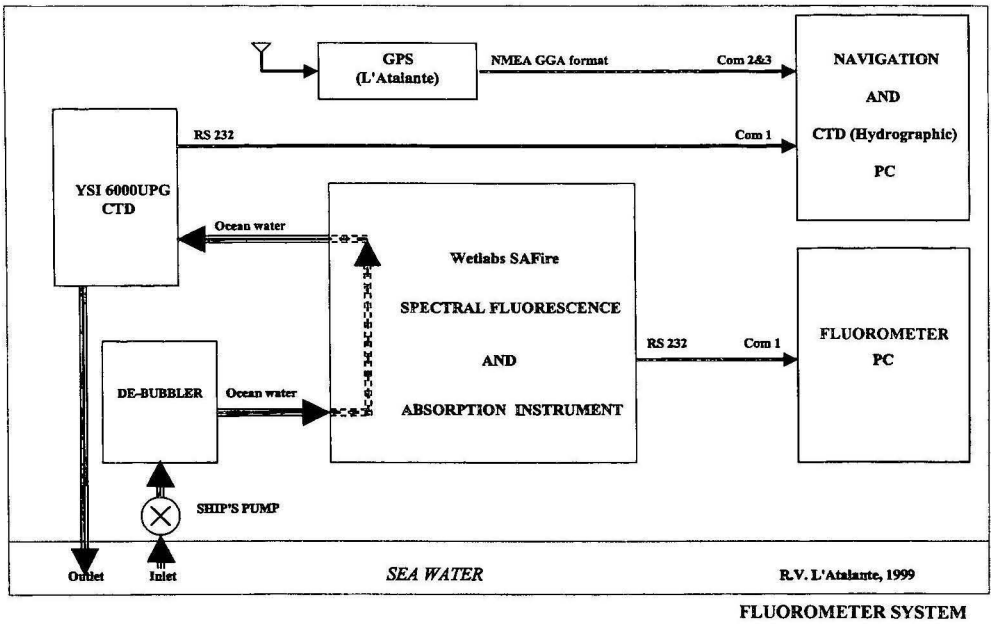

Figure 2(a). System schematic

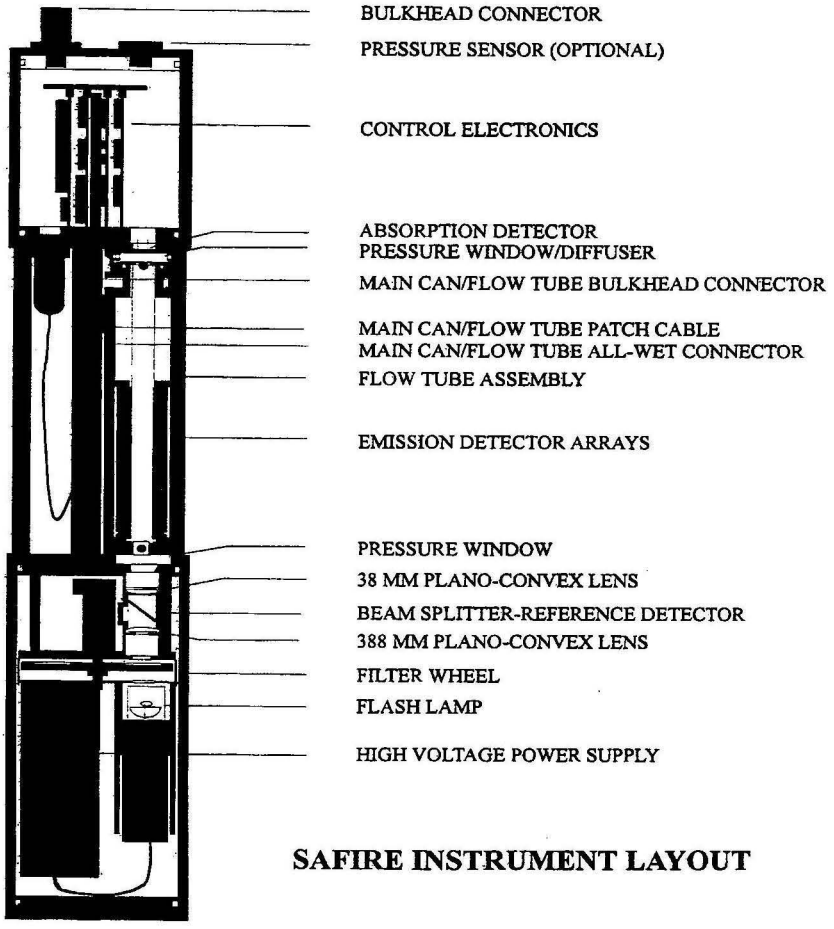

Courtesy:

WET Labs Inc. SAFIRE Users Manual V 1.1 08 June 1999

Figure 2(b). Fluorimeter with principal components labelled

to install the standard device file (SAF0116) and use the minimum regional reading from the survey as the baseline.

Fluorescence values for the emission wavelengths were then checked at each cleaning and calibration point and therefore only required corrections for optical drift (see below).

The fluorescence field results outlined in this paper are relative emissions only. They are not quantum corrected to normalise to the excitation energy or corrected for 'inner filter effect' to compare relative emission values. They do show the precise measured value for each channel. If required, further corrections can be implemented using the methods of Desiderio & Twardowski (1999).

The WET Labs calibration curves are shown in Appendix Figure1, p 56.

Processing

As outlined above, the fluorescence measurements were binned in WET Labs SAFview software every 5 seconds. The GPS data and YSI CTD data were recorded at the same rate using YSI Ecowin data acquisition software. Cruise data processing and post acquisition processing was all undertaken using Microsoft Excel.

The processing involved synchronising and merging data streams, de-spiking remnant bubble spikes (which occurred on average once every 5 nautical miles), data averaging and decimating and normalising instrument drift.

Particulate matter or bubble interference from time to time caused a gradual increase in signal to noise response. On most occasions this was corrected by simply disconnecting the intake to the fluorometer and allowing the seawater to back-flush for a few seconds. However an overall increase in noise in the fluorescence channels compared with earlier results was noted in the latter part of the survey from Line 21 to Line 33.

Binning rate

It was discovered that the binning rates of the fluorometer are not exact multiples of a second as might reasonably be supposed. For example a 25 bin average occurs approximately every 4.82 seconds – not 5 seconds as anticipated. This caused a problem merging this data with the navigation and CTD data, which were recorded exactly every 5 seconds.

An algorithm was therefore applied, to adjust the fluorimeter data to a 5 second sample rate before combining all data into one file.

Despiking

The efficiency of the de-bubbler was acceptable throughout but remnant bubble spikes restricted the rate of data processing on board, because the data was processed manually

In post processing, despiking was undertaken using an algorithm that removed most of the spikes automatically. The data was then analysed manually to remove any remaining bubble noise and confirm that the remaining data included only true anomalous measurements.

Lamp aging

The fluorimeter has a built-in capability to allow for flash-to-flash lamp variations and flash lamp aging. Reference values are derived in internal software from the amount of light from the flash tube incident on a reference detector. Thus the SAFview 'Use Refs' facility was used on this survey and there was no requirement for further lamp calibration.

Optical drift

The internal optical surfaces gradually attracted a residue (algae/bacteria) deposited by the passing seawater. These were cleaned every two or three days using a non-abrasive lint free 'wipe' and a dilute water – detergent mix. A small piece of the 'wipe' was pushed through the flow tube several times using a nylon rod to thoroughly clean the tube. The effect of the build up of grime is to increase the absorption values in an approximately linear manner over time and (very slowly), reduce the fluorescence signal. This result means that at background and near background levels, profiles on adjacent lines were difficult to compare and contouring was not practical unless corrections were applied and anomalies were very large and continuous.

The fluorometer has a facility to re-calibrate its device files. This applies offset values to re-zero each data column. Providing these device file offsets are recorded and saved frequently, this provides one method of drift correction. A

second option (the one taken on this survey) is to use the same device file (SAF0116) throughout and correct the drift in post processing, by normalising at each cleaning point. A drift correction algorithm was written, that automatically adjusts the data to the 'before and after' values at each cleaning point.

Fluorescence spectra

The study and description of petroleum hydrocarbons in sea-water, using UV and visible light fluorescence spectroscopy, in both laboratory and field experiments, has been the subject of considerable research over several decades (Freegarde et al, 1971; Hornig, 1974). Frank (1978), reviewed and evaluated methods for oil source identification in the context of a complete 3-D fluorescence system using all possible data, ie. emission spectra, excitation spectra and fluorescence intensity, allowing contour analysis and fingerprinting of oil types. More recently, laser induced fluorescence studies of PAH in sea-water have sought further to discriminate oils using time-delayed fluorescence techniques, (Rudnick and Chen, 1998).

Hydrocarbon detection

The method has been used for environmental monitoring and source identification of oil spills, but can also be used for prospecting for oil at sea by identifying naturally occurring oil seeps. The search for oil seeps, the determination of the fate of oil spill constituents, remediation experiments and environmental response studies, all benefit from rapid identification of fluorescing oil components. The shape of the UVF spectrum and emission intensity of an oil is determined mainly by the quantity and distribution of polycyclic aromatic hydrocarbons (PAHs). This composition is in turn influenced by the type of precursor material, burial history, maturity and subsequent alteration or weathering effects such as water-washing, biodegradation and fractionation caused by exposure to the hydrosphere and atmosphere (Ehrhardt & Petrick, 1984; Ehrhardt & Burns, 1993; Burns & Codi, 1999). The spectra are further modified by *in situ* interference effects such as quenching, scattering and solvent interactions, (Frank, 1978).

A recent UVF study of pristine Western Australian oils using a 266 nm excitation wavelength (identical to that used by the Airborne Laser Fluorescence (ALF) system), describes the variations and broad classifications of these oils. It also emphasises the difficulty of recognising the source of the resultant weathered oil, particularly when seen as a slick by remote sensing or towed fluorimetry methods (Edwards et al., 1998). The other challenge is to be able to differentiate petroleum hydrocarbons from naturally occurring oils such as fish oils and gelbstoff. Fish oils fluoresce in the 350-500 nm region and gelbstoff (a complex mixture of water soluble decayed organic material), generally in the 400-450 nm region, (Hornig, 1974). Both potentially overlap with thermogenic hydrocarbons.

The principal window used to detect and classify oils is in the 300 nm to 400 nm range of the emission spectra at 220 to 320 nm excitation. Edwards et al (1998), specifically use the emission intensity ratio of the 320 nm and 360 nm emission wavelengths to differentiate between oil types. Secondary responses of crude oils can also be expected around 500 nm and also beyond 600 nm at diminishing levels. From quantum fundamentals it has also been determined that 'see through' (*in situ* fluorescence measurements) and reflectance spectra are identical in wavelength response. This means that direct comparisons can be made between spectra obtained from 'towed' fluorimetry and those obtained from surface reflection, ie. remote sensing systems such as ALF (Goldberg & Devonald, 1973).

3D emission-excitation spectra can be produced using the SAFire data and are very convenient for comparing and contrasting sites at a glance. Comparisons with 3D spectra generated by laboratory instruments can also be made, providing only the corresponding laboratory emission wavelengths are used. Examples of SAFire 3D spectra are shown in Figs 23 - 40.

By using 265 nm excitation with emission detectors in the UV range at 307, 326, 340, 365 and 375 nm, measurements within the most oil sensitive emission range can be made. These wavelengths can also be summed and intensity ratios calculated in order to broadly classify fluorescence spectra and thus oil types. In this survey the 326 / 365 nm ratio is used as a proxy for the 320 / 360 used by Edwards et al, (1998).

Biological identification

Fluorescence characteristics also have the potential to differentiate between biological types, such as the phytoplankton and macro algae classes and may even discriminate between individual algae where fluorescence characteristics do not overlap, (Blumer et al, 1971; Yentsch and Yentsch, 1979). The technique is complicated because of the disparity in the total amount of light fluoresced from different algae and variability due to environmental conditions (such as nutrient and light stress), but offers the possibility of a continuous, semi-automated non-taxonomy based method of classification.

Yentsch and Yentsch, (1979), proposed a broad classification scheme to discriminate between brown, green and blue-green algae, dinoflagellate and diatoms using ratios of spectral intensity in the 540 nm and 685 nm region and at various excitation wavelengths. For example, at 440 nm excitation, chlorophyl *a* has a maximum fluorescence at 685 nm emission and cyano-bacteria (blue-green algae) have a prominent fluorescence at 540 nm. Another bacteria (cytochromus) fluoresces at 440 nm at 375 nm excitation. A characterisation scheme for macroalgae has also been proposed. Similarly, by measuring fluorescence at 685 nm (the chlorophyl *a* emission wavelength) and comparing the ratio of 540 / 465 nm excitation at this emission wavelength, various brown, red and green algae have been shown to have characteristic signatures of about 0.59, 3.67 and 0.28 respectively (Topinka et al, 1990).

Recognising the spectral characteristics associated with biological effects is important for hydrocarbon detection. Firstly, direct hydrocarbon indicators should not be confused with biological signatures. Secondly, there may be some potential for indirect hydrocarbon detection by using certain oil-consuming micro-organisms as a proxy for detecting oils in water. Bacteria isolated from wastewater such as *Pseudomonas* and *Sphingomonas* have been shown to degrade PAH's in the laboratory (Meyer et al, 1999).

Spectral subset used

An appraisal of the spectral data from the survey indicates that the hydrocarbon response can be mostly described by the 265 nm excitation data subset. In addition, the combination of emission spectra resulting from the 265 nm and 440 nm excitation wavelengths describe the salient features of the 400 - 810 nm portion of the spectrum used to classify biological types.

Thus the following discussion and the classification of the selected sites are based predominantly on the emission spectra resulting from the 265 and 440 nm excitation wavelengths (including the 685 nm excitation spectra). This schema is illustrated in the spectral 'fence' diagram in Figure 3.

Nevertheless the 228, 307, 375 and 487 nm data help to 'fingerprint' the spectra by adding detail which is usefully displayed as 3D contour plots (Figs 23-40) as described above.

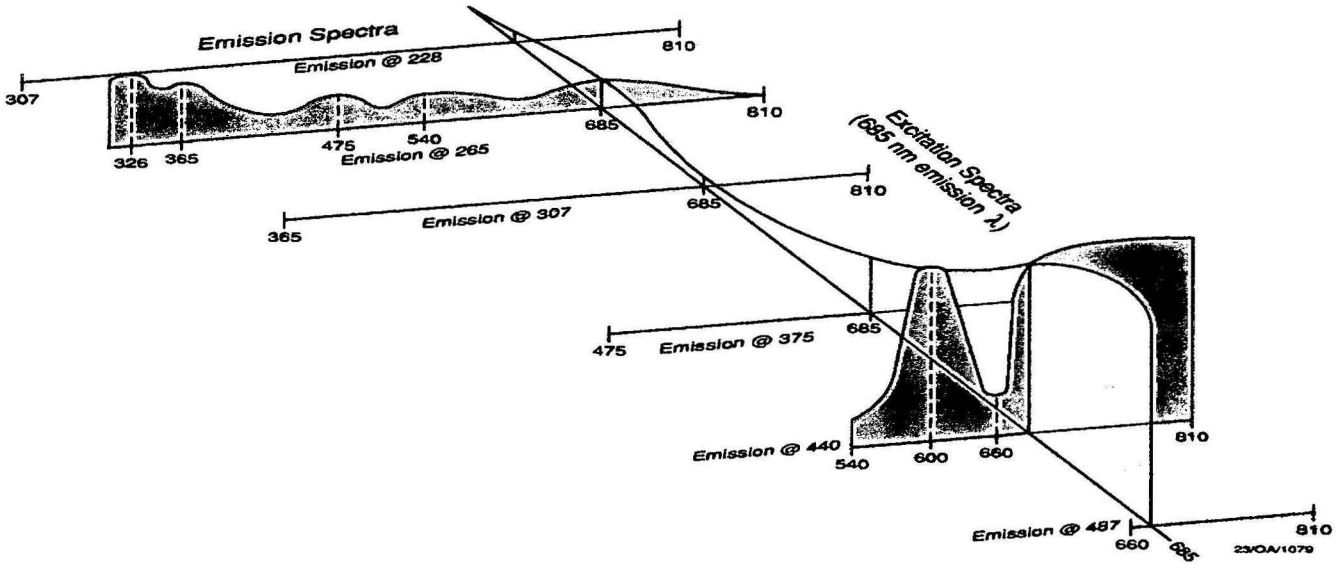

Figure 3. Fluorescence spectra - emission and excitation 'fence' diagram

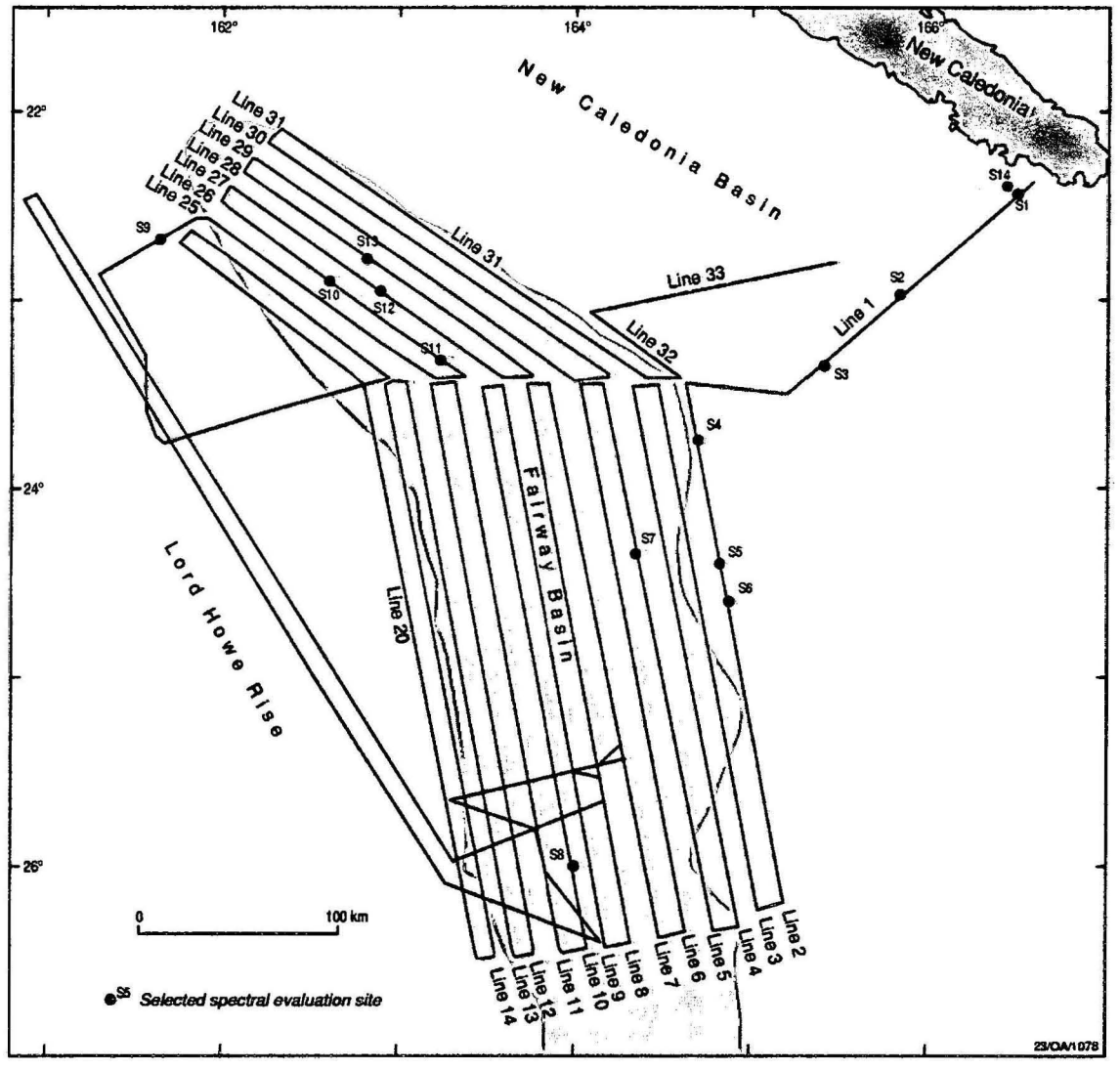

Figure 4. Survey lines and spectral evaluation site locations

Results

A total of 6,000 line kilometres of fluorimeter data extending over an area of 65,000 square kilometres was collected. This included transit lines from Noumea, New Caledonia to the main survey area. The survey was conducted in consistently good, mild weather and calm seas with only the occasional moderate swell and rising winds.

Sea surface temperatures were in the range 21 °C to 25 °C with the coolest temperatures recorded by thermo-salinograph and CTD at the southern extremities of Lines 2 to 10.

The survey Line locations and selected sites for spectral analyses are shown in Figure 4. The sites include those with elevated responses in one or more emission or absorption wavelengths as well as sites with typical regional background levels. The exact co-ordinates of each site are shown in Table 1. The fluorescence and absorption profiles of the lines chosen for discussion are shown in Figures 5 to 13 and the averaged results of all significant parameters at the sites are shown in Table 2.

Spectral responses

As described above, of the 102 fields of data captured by the instrument, anomalous hydrocarbon indications would be expected in the UV range using 228 nm and 265 nm excitation, particularly through the emission wavelengths of 326 to 375 nm. This description is confined to the ALF compatible 265 nm emission spectra but the 228 nm emission spectra were always similar and in some cases gave slightly higher responses. Figs 14 & 15.

Although slight anomalies were seen at these UV wavelengths, they were all associated with similar or slightly larger levels in the 400 to 685 nm region of the spectra. This is indicative of the presence of biological activity rather than petroleum oils.

Thus no distinctive 'hydrocarbon only' anomalies were detected during the survey. Various other combinations of elevated responses, however, were noted.

Transit line

The first and largest anomaly encountered was on the transit line from Noumea to the survey area (Line 1), between 166° 45'E, 22° 25'S and 166° 15'E, 22° 40'S,). It was a broad 100 km long anomaly with a response at 540 nm of about 12 counts, commencing in shallow reef waters on the Norfolk Ridge and extending out to about 2 km water depth to the south west. (Figure 5). A level of about twice background was recorded at the biological sensitive wavelengths (540 and 685 nm) and a slightly weaker response noted on the hydrocarbon channels. Background level for all wavelengths was less than 6 counts. The 326 and 365 nm hydrocarbon emission channels were only slightly elevated above background. This area is on or adjacent to the Norfolk Ridge in shallow reef water with the westernmost extent of the anomaly extending rapidly into 2000 m water depth. It was parallelled by an absorption coefficient (α) rising to nearly 0.3 m^{-1} at 265 nm wavelength. The absorption increase was seen at all wavelengths although at reduced levels at 440 and 487 nm.

The emission spectra at 265 excitation showed high levels from 440 to 600 nm and 865 to 810 nm compared to background sites such as Site 2, (which was chosen as a background spectral site for this area). Responses were also elevated on the 440 nm emission spectra at 600 nm and in the 685-810 nm region (Figures 15, 18 and 23). Thus a broad band biological response is indicated.

Radarsat targets

Prior to the survey, several Radarsat scenes of the North Lord Howe Rise area were obtained and three low probability (Rank 3 seepage) sites and several Natural Film Slicks (NFS's) were identified as possible targets for ground truthing. The Rank 3 sites were at the eastern edge of the BSR survey area and were intersected early in the survey (Lawrence [NPA Report], 1999). A slightly elevated response of about 5% above background (around Site 3), approximately coincided with the first of the Radarsat Rank 3 seepage sites at 165° 20' to 164° 50' at latitude 23° 30' on the absorption profiles. On the basis of this result the SAR anomaly in this area (in water depths over 3 km) was most likely to be a natural film slick only.

South-east

On Line 2, the first north-south traverse, the fluorescence response was slightly elevated at spectral Site 5, representative of a broad area

around 24.5 °S which continued onto Site 6 where a 540 nm emission peak indicated a biological anomaly for about 2 km. This was associated with a temperature drop of 1° C in the surface waters as indicated by the temperature profile (Figures 6, 15 and 18). This temperature front, and the higher slightly anomalous measurements persisted through to Line 4 in the west at approximately the same latitudes but with decreasing amplitude.

The 487 and 540 nm emission response (at 265 excitation) were distinctly higher than background, but unlike Site 1, there was no 685-810 nm response (above background) and no response at 600 nm and 685-810 nm at 440 nm excitation.

Absorption event – Line 5

Line 5 had typical baseline fluorescence characteristics overall (Figure 7). At Site 7, excitation wavelengths 228 nm to 375 nm had baseline emission levels only, although at 265 nm excitation, there was a distinctive dip in the emission spectra at 475 nm (Figure 15a). However, the 440 nm and 487 nm emission spectra exhibit strong responses at 600 nm and 685-810 nm (Figures 18 and 19).

Site 7 also had a significant absorption anomaly rising to 0.45 m^{-1} at 24.3 °S almost 1 km in width. As shown in Figures 7 and 20, all absorption wavelengths responded fairly uniformly.

West and north-west baseline

Lines 10 and Lines 24 & 25 showed typical background fluorescence characteristics in the south-west and north-west portions of the survey area respectively. Site 8 on Line 10 is representative of slightly elevated fluorescence levels over a broad area (probably 50% of the line extent) and has similar fluorescence characteristics to the previous site, ie, low fluorescence intensity at 265 nm excitation but relatively high at 440 nm excitation (Figures 8 and 15). There was no absorption anomaly on the line profile but the absorption spectral characteristics showed higher than average 265/228 and 265/440 intensity ratios (Figure 18).

An increase in noise levels on the 265 nm fluorescence profiles may have been due to a problem associated with equipment breakdown on Line 14. This is reflected in the error bars on the baseline spectra. These are set at one standard deviation of the samples per 100 measurements spaced at 5 second intervals (Figures 15 to 20). The variation, therefore, has an environmental component as well as statistical noise.

Absorption anomaly – Lines 26 & 27

The outstanding feature of Line 26 and 27 was a high absorption anomaly at 162.62 °E, 22.9 °S and 162.9 °E, 22.95 °S respectively. It was accompanied by strong fluorescence levels on both lines of up to 75 counts at 600 nm and 685-810 nm for the 440 nm emission spectra. This was a similar combination of characteristics to Site 7 in the south. The 265 nm emission spectra was also similar to Site 7, which had typical baseline characteristics except for a distinctive 'dip' at 475 nm (Figures 9, 10 and 11). The anomalies were approximately 1 km wide, along track, on both survey lines, and presumably represent a long ribbon of suspended absorbent and fluorescing material in the near surface. Significantly, the anomaly was not encountered on Line 25 (to the west) and decreased slightly in amplitude on Line 27 with perhaps a remnant still evident on Line 28 (Site 13), shown in Figure 12. Spectra are shown in Figures 15, 18 and 20. Contour maps of the 265 nm absorption coefficient are presented in Figure 21.

Site 11, to the southern and eastern end of Line 26, has high 487 and 540 nm emission responses at 265 nm excitation but no response at 440 nm excitation. This site was therefore spectrally similar to Site 6 (Line 2). Overall, higher fluorescence levels were observed in the eastern region of the survey area rather than in the west.

Transit to Noumea

The transit line from the survey area to Noumea (Line 33) had similar absorption characteristics to Line 1 (as would be expected) with higher absorption levels at all wavelengths approaching the Norfolk Ridge and shelf waters of Noumea (Figures 13 and 20).

The fluorescence anomalies seen on Line 1 (on the 265 emission spectra) were not repeated on this transit. This may be because of changes in the water mass or because of the increased instrument noise experienced in the latter stages of the survey. The 440 nm emission data, however, was similar, with levels near the baseline (Figures 15 and 18).

Table 1. Selected spectral evaluation sites with positions and reference criteria

Site	Line No.	Figure references	Coordinates	
			Longitude (decimal degrees)	Latitude (decimal degrees)
1	1	Figures 5, 14 - 20	166.50	22.45
2	1	Figures 5, 14 - 20	165.84	22.97
3	1	Figures 5, 14 - 20	165.37	23.34
4	2	Figures 6, 14 - 20	164.70	23.76
5	2	Figures 6, 14 - 20	164.83	24.42
6	2	Figures 6, 14 - 20	164.90	24.78
7	5	Figures 7, 14 - 20	164.35	24.34
8	10	Figures 8, 14 - 20	163.99	26.01
9	24	Figures 8, 14 - 20	161.64	22.72
10	26	Figures 9, 10, 14 - 20, 21	162.62	22.90
11	26	Figures 9, 14 - 20	163.23	23.32
12	27	Figures 10, 11, 14 - 20	162.90	22.95
13	28	Figures 12, 14 - 20	163.00	22.90
14	33	Figures 13, 14 - 20	166.44	22.39

Table 2. Average intensity levels and ratios of key parameters measured at spectral sites

Site	Absorption		265 EX			HC TYPE			BIO TYPE HC/BIO		440 EX				685 EM
	265Ab	265/228	265/440	326 em	365 em	326/365 em	540 em	685 em	540/685 em	326/540 em	600 em	685 em	600/660 em	600/685 em	265/440 ex
1	0.195	0.996	4.491	19.849	17.529	1.132	25.749	23.020	1.119	0.681	26.766	40.584	1.715	0.660	0.567
2	0.077	0.737	2.267	18.562	16.691	1.112	20.667	19.920	1.038	0.808	24.013	25.942	2.536	0.926	0.768
3	0.069	0.638	2.749	18.155	16.511	1.100	20.829	19.898	1.047	0.793	24.843	28.600	2.389	0.869	0.696
4	0.119	0.933	2.824	17.687	16.589	1.066	20.037	19.094	1.049	0.828	27.360	28.083	2.804	0.974	0.680
5	0.178	1.045	3.675	17.998	16.560	1.087	20.364	18.712	1.088	0.813	30.693	30.102	2.928	1.020	0.622
6	0.168	1.282	3.369	17.749	16.233	1.093	25.695	18.684	1.375	0.632	33.169	33.273	2.822	0.997	0.562
7	0.285	1.001	3.086	22.307	16.276	1.371	19.379	18.720	1.035	0.840	100.185	84.048	4.464	1.192	0.223
8	0.107	1.120	2.543	16.249	16.220	1.002	17.487	12.580	1.390	0.928	143.341	113.896	4.467	1.259	0.110
9	0.100	0.440	2.234	4.362	14.307	0.305	14.600	6.315	2.312	0.980	13.979	15.403	1.657	0.908	0.410
10	1.764	1.238	1.472	12.810	17.741	0.722	18.362	10.063	1.825	0.966	74.609	69.901	3.426	1.067	0.144
11	0.119	1.124	2.067	11.667	16.386	0.712	29.711	8.474	3.506	0.552	8.956	9.222	0.981	0.971	0.919
12	1.246	1.049	1.557	10.934	16.712	0.654	15.876	8.662	1.833	1.053	54.228	49.647	3.364	1.092	0.174
13	0.133	1.566	2.976	7.561	15.537	0.487	14.777	7.412	1.994	1.051	5.928	7.519	0.797	0.788	0.986
14	0.448	1.912	6.699	4.094	15.856	0.258	16.818	7.101	2.369	0.943	11.478	19.619	0.721	0.585	0.362

Discussion

Hydrocarbons

The criteria selected in this work for evaluating sites as hydrocarbon 'positive' are: the 326 nm emission response, the 365 nm response and the 326/365 ratio at 265 nm excitation, which is used to 'type' the oil, if detected, (Edwards et al, 1998). These values are only significant, however, if the emission intensity response in the 326 nm to 365 nm region is high enough to suggest the presence of fluorescing PAH hydrocarbons. One way of quantifying this is to use the ratio of the 326 nm emission intensity (hydrocarbons) to the emission intensity of a non-hydrocarbon wavelength, eg. 540 nm; ie. a UV / visible-green ratio.

Tables 2 and 3 show that this ratio rarely exceeded an intensity of 1.00 and varied between 0.55 and 1.052. This is interpreted to mean that there were no hydrocarbon anomalies at any of the sites. The slight hydrocarbon responses that were measured, eg. at Site 1 on the transit line, were all associated with a similar response in the visible spectral range (460-810 nm range) and therefore any anomalous response is interpreted as due to biological origin and/or to mixed biological and perhaps anthropogenic origin.

Typical intensities were less than 25 counts (emission) at 265 nm and 228 nm excitation. These are less than 1 ppb 'diesel equivalents' (Figure 23) and are at the limit of detectable background levels. This compares with petroleum hydrocarbon levels measured in the shelf waters of the Great Barrier Reef of 0.29 ppb and the embayment waters of Port Phillip Bay of 0.2 - 22.6 ppb. Typical measurements of PAH's in Australian rivers are 0.1 - 0.13 ppb in the Brisbane River and 0.17 - 0.41 ppb in the Parramatta River. Concentrations of petroleum hydrocarbons plus biogenic hydrocarbons can be as high as 10 ppb in ocean waters, (Swan et al, 1994).

3D spectral data of diesel and North Scott Reef condensate generated in laboratory tests at AGSO (Figures 23 to 26) show the type of anomaly expected from a relatively high concentration of petroleum hydrocarbons. These can be compared with 3D spectra from the sites evaluated on this survey and discussed below (Figures 27 to 40).

None of the 3D spectra from the sites show any evidence of significant hydrocarbon concentrations above background level. There were no signs of fluorescing hydrocarbons that might have originated from point sources at sea.

Biological indicators

The sites have been classified into five groups. There are two groups with 'ocean background', characteristics. These groups are representative of broad areas in a deep-water oceanic setting. Of the other groups, two had very localised spectral characteristics which can be considered 'anomalous' in that they were obviously different from oceanic conditions. The other group was more extensive and representative of shallow water conditions. The results pertinent to biological classifications are shown in Tables 2 and 4, and Figure 22 (a) and (b). The spectra are shown in Figures 14 to 20. Sites 2 to 5, 9 and 13 (**OB1**) were oceanic background sites characterised by low absorption (at 265 nm), low to medium levels at 540 nm and 685 nm (265 nm ex.) and very low to low levels of fluorescence on the 440 nm emission spectrum.

Site 8 (**OB2**), typical of much of Line 10, is also classified as oceanic background and was similar to the OB 1 group except that there was a particularly high fluorescence response on the 440 emission spectrum at 600 nm and a high response in the range 685 - 810 nm. Classifying this response using both emission and excitation spectra as did Yentsch & Yentsch (1979), and making comparisons with their results is difficult because they used a broader excitation and absorption spectrum than that obtained using our SAFire instrument which is tailored for hydrocarbon fluorescence in the UV range. For example, an absorption spectra from 400 nm to 700 nm allows better differentiation of photo-synthetic pigments than the 228 nm to 487 nm range available with SAFire. Similarly, the excitation spectra used by Yentsch & Yentsch (1979), from 350 to 600 nm enabled them to distinguish between diatoms, dinoflagellates and chlorophytes, whereas we were restricted to the excitation spectrum below 487 nm. Only the emission spectrum has comparable coverage.

Nevertheless the high response at 600 nm (440 nm excitation) is interpreted as an indicator of the presence of phycobilin pigments such as

phycoerythrin which are characteristic of blue-green algae blooms like *Oscillatoria erythraea* (*Trichodesmium*). These have been shown to have a fluorescence peak at 576 nm in laboratory experiments and have been frequently reported in open sea environments, (Yentsch & Yentsch, 1979; Exton et al, 1983). The high response at 685 nm is the classic response expected of chlorophyl *a*. This identification is somewhat ambiguous however, since similar emissions could be due to diatoms, dinoflagellates or green algae.

Sites 1 and 14 were in the same area close to Noumea in shallow reefal waters and have been designated **CO** (coastal). The spectral characteristics varied somewhat over the period of the survey. This may in part be due to temporal environmental variations but excessive instrument noise at the close of the survey was also a likely contributor. Algal growth was removed on a regular basis and therefore was not a factor.

Generally though, the shallow water sites had above ocean background absorption intensity, but with absorption declining rapidly at 440 and 487 nm; medium to high fluorescence at 487 nm and 540 nm and above background levels at 685 nm (at 265 nm excitation). Fluorescence intensity at 440 nm was low to medium.

The broad absorption high was indicative of the increased turbidity caused by currents driving dissolved organic material and total suspended solids (TSS), that might be expected in shallow waters. A dip in absorption between 440 and 487 nm (Figure 20) may indicate the presence of minor blue-green algae, perhaps containing biliproteins such as c-phycocyanin or allo-phycocyanin. These transmit light in the blue 460-520 nm region, in contrast to green algae (500-560 nm) or *c* carotenoid containing algae such as diatoms, dinoflagellate, browns and chrysophytes (550-560 nm), (Prezelin & Boczar, 1986). The slightly higher (relative to background) response at 600 nm and 685-810 nm range at 265 nm excitation. may support this and the presence of chlorophyls. However the low response on the 440 emission spectra at all wavelengths, suggest the **CO** sites (reef waters), unlike the previous sites, were relatively depleted in organisms with phyco-pigments and chlorophyl *a* and therefore *Trichodesmium* and similar blue-green algae are not as dominant.

Sites 6 and 11 were very localised areas where there was a high emission intensity at 487 and 540 nm (265 excitation). Otherwise they were characterised by background conditions of very low absorption and low fluorescence response at 440 nm excitation. These are classified as **D** sites. The cause of these 540 nm anomalies is unclear. They may be caused by phytoplankton but are more likely to be the result of fish oils or gelbstoff (Hornig, 1974).

Sites 7 and particularly Sites 10 and 12 were localised areas with very high absorption coefficient values. The absorption intensities, particularly at Sites 10 and 12, were very high (3.5 m^{-1}) and also consistent across the spectrum (Figure 20), with anomalous values recorded at all wavelengths. Site 7 was similar but with decreasing absorption at 440 nm and 487 nm. Fluorescence at 540 nm (265 nm excitation) was low to medium at these sites but high at 600 nm and 685-810 nm on the 440 nm emission spectrum similar to **OB2** Site 8. These are designated as **AB** (absorption) sites and the 440 nm emission spectra indicate the presence of a variety of phytoplankton groups, with fluorescence characteristics similar to Site 8. The similarity with Site 8 (**OB2**) suggest that the absorption plumes may be extreme examples of algal blooms. Recent satellite and ocean surface studies in the area by Dupouy et al (2000), show the widespread nature of *Trichodesmium* blooms in the Vanuatu - New Caledonia region. In addition, their study also detected a wide variety of other cyano-bacteria and symbiotic associations between diatoms and *Richella*.

The high absorptions at all wavelengths at the **AB** sites may be due to a high density combination of the above biota and differs from the Site 8 population where only moderate to background absorption intensities were measured. Other possible natural causes include suspended or dissolved inorganic detrital material, sea-floor derived sediment plume from a dynamic event (such as a turbidity current, volcano or mud volcano) or an atmospheric sourced, surface-entrained dust. The bathymetric and seismic profiles from Lines 26 and 27 give no indication of sea-floor activity at the anomaly site. Of course, this does not preclude the possibility that material from a seep or vent might be transported some distance from the source by sub-sea currents.

Table 3. Hydrocarbon classification of spectral evaluation sites

Site	Description				Class
	HC's 326 nm emission @ 265 nm ex.	**HC's** 365 nm emission @ 265 nm ex.	**HC Type** 326/365 emission ratio @ 265 nm ex.	**HC / Bio Ratio** 326/540 emission ratio @ 265 nm ex.	
1	Low	Low	Medium	Low (ratio about 1)	No oil
2	Low	Low	Medium	Low	No oil
3	Low	Low	Medium	Low	No oil
4	Low	Low	Medium	Low	No oil
5	Low	Low	Medium	Low	No oil
6	Low	Low	Medium	Low	No oil
7	Low	Low	Medium	Low	No oil
8	Low	Low	Medium	Low	No oil
9	Very Low	Low	Low	Low	No oil
10	Very Low	Low	Medium	Low	No oil
11	Very Low	Low	Medium	Low	No oil
12	Very Low	Low	Medium	Low	No oil
13	Very Low	Low	Medium	Low	No oil
14	Very Low	Low	Low	Low	No oil

Table 4. Biological classification of spectral evaluation sites

Site	Description								Class
	265 nm absorption intensity	265/440 absorp. ratio	**540 nm em. @ 265 ex.**	**685 nm em. @ 265 ex**	540/685 em. ratio @ 265 ex.	**600-685 nm em. @ 440 ex.**	600/685 em. ratio @ 440 ex.	265/440 ex. @ 685 em.	
1	**Medium**	*Very high*	**High**	**Medium**	*Low*	**Medium**	*Low*	*Medium*	**CO**
2	**Very low**	*Medium*	**Medium**	**Medium**	*Low*	**Low**	*Medium*	*Medium*	**OB1**
3	**Very low**	*Medium*	**Medium**	**Medium**	*Low*	**Low**	*Medium*	*Medium*	**OB1**
4	**Very low**	*Medium*	**Medium**	**Medium**	*Low*	**Low**	*Medium*	*Medium*	**OB1**
5	**Very low**	*High*	**Medium**	**Medium**	*Low*	**Low**	*Medium*	*Medium*	**OB1**
6	**Very low**	*High*	**High**	**Medium**	*Medium*	**Low**	*Medium*	*Medium*	**D**
7	**Medium**	*High*	**Medium**	**Medium**	*Low*	**High**	*High*	*Very low*	**AB**
8	**Very low**	*Medium*	**Medium**	**Low**	*Medium*	**High**	*High*	*Very low*	**OB2**
9	**Very low**	*Medium*	**Medium**	**Low**	*High*	**Very low**	*Medium*	*Low*	**OB1**
10	**Very high**	*Low*	**Medium**	**Low**	*High*	**High**	*High*	*Very low*	**AB**
11	**Very low**	*Medium*	**High**	**Low**	*Very high*	**Very low**	*Medium*	*High*	**D**
12	**Very high**	*Low*	**Medium**	**Low**	*High*	**High**	*High*	*Very low*	**AB**
13	**Very low**	*Medium*	**Medium**	**Low**	*High*	**Very low**	*Medium*	*High*	**OB1**
14	**Medium**	*Very high*	**Medium**	**Low**	*High*	**Low**	*Low*	*Low*	**CO**

NOTE: Only key characteristics used to classify sites are tabled. Italicised data are of secondary importance.

Conclusion

A WET Labs SAFire spectral fluorescence and absorption instrument was used to directly detect dissolved hydrocarbons and anomalous biological activity in the water column that might be the result of seafloor petroleum seepage or the venting of natural gas from the sub-surface. The excitation and emission filters were selected specifically for hydrocarbon detection, but were also useful for a limited biological assessment.

Approximately 6000 kilometres of multi-channel fluorescence and absorption data were collected at a sampling interval of five seconds (approximately every 25 metres) at a ship speed of 10 knots. Typical background fluorescence levels at 326 - 685 nm emission wavelengths and 265 nm excitation were less than 5 counts (emission). Only occasionally were elevated fluorescence levels (2 to 3 times background) measured on the survey.

The most extensive of these was on the transit line from Noumea to the survey area in the shallow shelf waters of the Norfolk Ridge. This was accompanied by above background absorption levels and was probably the result of the presence of planktonic algae and dissolved and suspended inorganic reefal material, driven by the prevailing south-east Trade Winds and the Southern Sub-Tropical Current.

Minor 487-540 nm fluorescence anomalies at 265 nm excitation, on Line 2 to the south and on Line 26 to the north-west, are of unknown but probably biological origin, the former corresponding with a cool surface water front encountered on the southern end of Lines 2 to 4.

A minor absorption anomaly (α = 0.45 m^{-1}) was detected on Line 5 (Site 7) in the central survey area and a high intensity (α = 3.5 m^{-1}), but narrow (1 km wide) absorption region was intersected to the north-west on survey Lines 26 and 27. These regions of increased absorption did not show any fluorescence excited at 265 nm emission but fluoresced to a level of 75 counts at 600 nm and 685-810 nm when excited at 440 nm. This fluorescence pattern, similar to that observed at Site 8 on Line 10, is likely to be due to the presence of phyco-pigmented cyano-bacteria, ie. blue-green algae.

The high absorption is of uncertain origin but could simply be due to unusually high levels of the algae or algal remnants. The most likely candidate is *Trichodesmium*, an algae previously identified and mapped by a combination of satellite and ship based analyses (Dupouy et al, 2000). It can be broadly dispersed or found in 'meanders' at higher concentration levels.

On the other hand, the algae could be attracted to material derived from the sea-floor (dissolved or suspended sediment from a dynamic event such as a volcano, mud volcano or turbidity current).

On the return transit to Noumea an extensive but low intensity absorption anomaly was again detected in the shallow Norfolk Ridge waters. The low level, near background, (20 counts; less than 1 ppb), fluorescence UV events, appeared to be too low in concentration to indicate anything other than normal shelf and oceanic variations caused by biological activity.

There was no fluorescence evidence to suggest the presence of any petroleum hydrocarbon related molecules in near-surface waters.

References

Auzende J-M., Beneton, G., Dickens, G., Exon, N., Francois, C., Holdway, D., Juffroy, F., Lafoy, Y., Leroy, A., Van de Beuque, S. & Voutay, O., 2000. Mise en evidence de diapirs mesozoiques sur la bordure orientale de la ride de Lord Howe (Sud-Ouest Pacifique): campagne ZoNeCo5. *Earth and Planetary Sciences*, 330 (2000) 209-215.

Blumer, M., Guillard, R.R.L. & Chase, T., 1971. Hydrocarbons of marine phytoplankton. *Marine Biology*, Vol. 8, 183-189.

Burns, K.A. & Codi, S. 1999. Non-volatile hydrocarbon chemistry studies around a production platform on Australia's Northwest Shelf. *Estuarine, Coastal and Shelf Science*. Vol. 49, 853-876.

Coble, P.G., Green, S.A., Blough, N.V. & Gagosian, R.B., 1990. Characterisation of dissolved organic matter in the Black Sea by fluorecence spectroscopy. *Letters to Nature*, Nature Vol. 348, 432-435

Desiderio, R.A. & Twardowski, M.S., 1999. Characterisation of the WET Labs SAFire: Data analysis and corrections. College of Oceanic and Atmospheric Sciences, Oregon State University unpublished report.

Dupouy, C., Neveux, J., Subramaniam, A., Mulholland, R., Montoya, J.P., Campbell, L., Carpenter, E.J. & Capone, D.G., 2000. Satellite captures *Trichodesmium* blooms in the Southwestern tropical Pacific. *EOS*, Vol. 81, 13-16.

Edwards, D., Radlinski, A., Crawford, N. & Hulskamp, N., 1998. ALF-compatible laboratory UV fluorescence spectra of 120 off-shore Western Australian oils. Multi-client AGSO Study.

Ehrhardt, M.G. & Burns, K.A., 1993. Hydrocarbons and related photo-oxidation products in Saudi Arabian gulf coastal waters and hydrocarbons in underlying sediments and bioindicator bivalves. *Marine Pollution Bulletin*, Vol. 27, 187-197.

Ehrhardt, M.G. & Petrick, G., 1984. On the sensitized photo-oxidation of alkylbenzenes in seawater. *Marine Chemistry*, Vol. 15, 47-58.

Exon, N.F., Dickens, G.R., Auzende, J-M., Lafoy, Y., Symonds, P.A. & Van de Beuque, S., 1998. Gas hydrates and free gas on the Lord Howe Rise, Tasman Sea. *PESA Journal*, No. 26, 148-158.

Exton, R.J., Houghton, W.M. & Esias, W., 1983. Spectral differences and temporal stability of phycoerythrin fluorescence in estuarine and coastal waters due to domination of labile cryptophytes and stabile cyanobacteria. *Liminological Oceanography*, Vol. 28(6), 1225-1231.

Frank, U., 1978. A review of fluorecence spectroscopic methods for oil spill source identification. *Toxicological and Environment Chemistry Reviews*, Vol. 2, 163-185.

Freegarde, M., Hatchard, C.G. & Parker, C.A., 1971. Oil spilt at sea: its identification determination and ultimate fate. *Laboratory Practice*, Vol. 20-4, 35-40.

Gaina, C., Müller, R.D., Royer, J-Y., Stock, J., Hardebeck, J. & Symonds, P., 1998. The tectonic history of the Tasman Sea: a puzzle with 13 pieces. *Journal of Geophysical Research*, Vol 103, B6, 12413-12433.

Goldberg, M.C. & Devonald, D.H., 1973. Fluorescent spectroscopy, a technique for characterising surface films. *Journal of Research, U.S. Geological Survey*, Vol. 1, No. 6, 709-717.

Hayes, D.E. & Ringis, J., 1973. Seafloor spreading in the Tasman Sea. *Nature*, Vol 243, 454-458.

Hornig, A.W., 1974. Identification, estimation and monitoring of petroleum in marine waters by luminescence methods. Proceedings of a Symposium and Workshop held at NBS, Gaithersburg Maryland, May 1974, 135-144.

Jongsma, D. & Mutter, J.C., 1978. Non axial breaching of a rift valley: evidence from the Lord Howe Rise and the Southeastern Australian margin. *Earth Planet. Sci. Lett.*, Vol 39, 226-334.

Lafoy, Y., Pelletier, B., Auzende, J.M., Missegue, F. et Mollard, L., 1994. Tectonique compressive cénozoïque sur les rides de Fairway et Lord Howe, entre Nouvelle-Calédonie et Australie, *C. R. Acad. Sci. Paris*, Vol 319, série.IIa, 1063-1069.

Lawrence, G., 1999. Lord Howe Rise offshore basin screening report, AGSO Schedule 4. NPA-TREIC Production, UK, 1-20.

Prezelin, B.B. & Boczar, B.A., 1986. Molecular bases of cell absorption and fluorescence in phytoplankton: potential applications to studies in optical oceanography. *Progress in Phycological Research*, Vol. 4 (Round & Chapman, eds.), section 8.

Rudnick, S.M., & Chen, R.F., 1998. Laser-induced fluorescence of polycyclic aromatic hydrocarbons (PAH) in seawater. Environmental Coastal and Ocean Sciences Program, University of Massachusettes Report, 1-24.

Shaw, R.D., 1978. Seafloor spreading in the Tasman Sea; a Lord Howe Rise-Eastern Australian reconstruction. In: P.J. Coleman (Ed), *Southwest Pacific Earth Science Symposium and IGCP Project Meeting, 2nd*, Australian Society of Exploration Geophysicists Bulletin, Vol 9, 75-81.

Swan, J.M., Neff, J.M. & Young, P.C., 1994. Environmental implications of offshore oil and gas development in Australia. *The Findings of an Independent Scientific Review for APPEA*, Sydney, Australia, 553-556.

Symonds, P.A., J.B., C., Struckmeyer, H.L.M., Willcox, J.B. & Hill, P.J., 1996. Mesozoic rift basin development off eastern Australia, *Mesozoic Geology of the Eastern Australia Plate Conference*, Vol 43, 528-542.

Topinka, J.A., Bellows, W.K. & Yentsch, C.S., 1990. Characterisation of marine macroalgae by fluorecence signatures. *International Journal of Remote Sensing*, Vol. 11, No. 12, 2329-2335.

Van de Beuque, S., Auzende, J.-M., Lafoy, Y. & Missegue, F., 1998. Tectonique et volcanisme tertiaire sur la ride de Lord Howe (Sud-Ouest Pacifique), *C. R. Acad. Sci. Paris*, Vol 326, série II, 663-669.

Weissel, J.K. & Hayes, D.E., 1977. Evolution of the Tasman sea reappraised, *Earth Planet. Sci. Lett.*, Vol 36, 77-84.

Wilcox, J.B., Symonds, P.A., Hinz, K. & Bennet, D., 1980. Lord Howe Rise, Tasman Sea - preliminary geophysical results and petroleum prospects. *BMR Journal of Australian Geology & Geophysics*, Vol. 5, 225-236.

Yentsch, C.S. & Yentsch, C.M., 1979. Fluorecence spectral signatures: The characterisation of phytoplankton populations by the use of excitation and emission spectra. *Journal of Marine Research*, Vol. 37, 471-483.

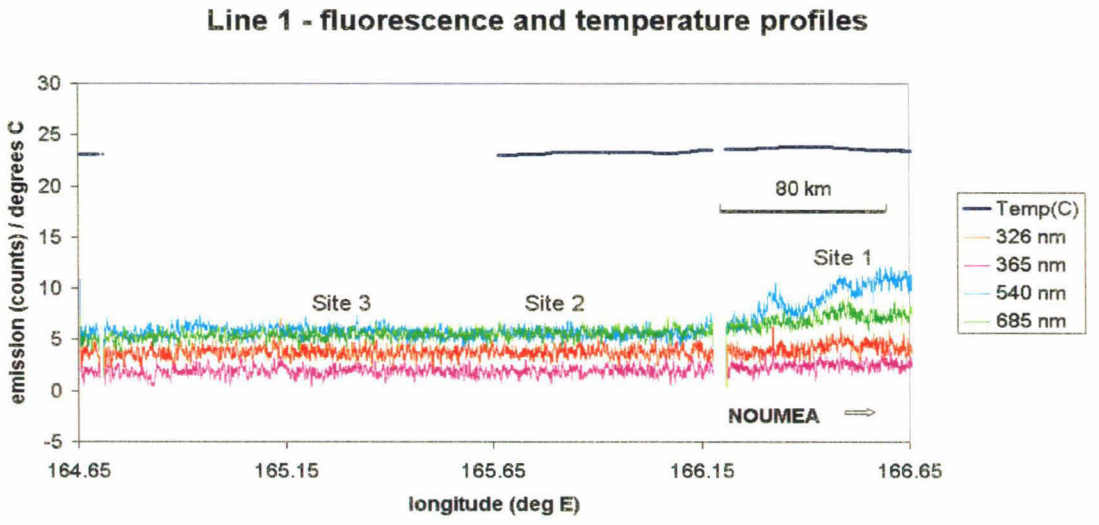

(a)

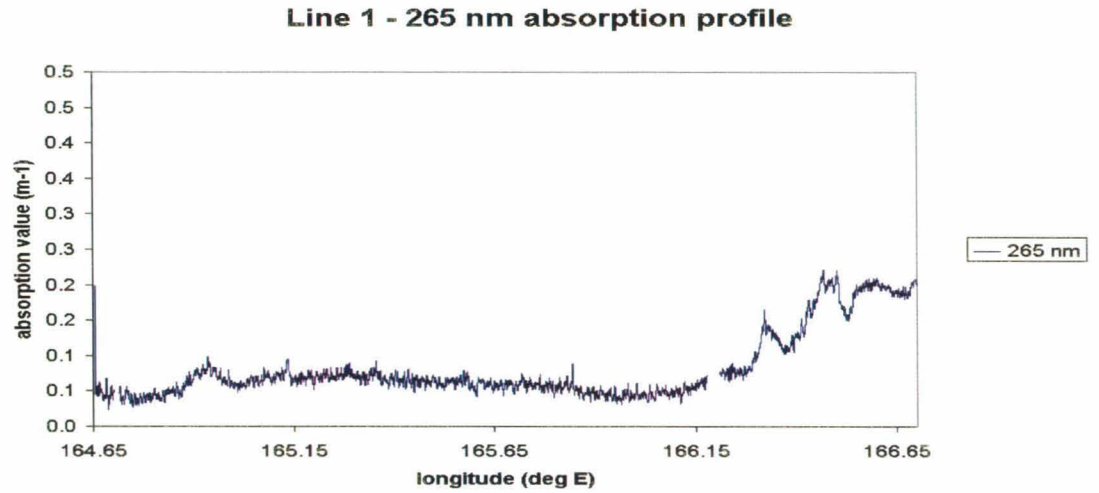

(b)

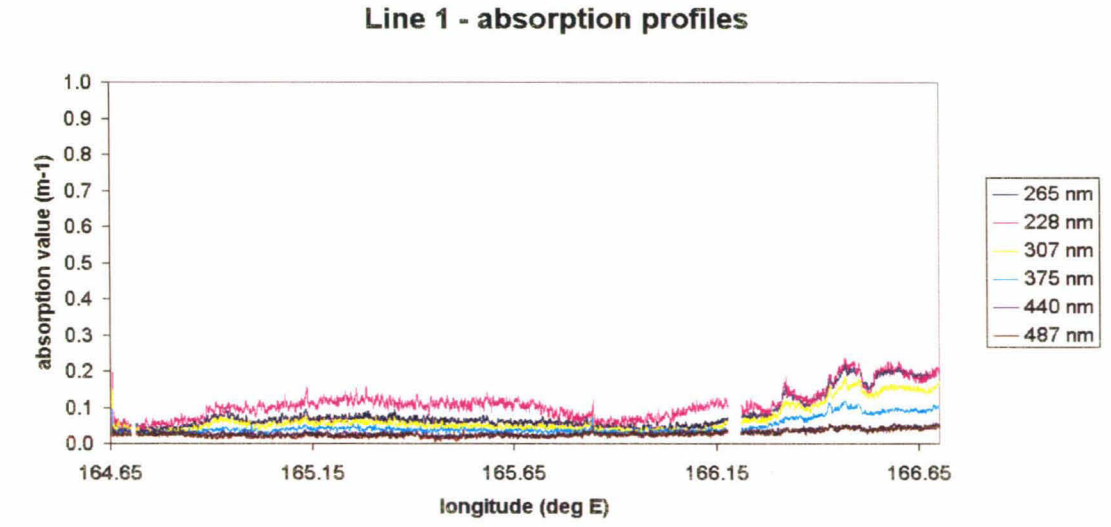

(c)

Figure 5. Line 1 - fluorescence, absorption and temperature profiles

(a)

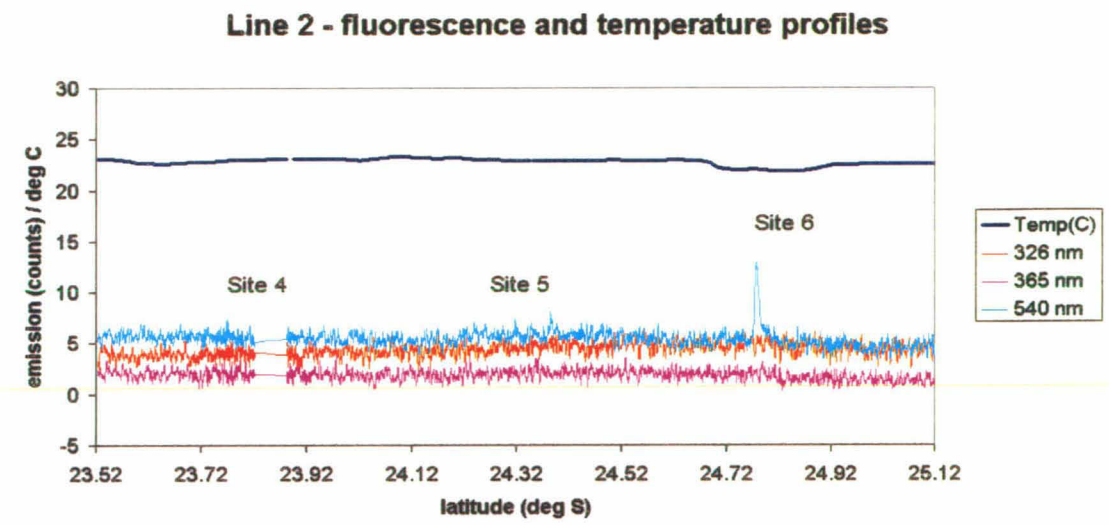

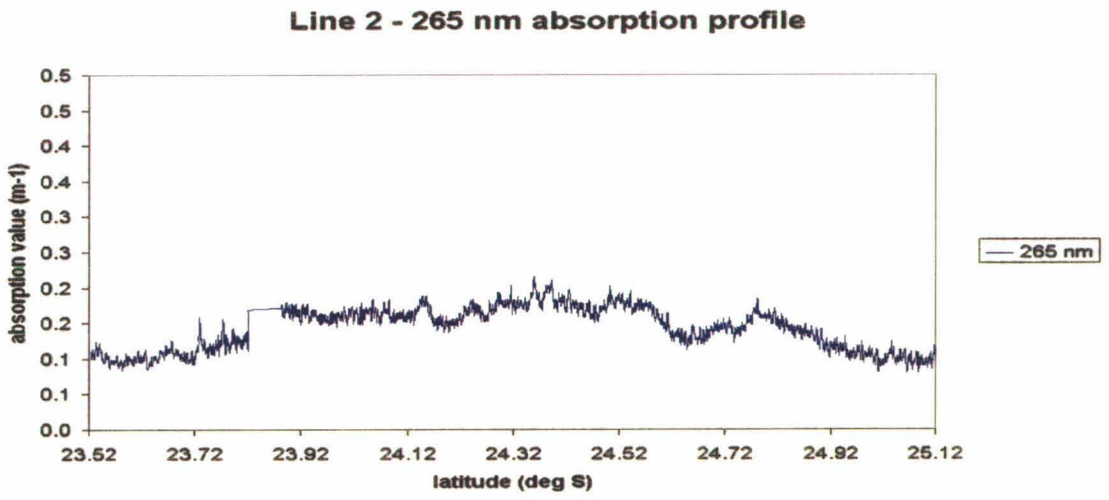

(b)

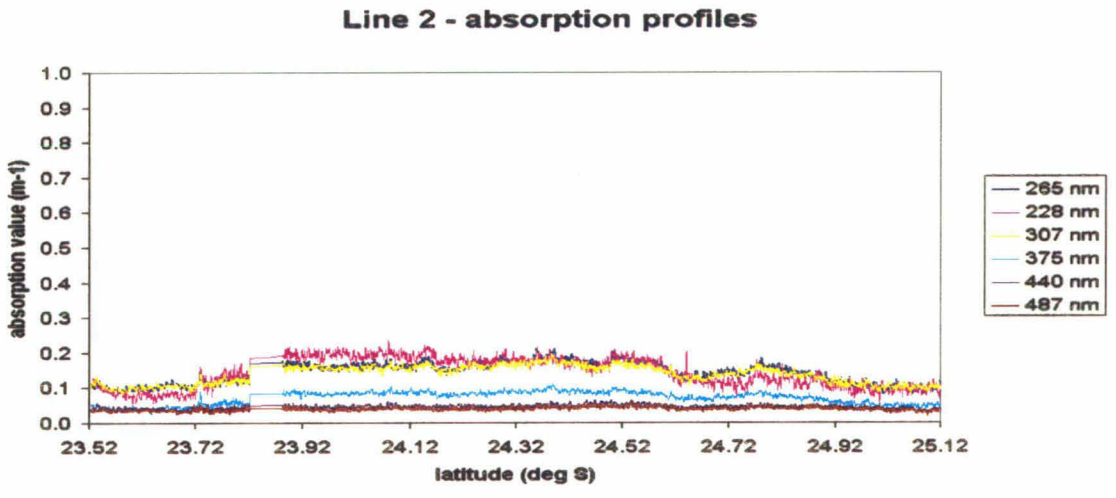

(c)

Figure 6. Line 2 - fluorescence, absorption and temperature profiles

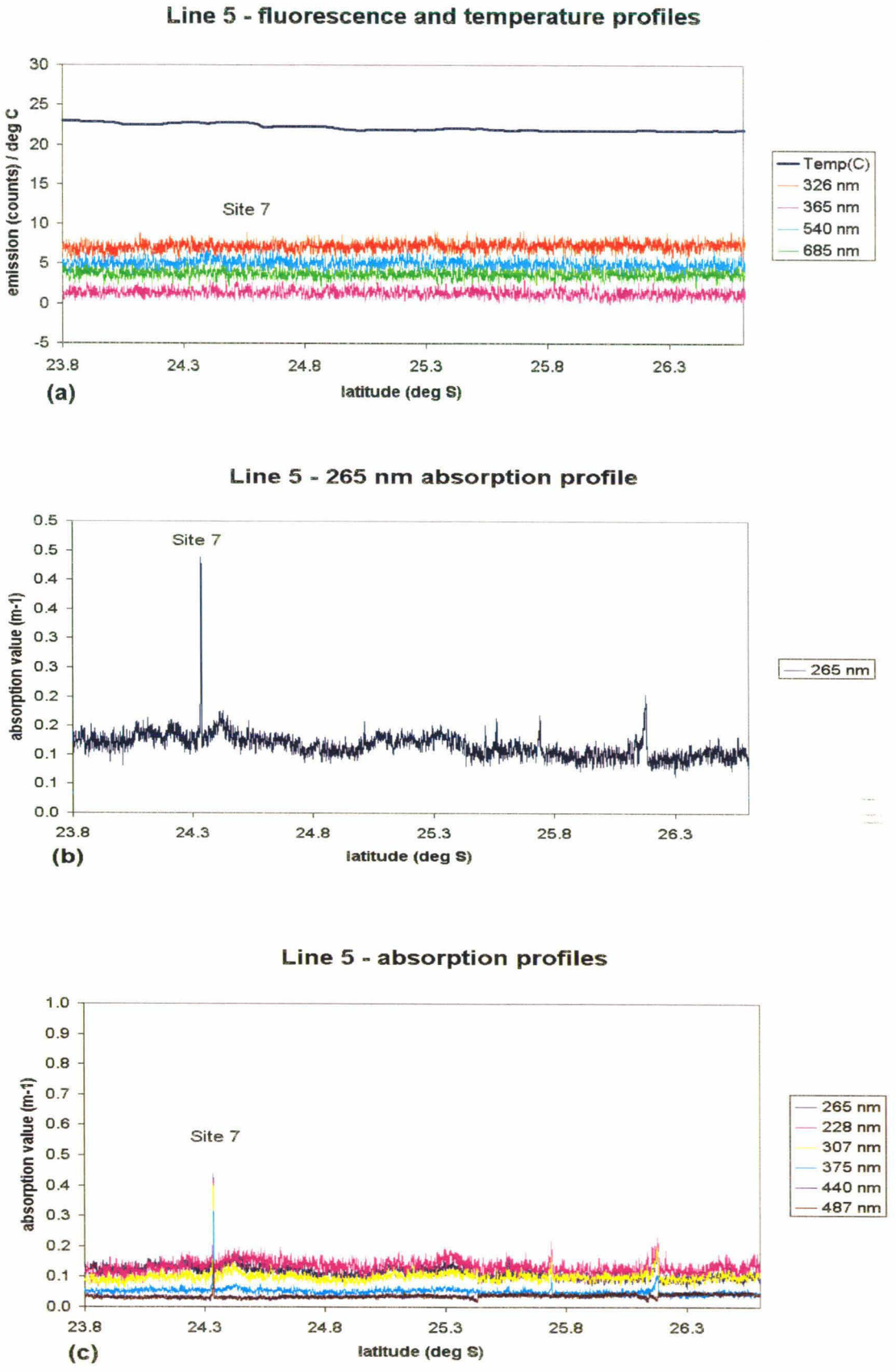

Figure 7. Line 5 - fluorescence, absorption and temperature profiles

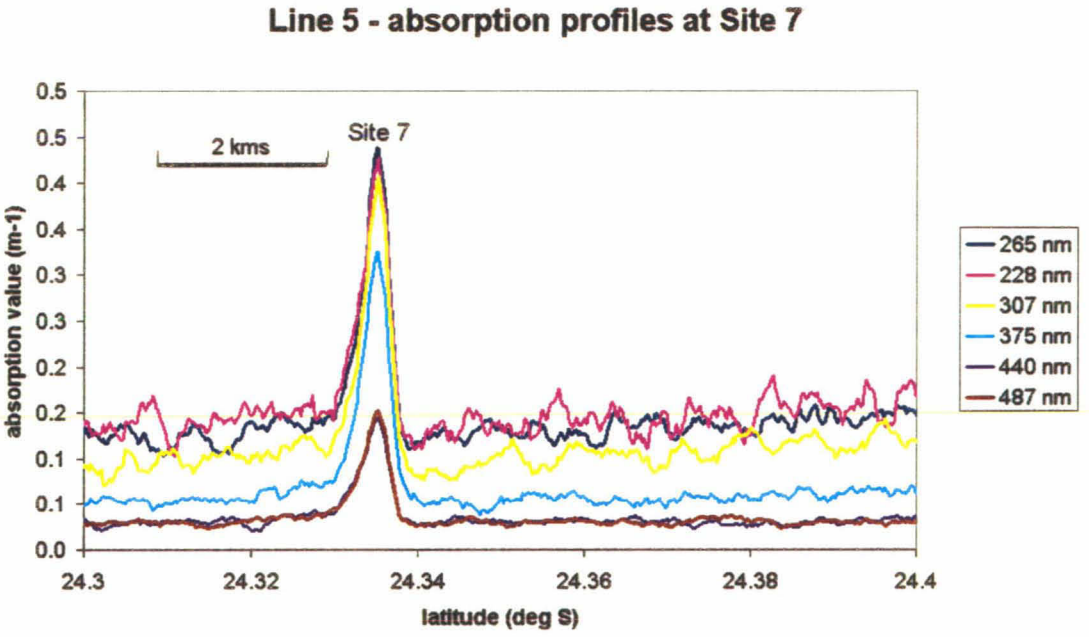

(d)

Figure 7. (continued)

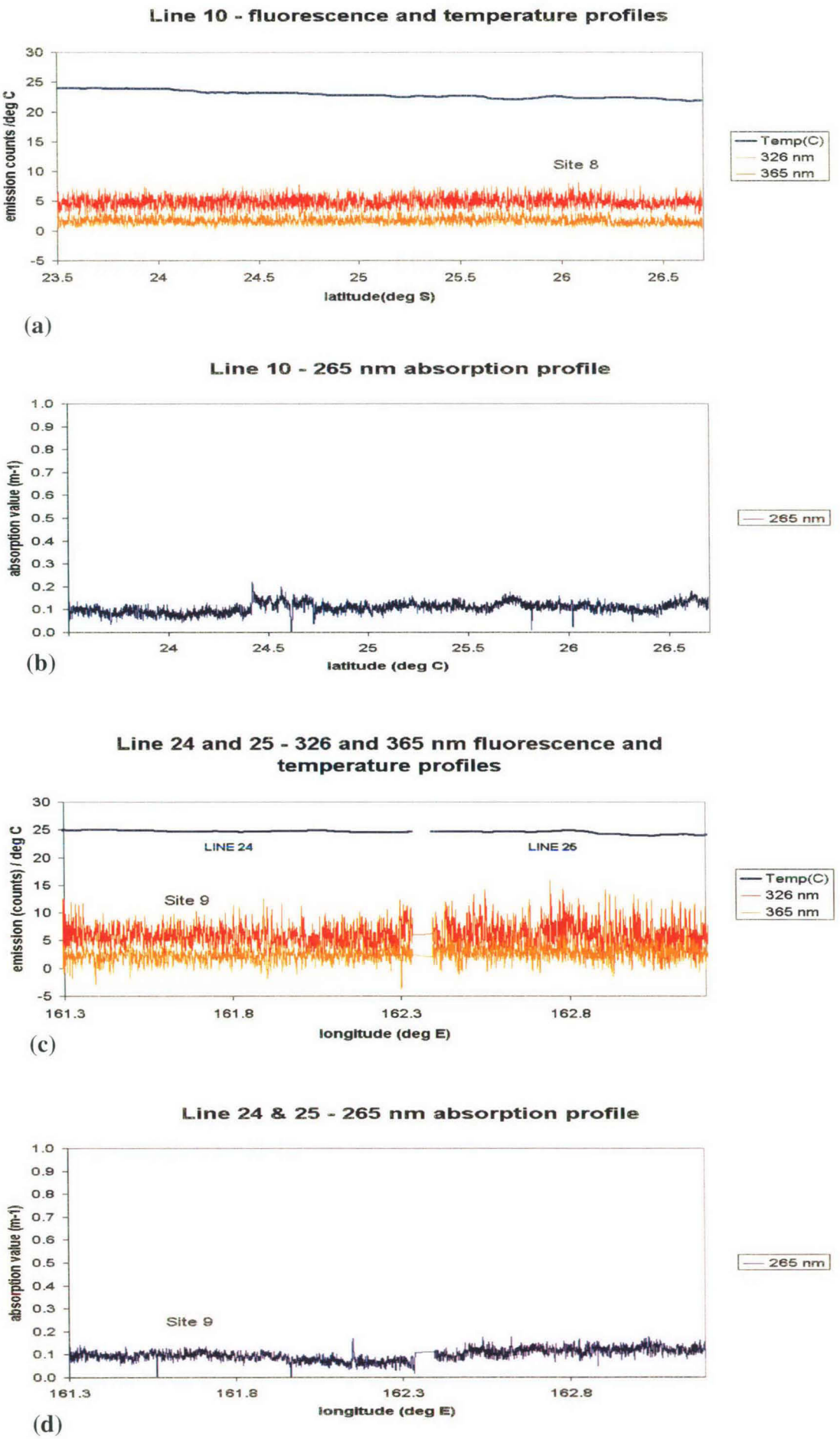

Figure 8. Line 10, Line 24 & 25 - fluorescence, absorption and temperature profiles

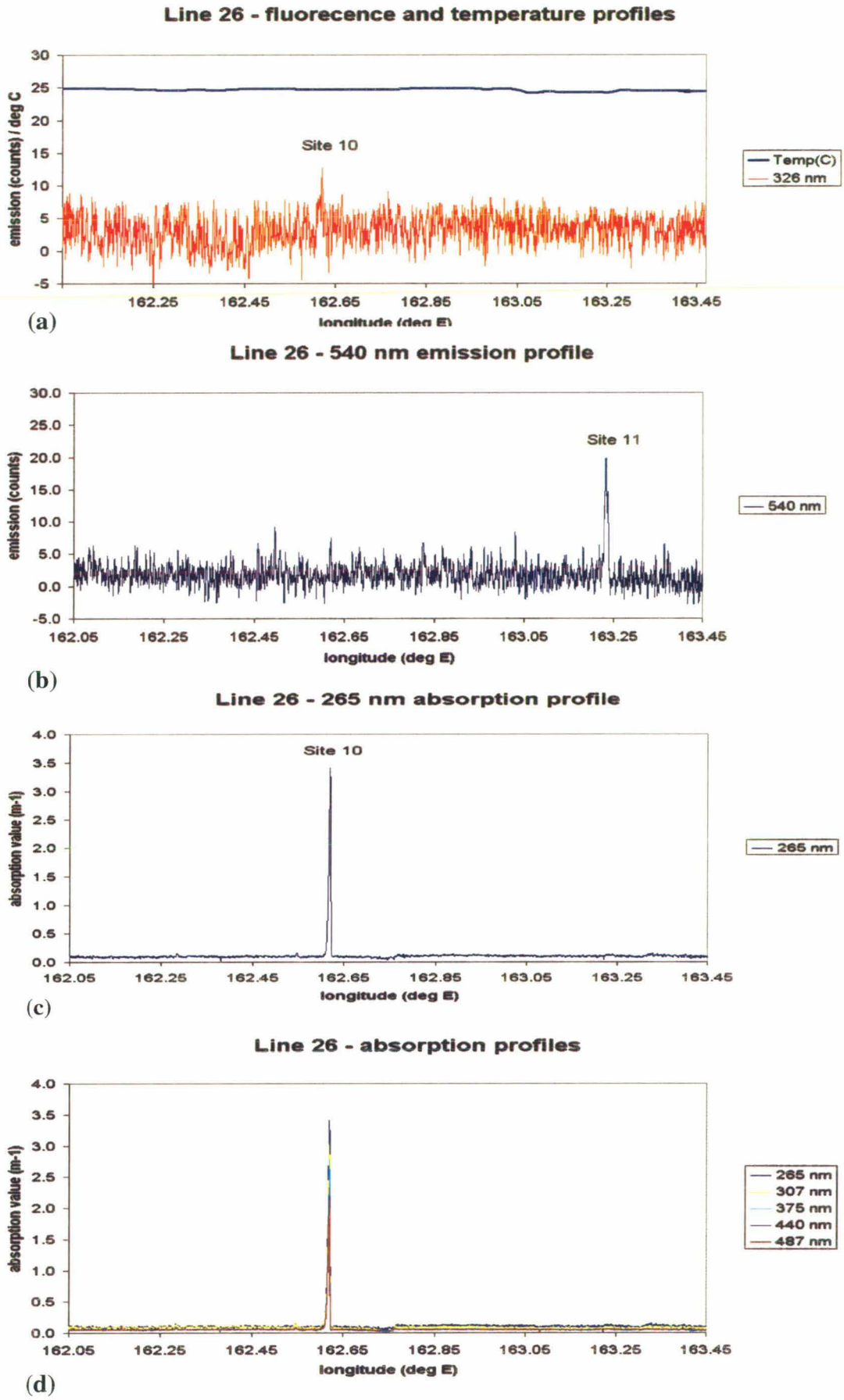

Figure 9. Line 26 - fluorescence, absorption and temperature profiles

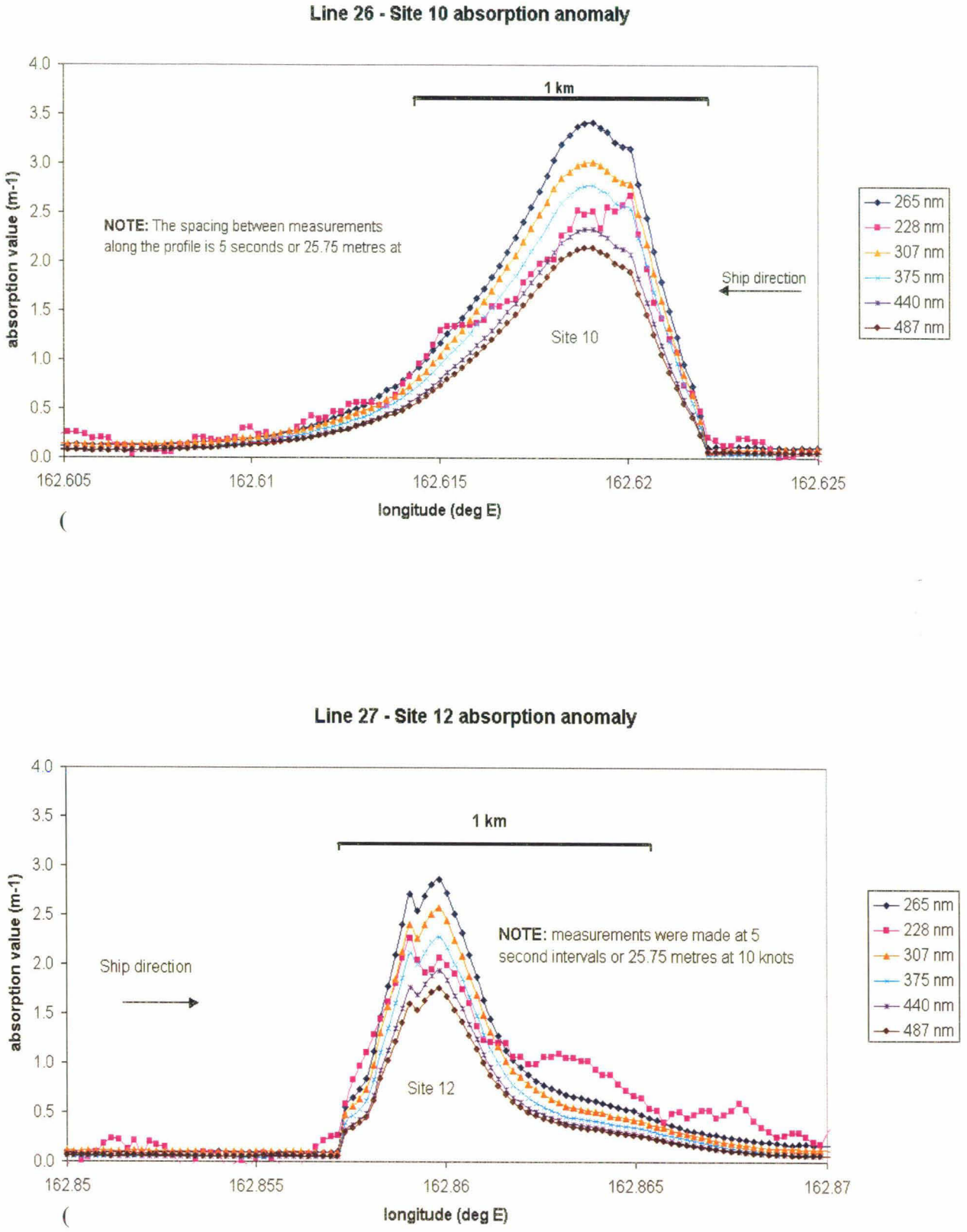

Figure 10. Line 26 & 27 - absorption anomaly

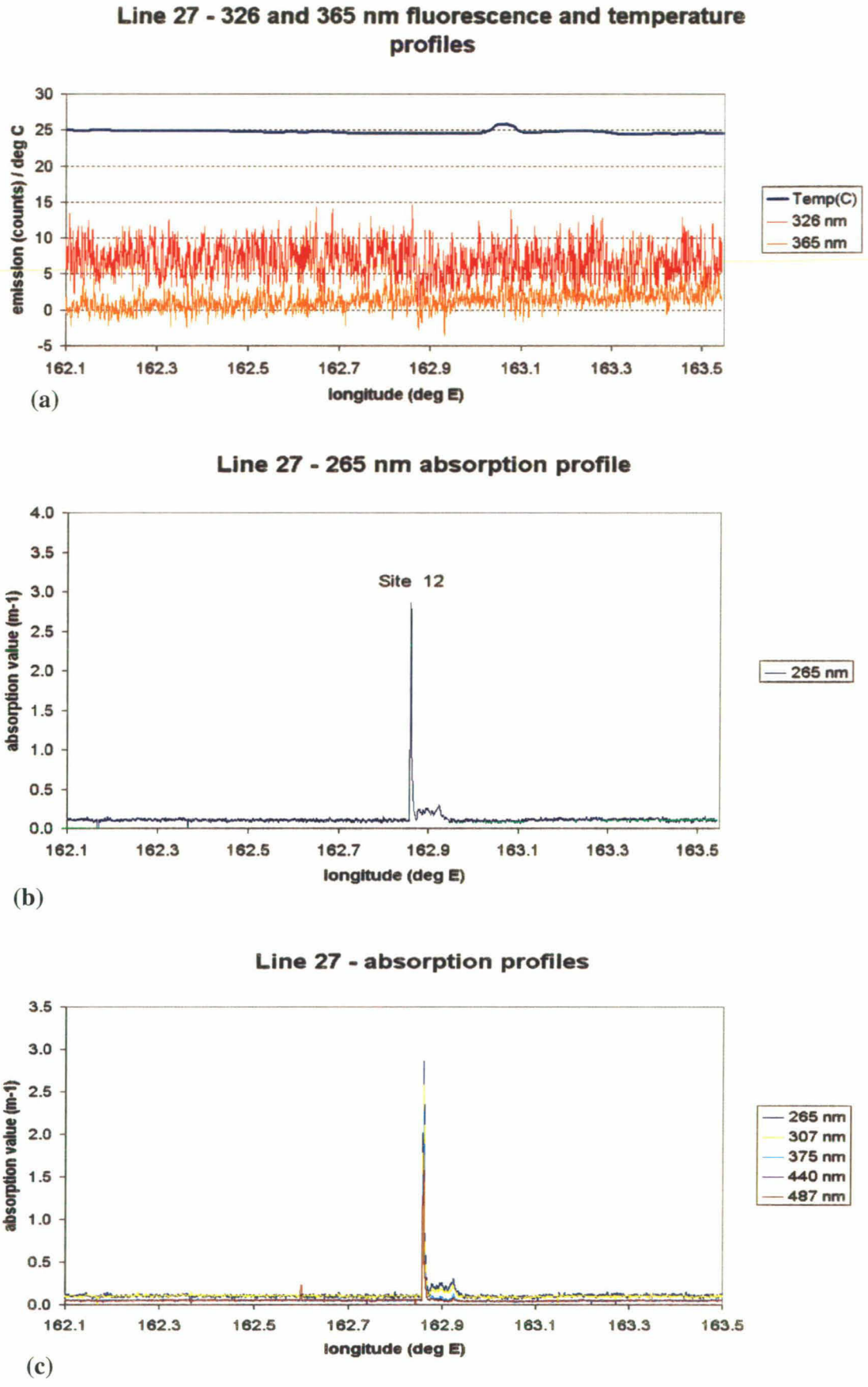

Figure 11. Line 27 - fluorescence, absorption and temperature profiles

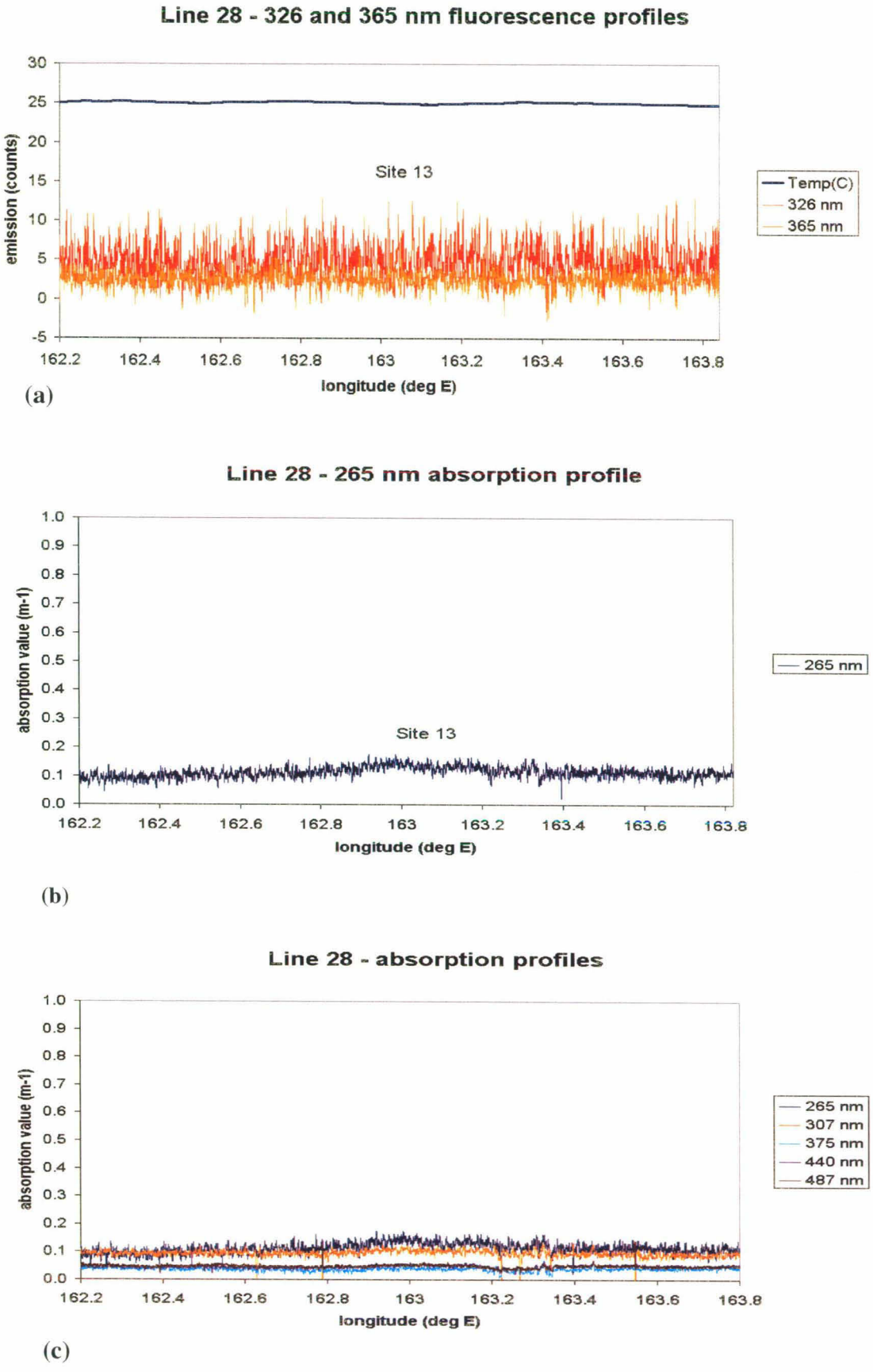

Figure 12. Line 28 - fluorescence, absorption and temperature profiles

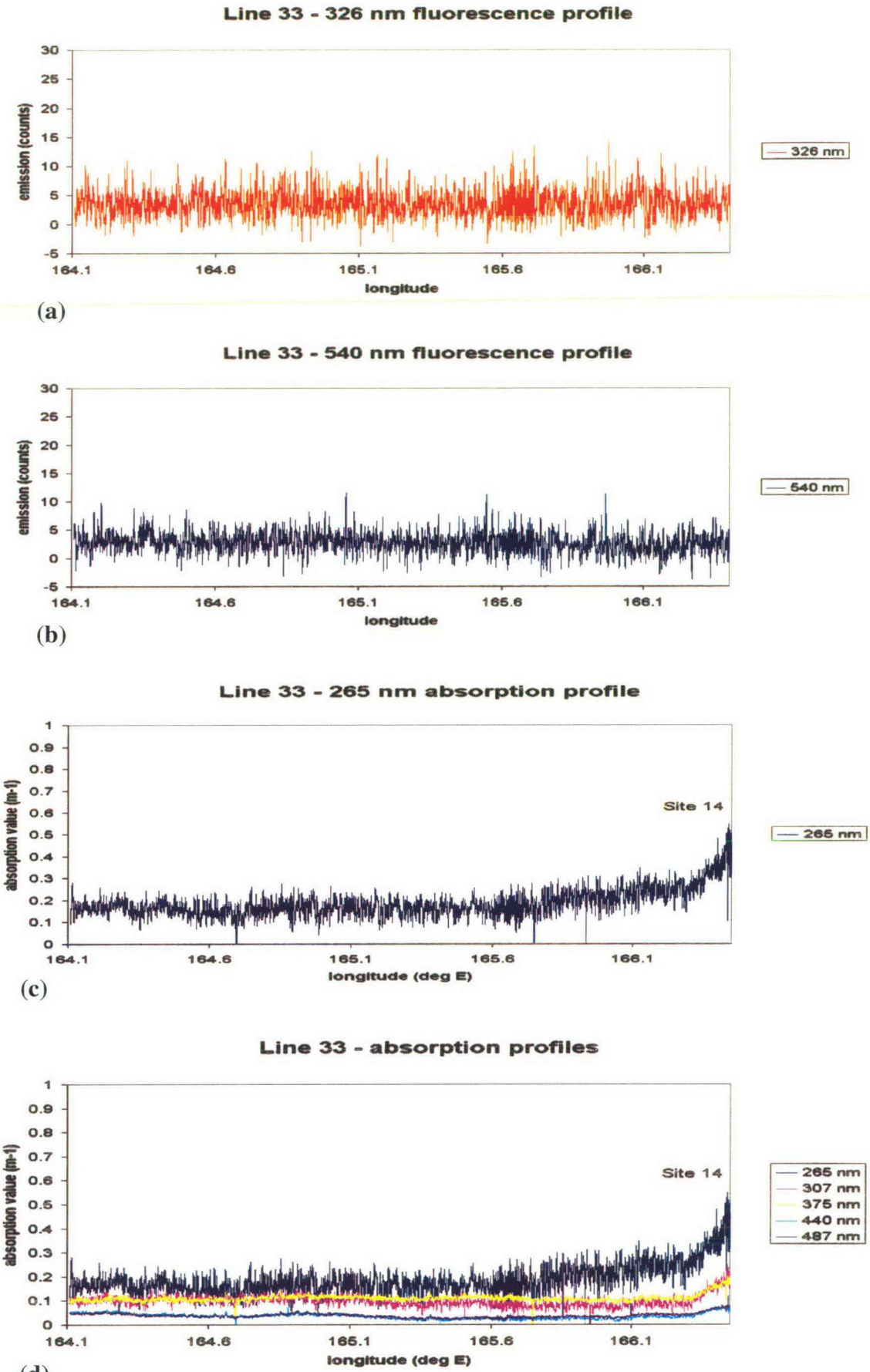

Figure 13. Line 33 - fluorescence and absorption profiles

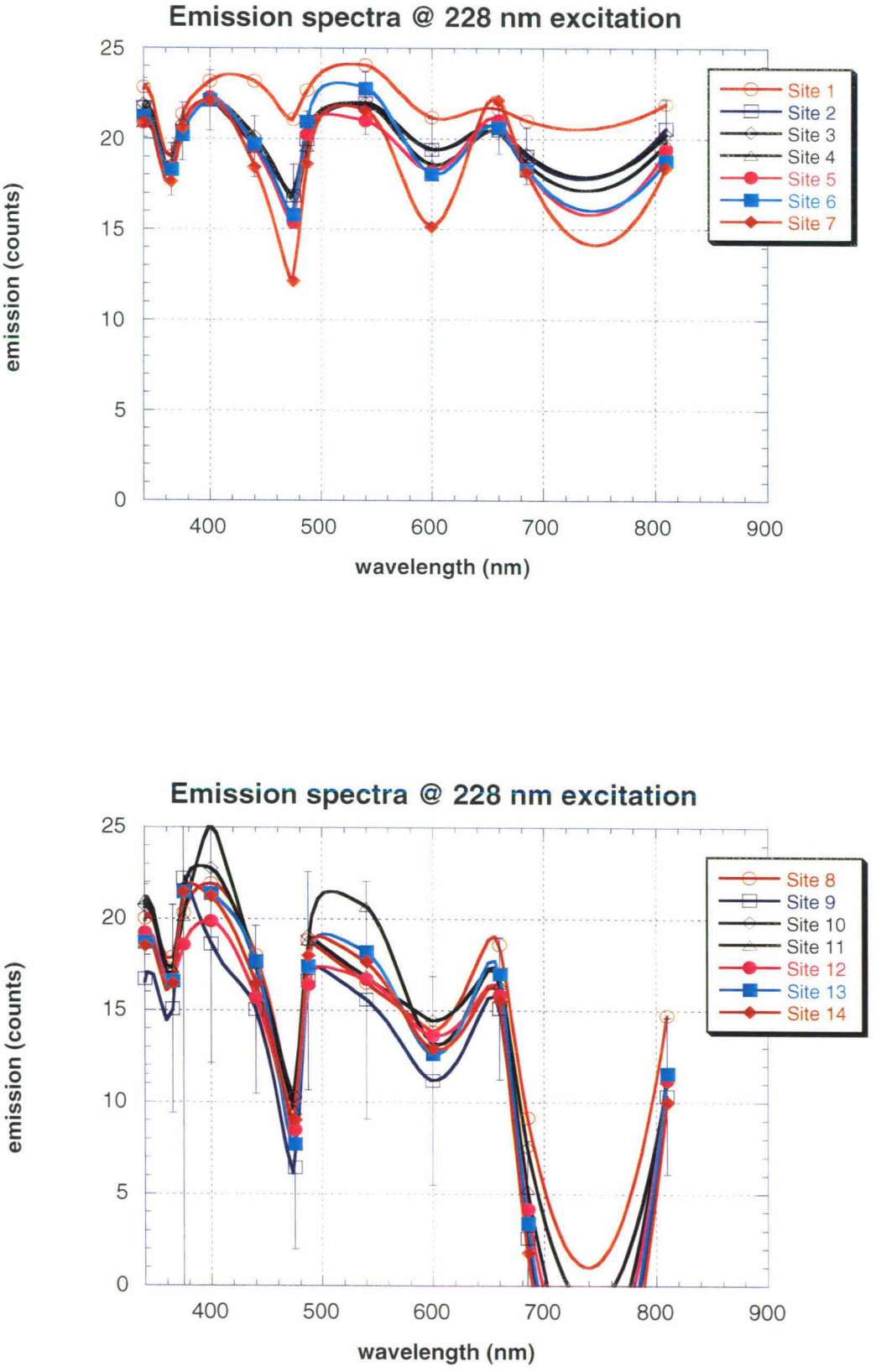

Figure 14. 228 nm emission spectra

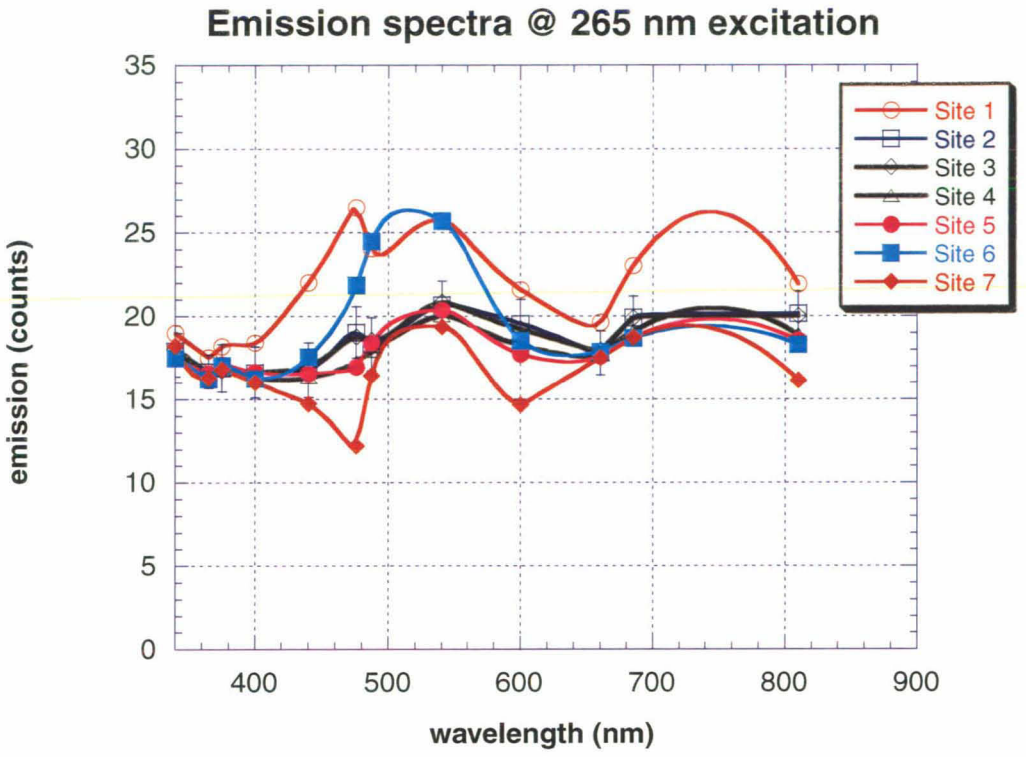

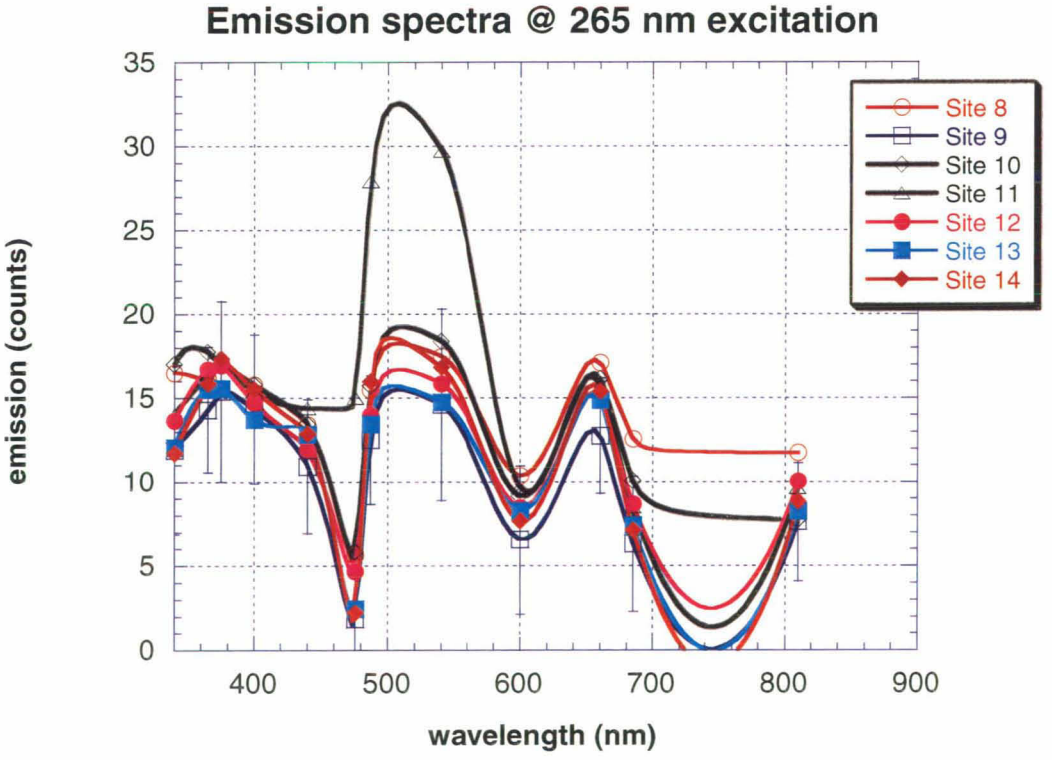

Figure 15. 265 nm emission spectra

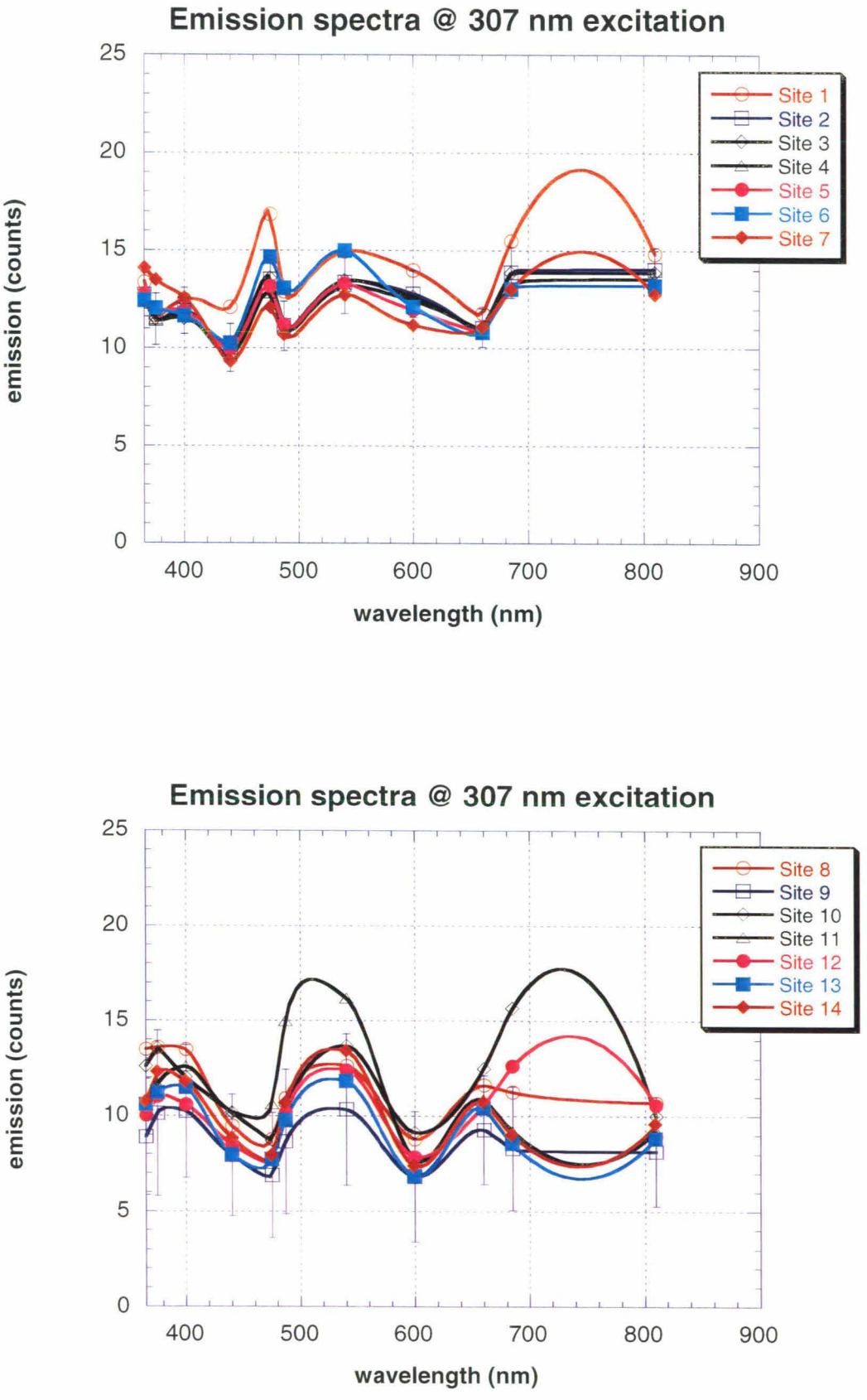

Figure 16. 307 nm emission spectra

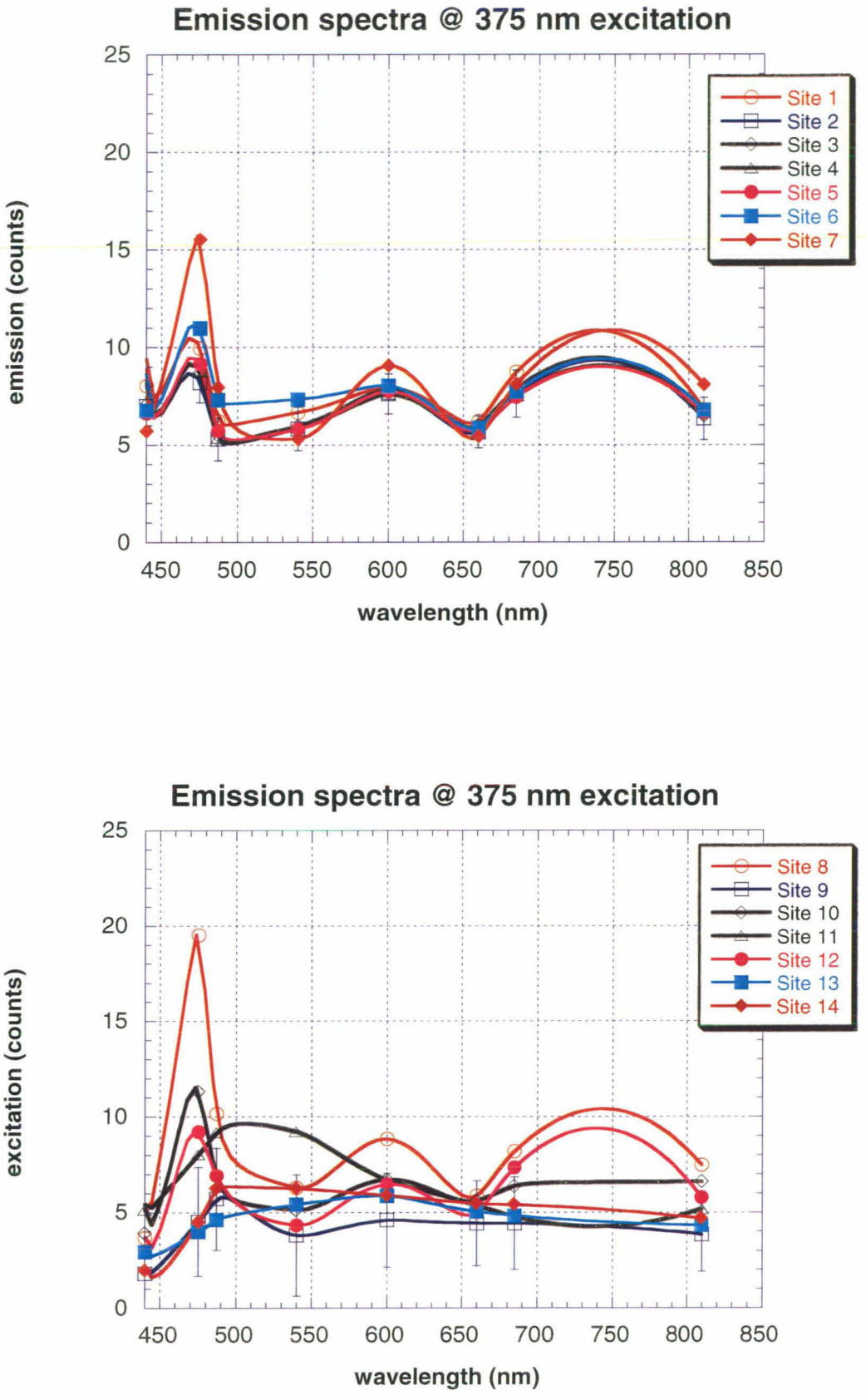

Figure 17. 375 nm emission spectra

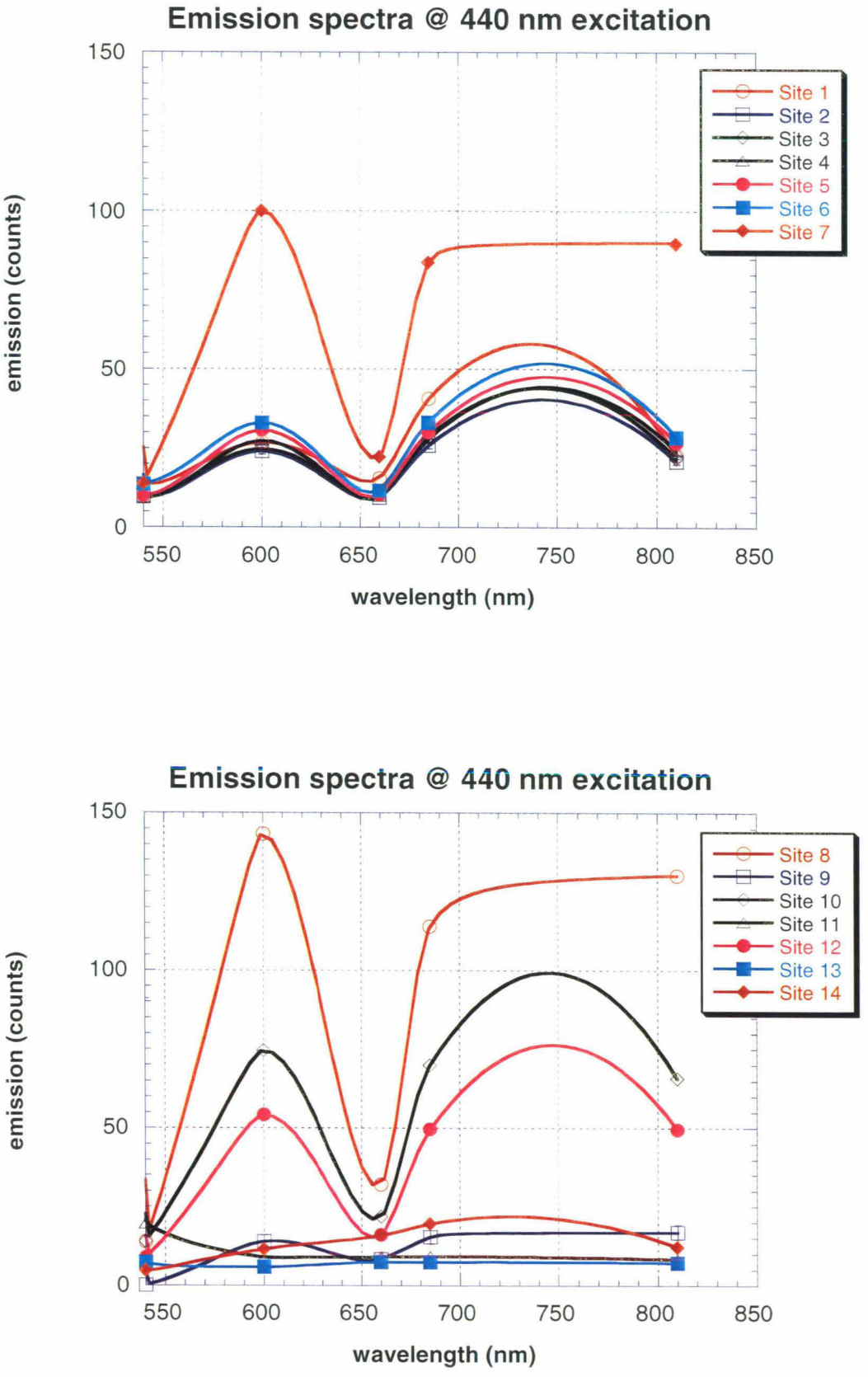

Figure 18. 440 nm emission spectra

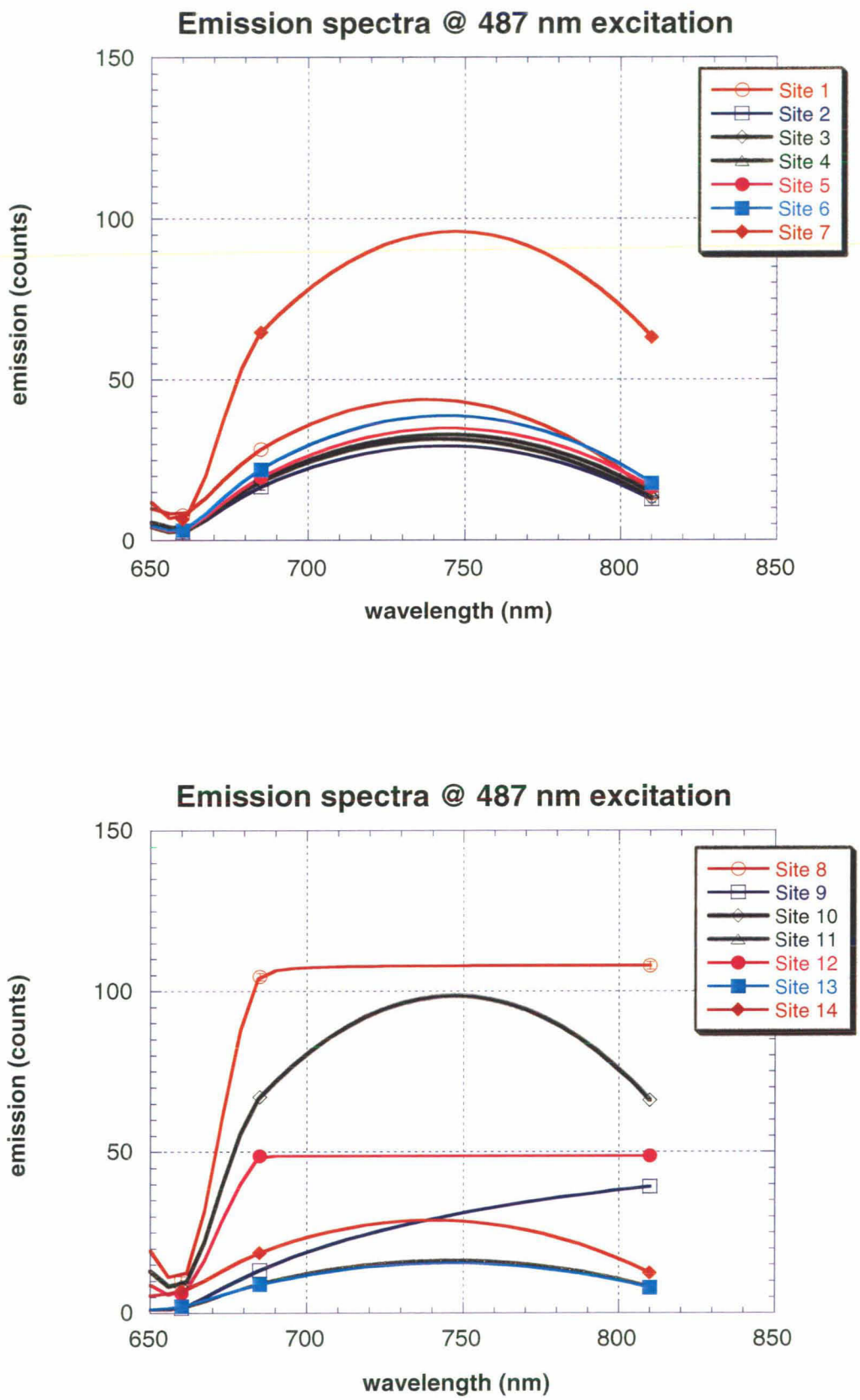

Figure 19. 487 nm emission spectra

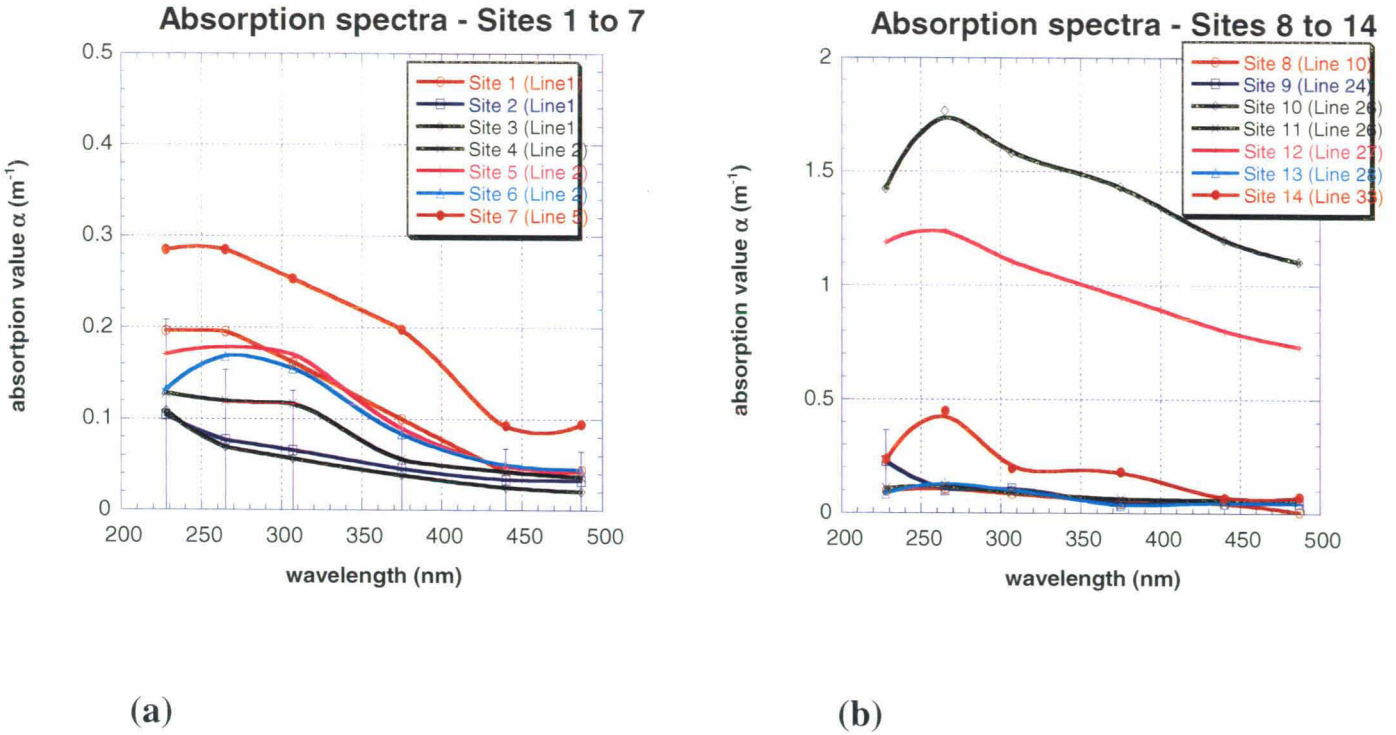

(a) (b)

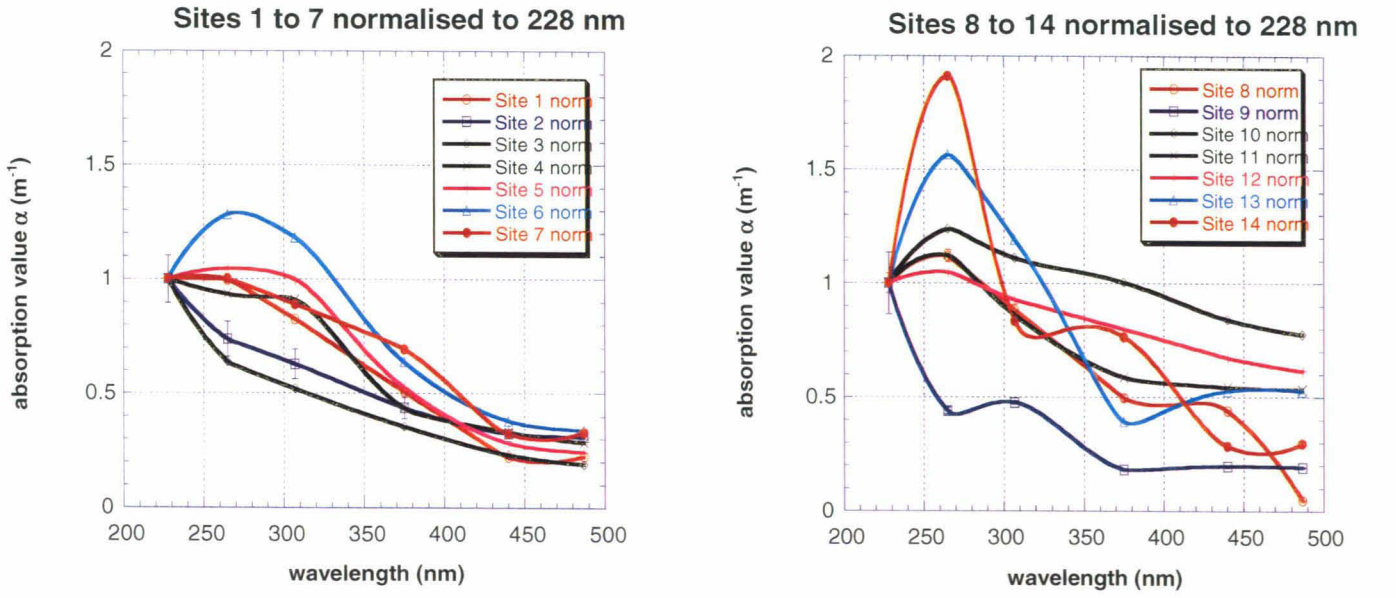

(c) (d)

Figure 20. Absorption spectra

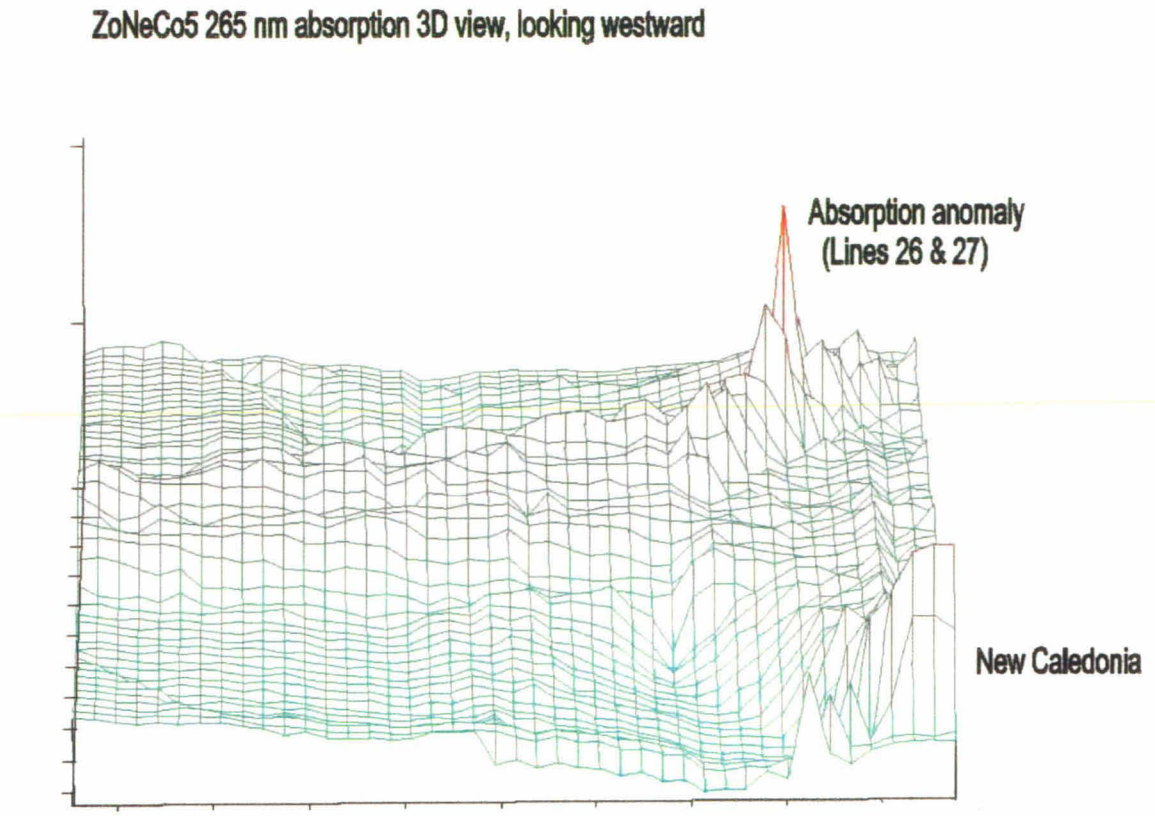

(a)

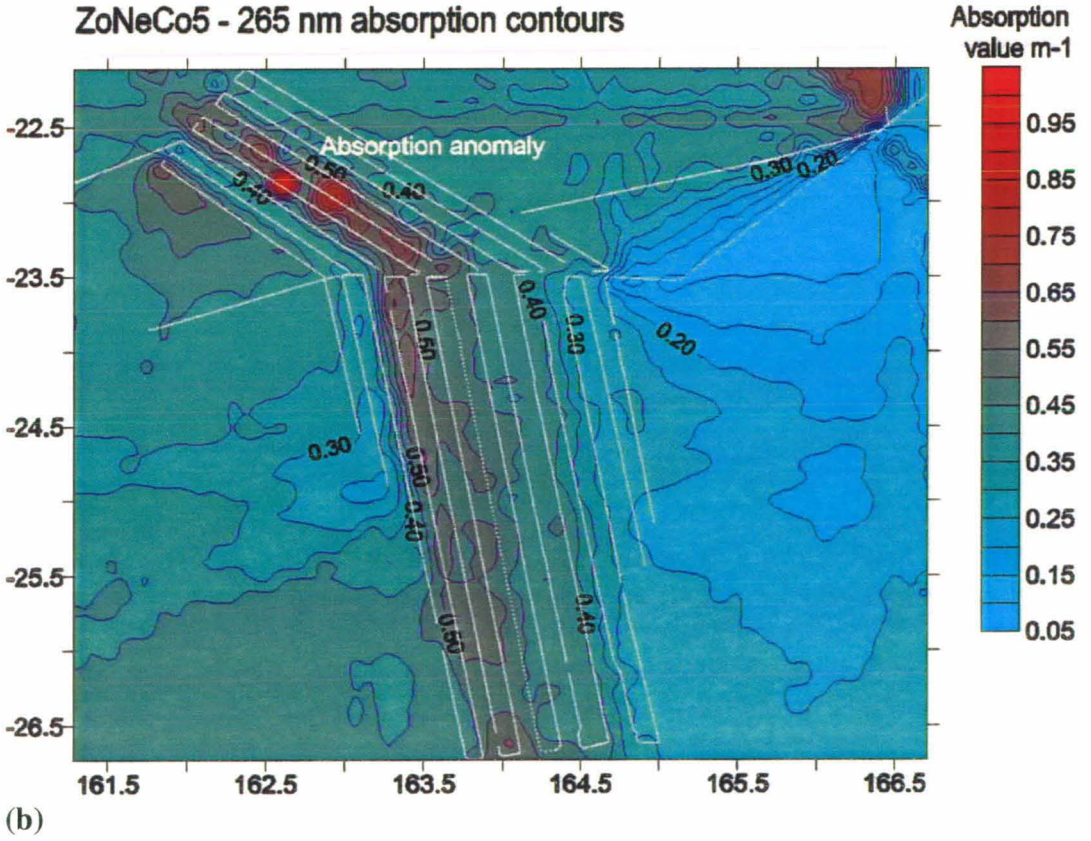

(b)

Figure 21. Absorption contour map of survey area

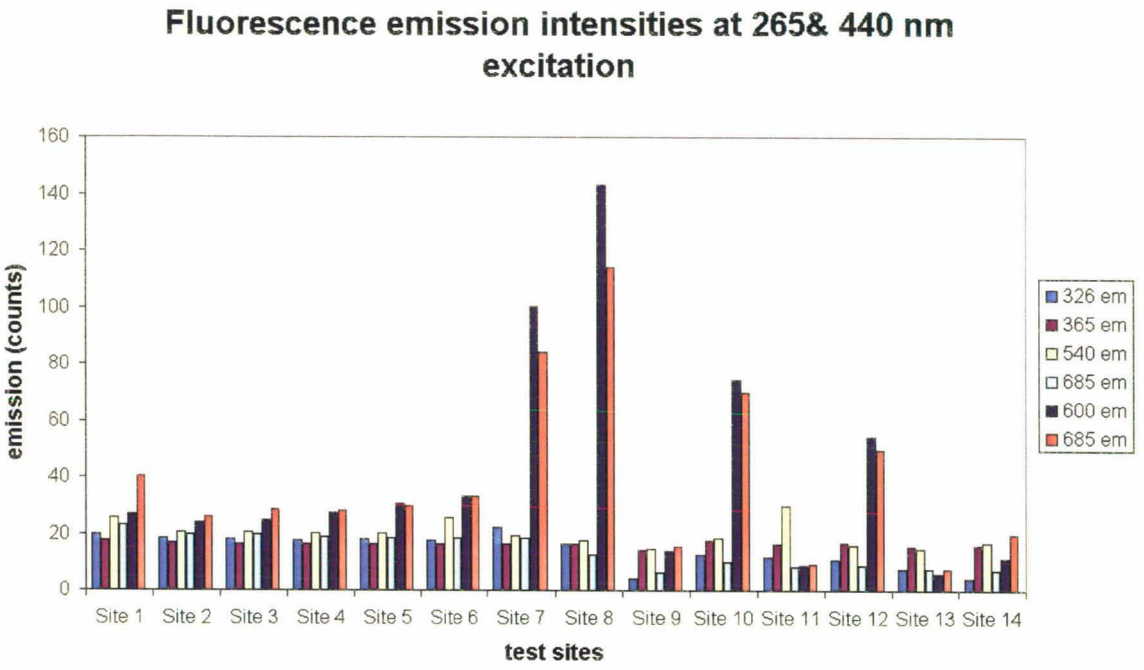

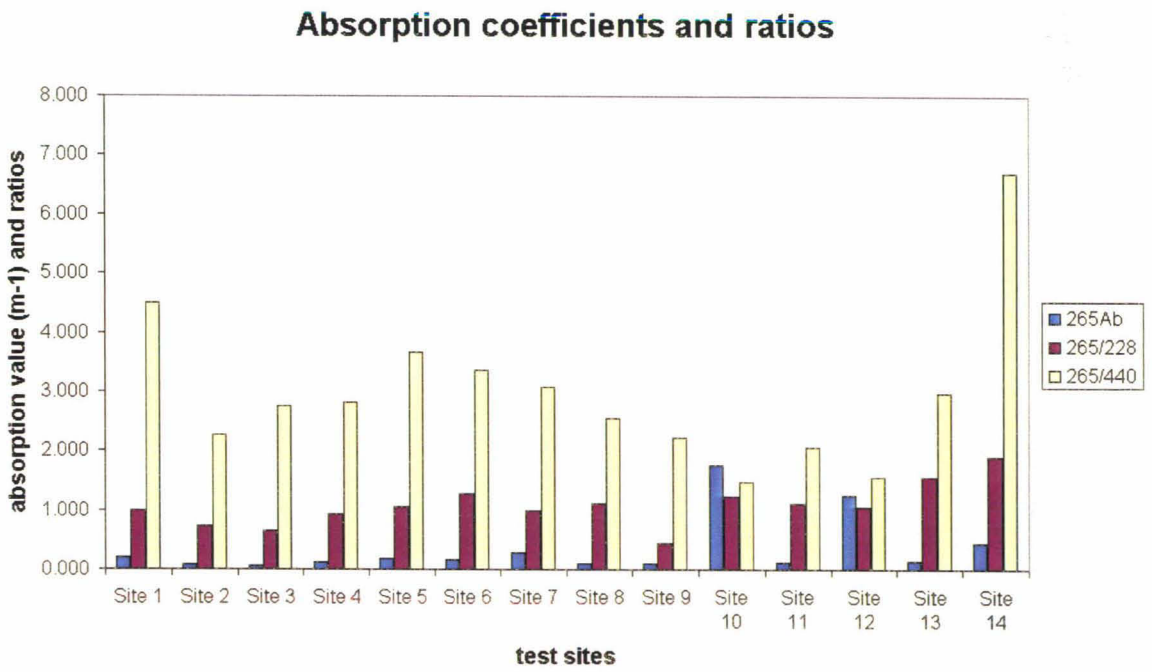

Figure 22. Fluorescence and absorption intensities at each test site

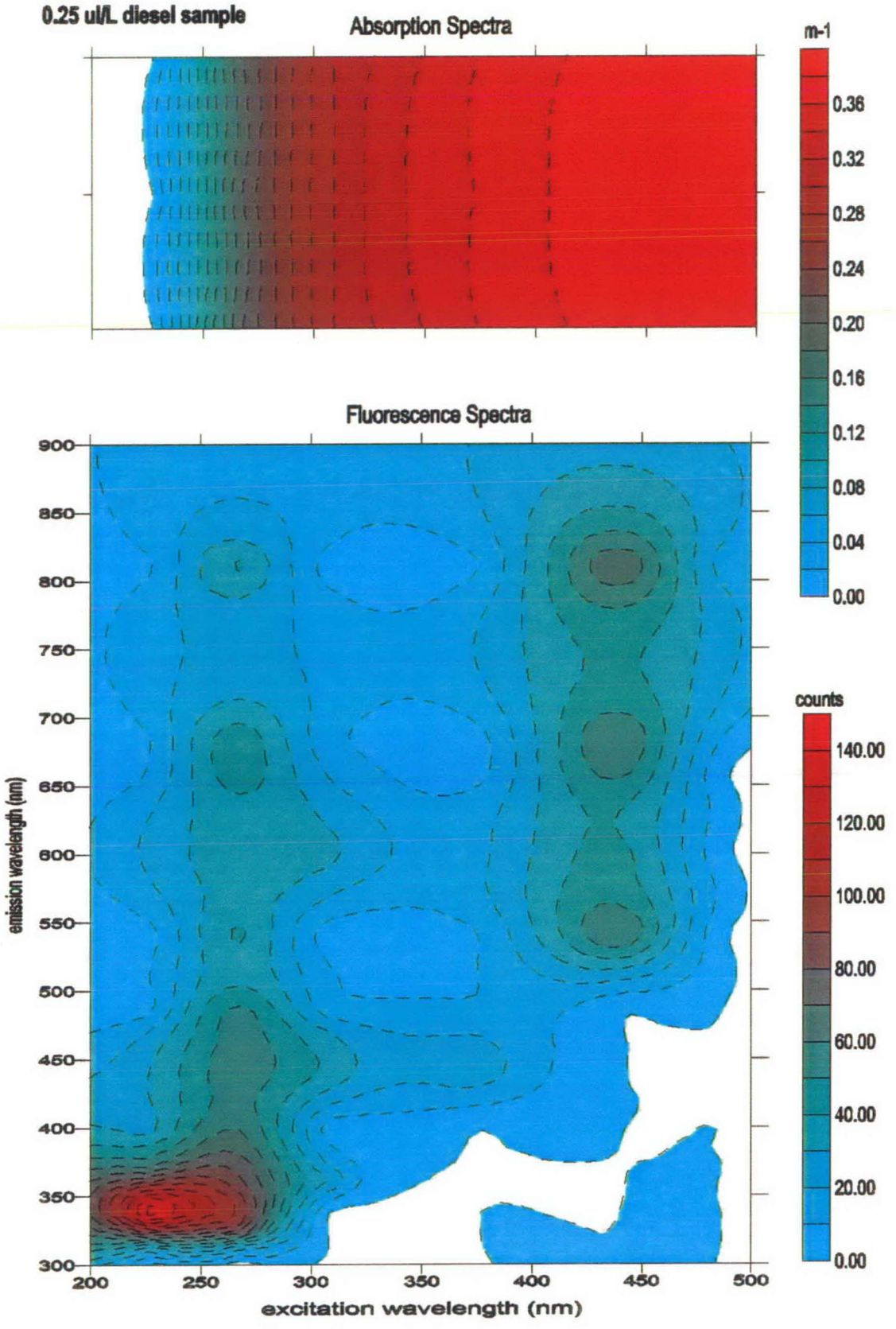

Figure 23. Diesel 3D spectra (0.25 ul/L)

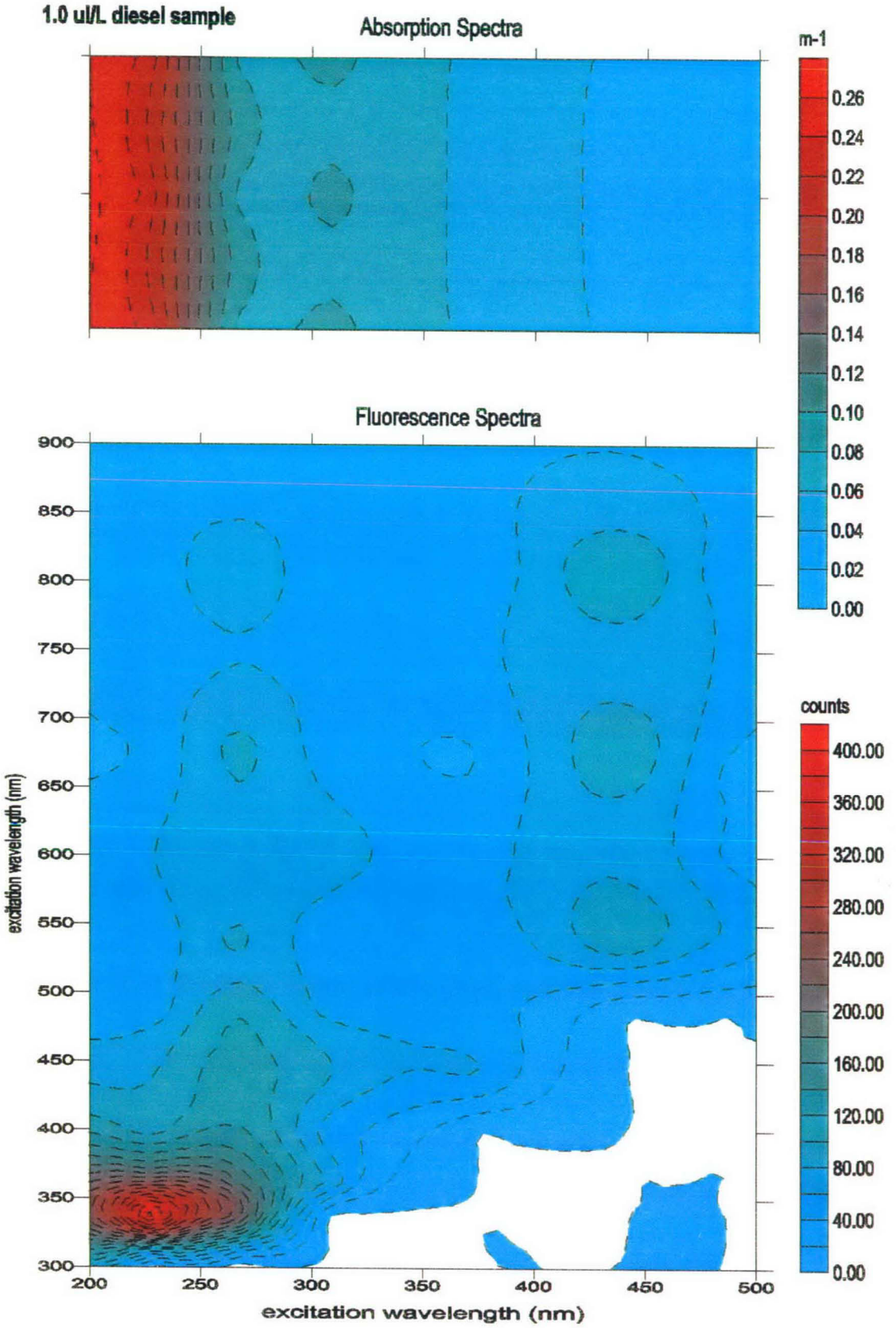

Figure 24. Diesel 3D spectra (1.0 ul/L)

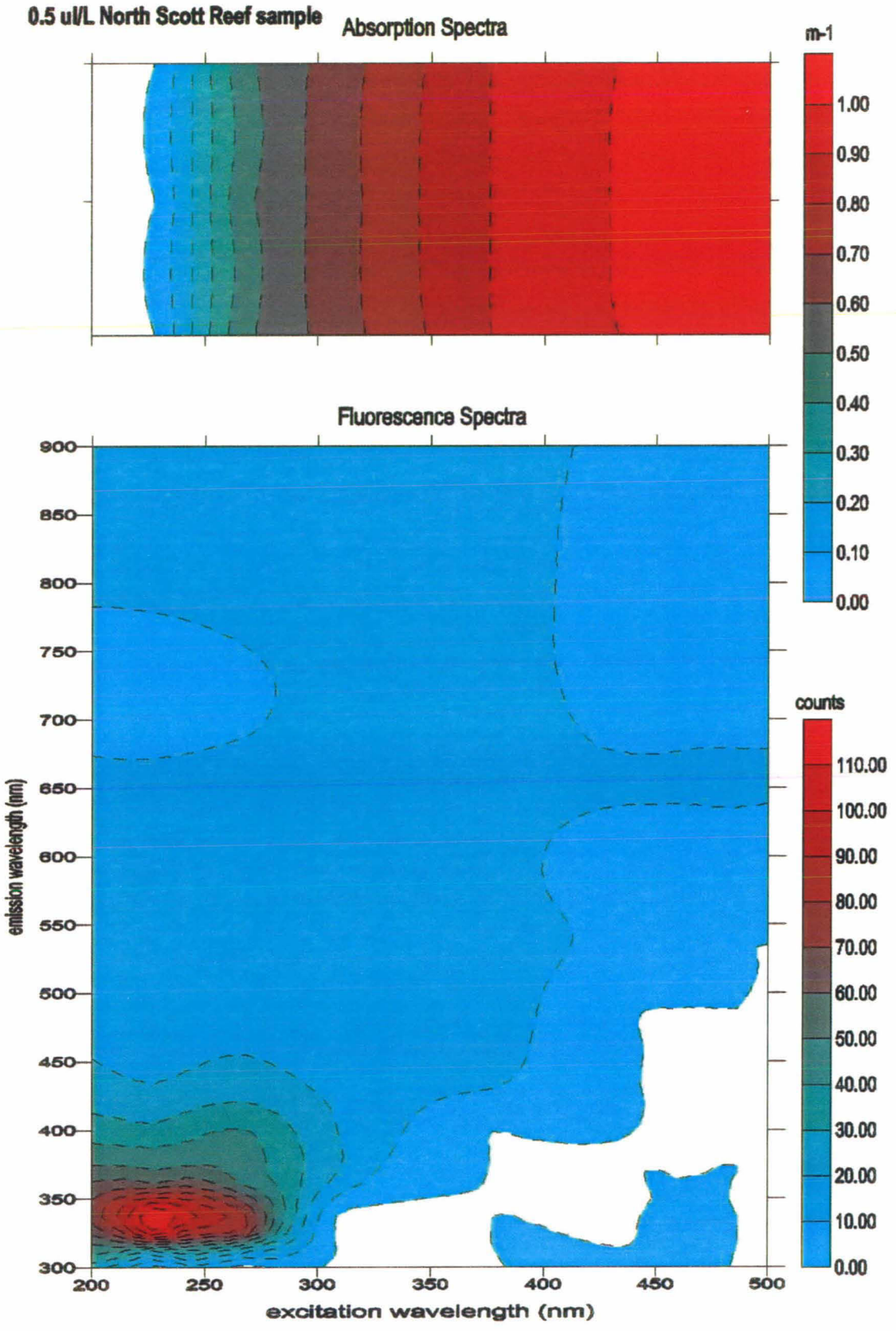

Figure 25. North Scott Reef 3D spectra (0.5 ul/L)

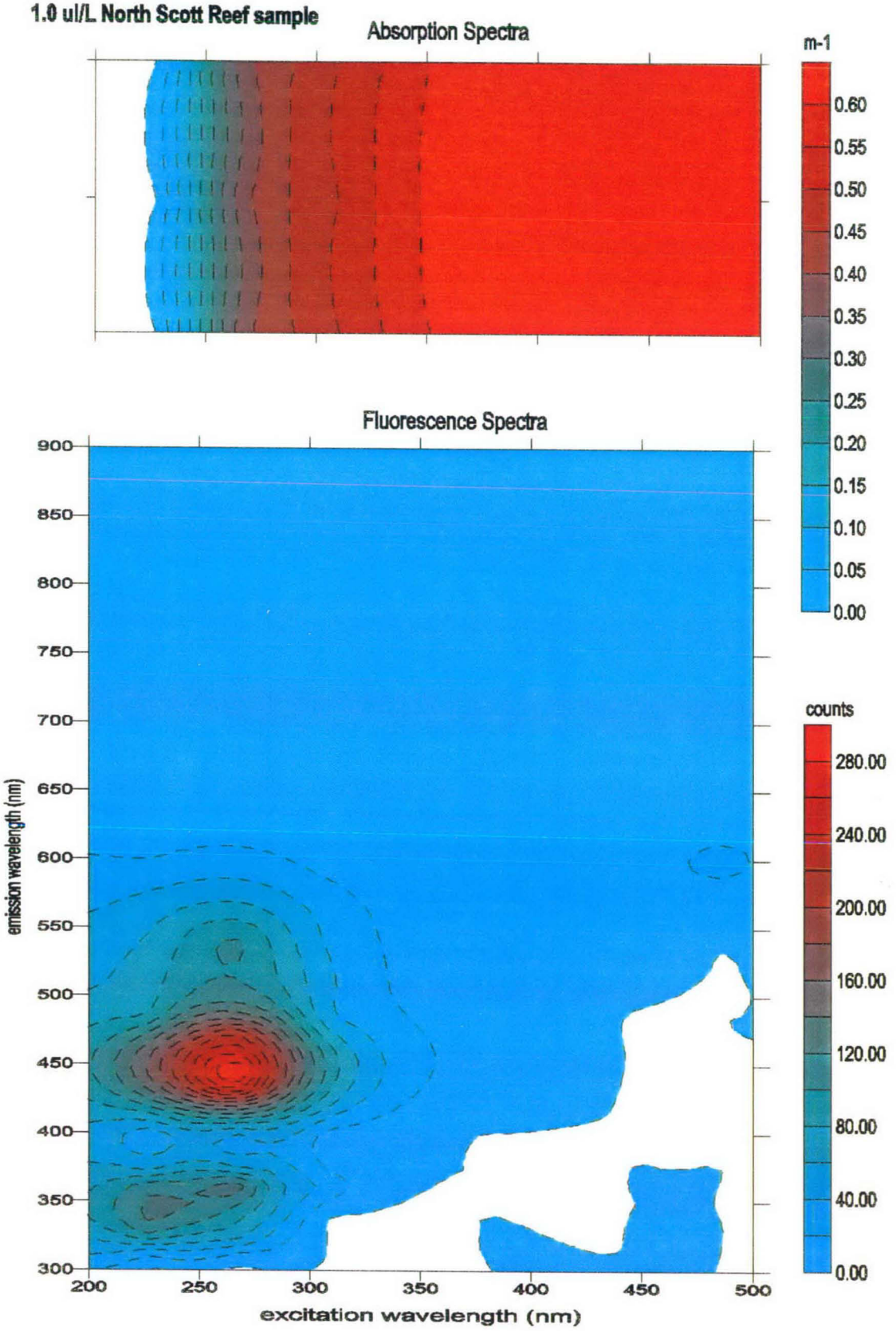

Figure 26. North Scott Reef 3D spectra (1.0 ul/L)

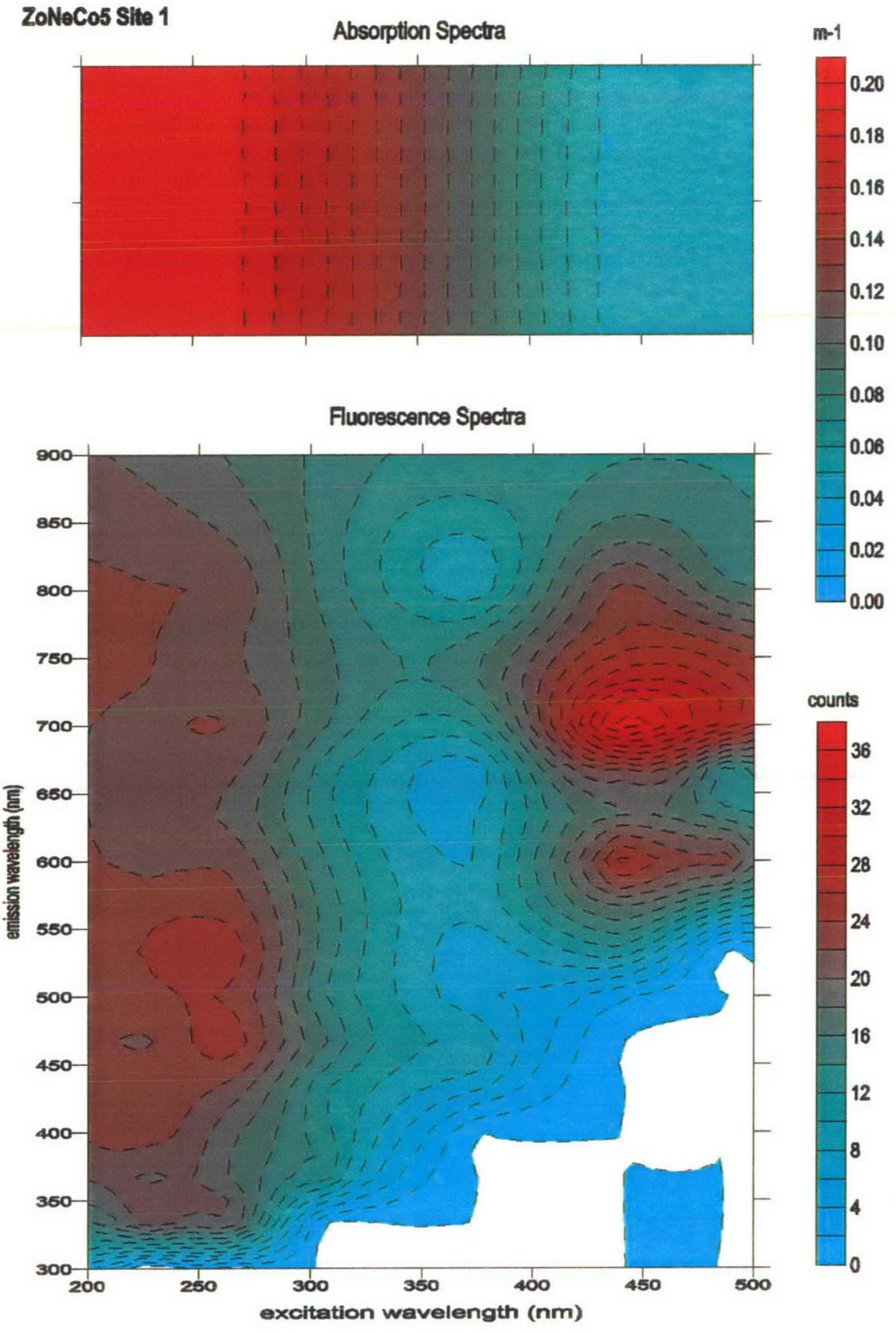

Figure 27. Site 1 - 3D fluorescence and absorption spectra

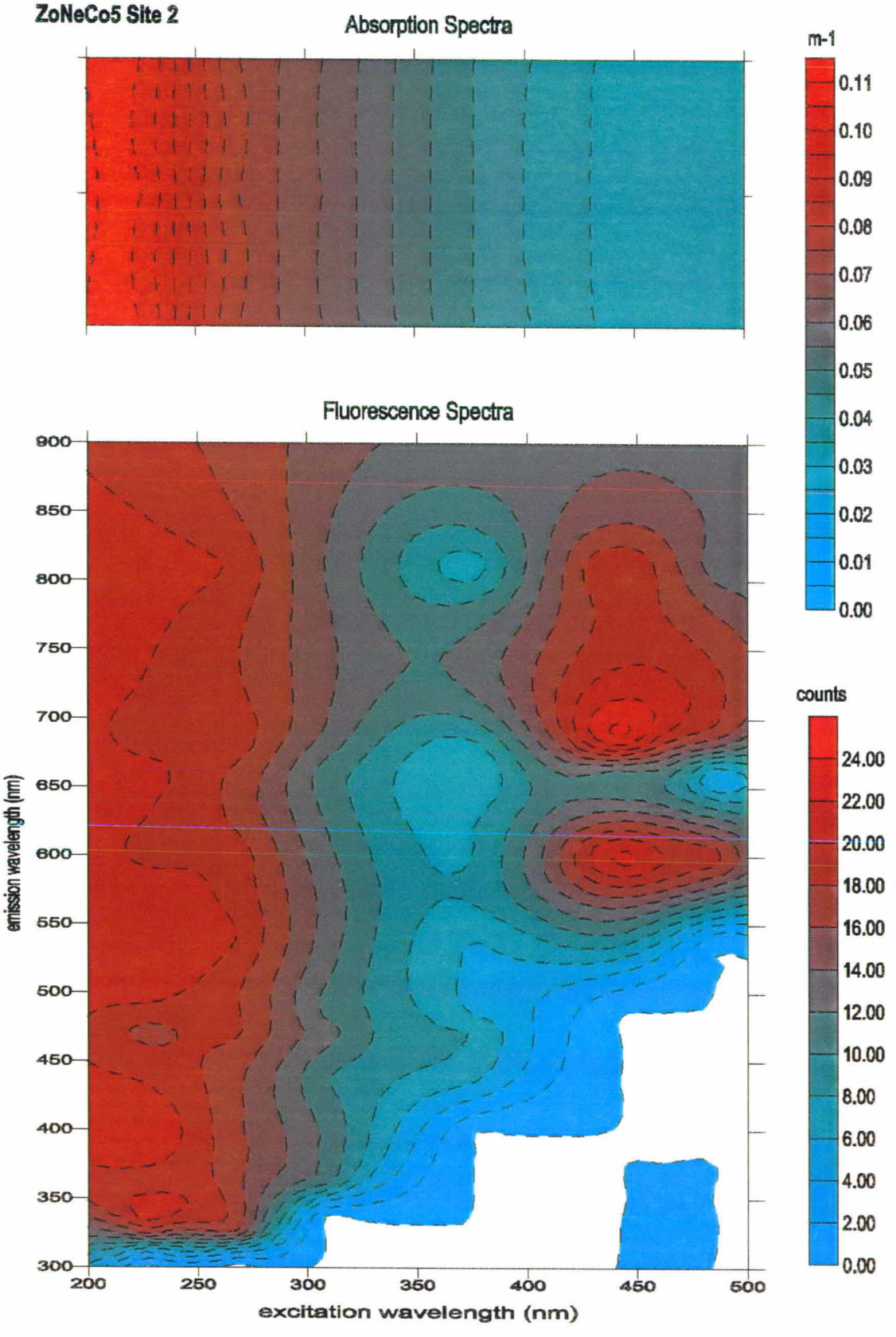

Figure 28. Site 2 - 3D fluorescence and absorption spectra

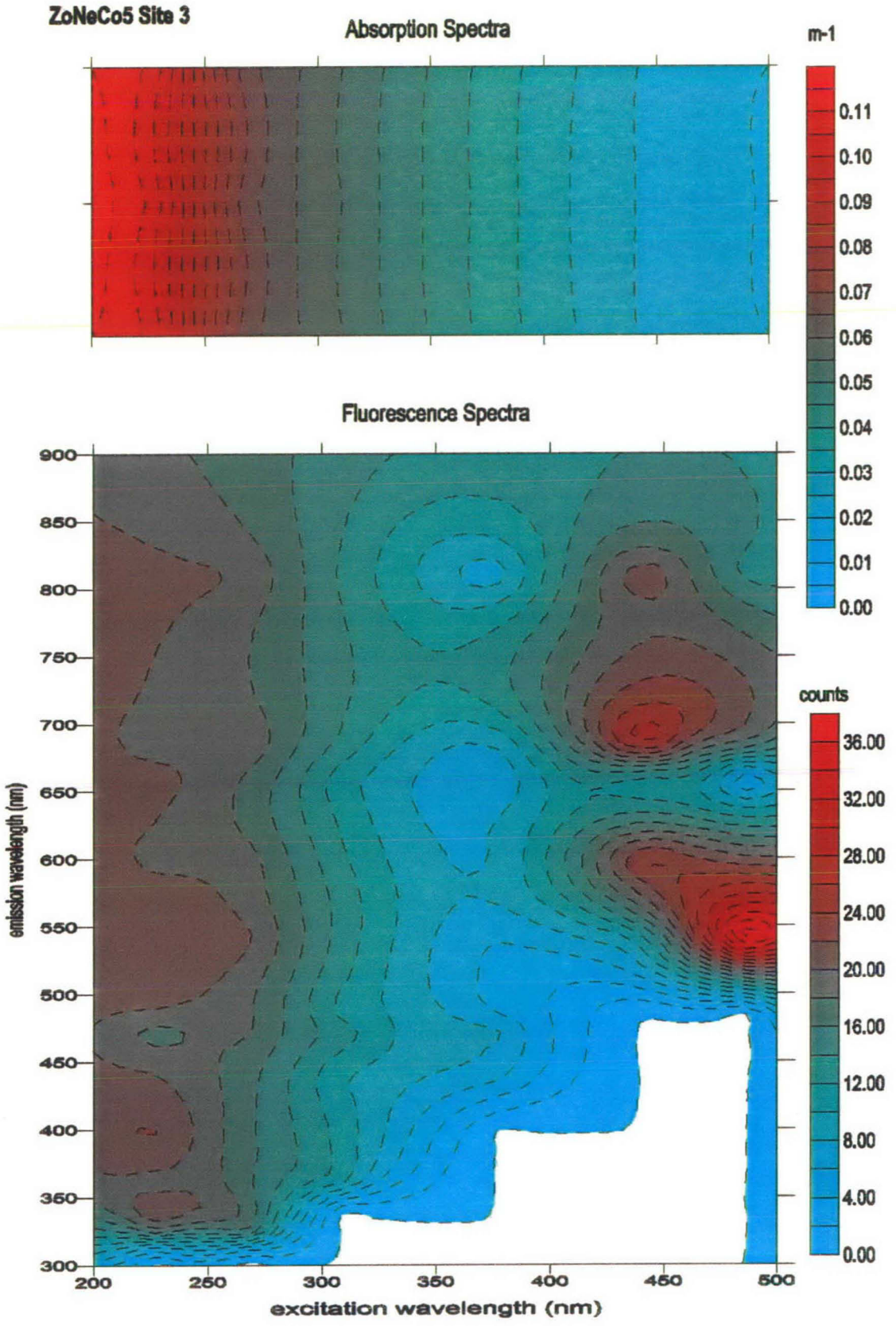

Figure 29. Site 3 - 3D fluorescence and absorption spectra

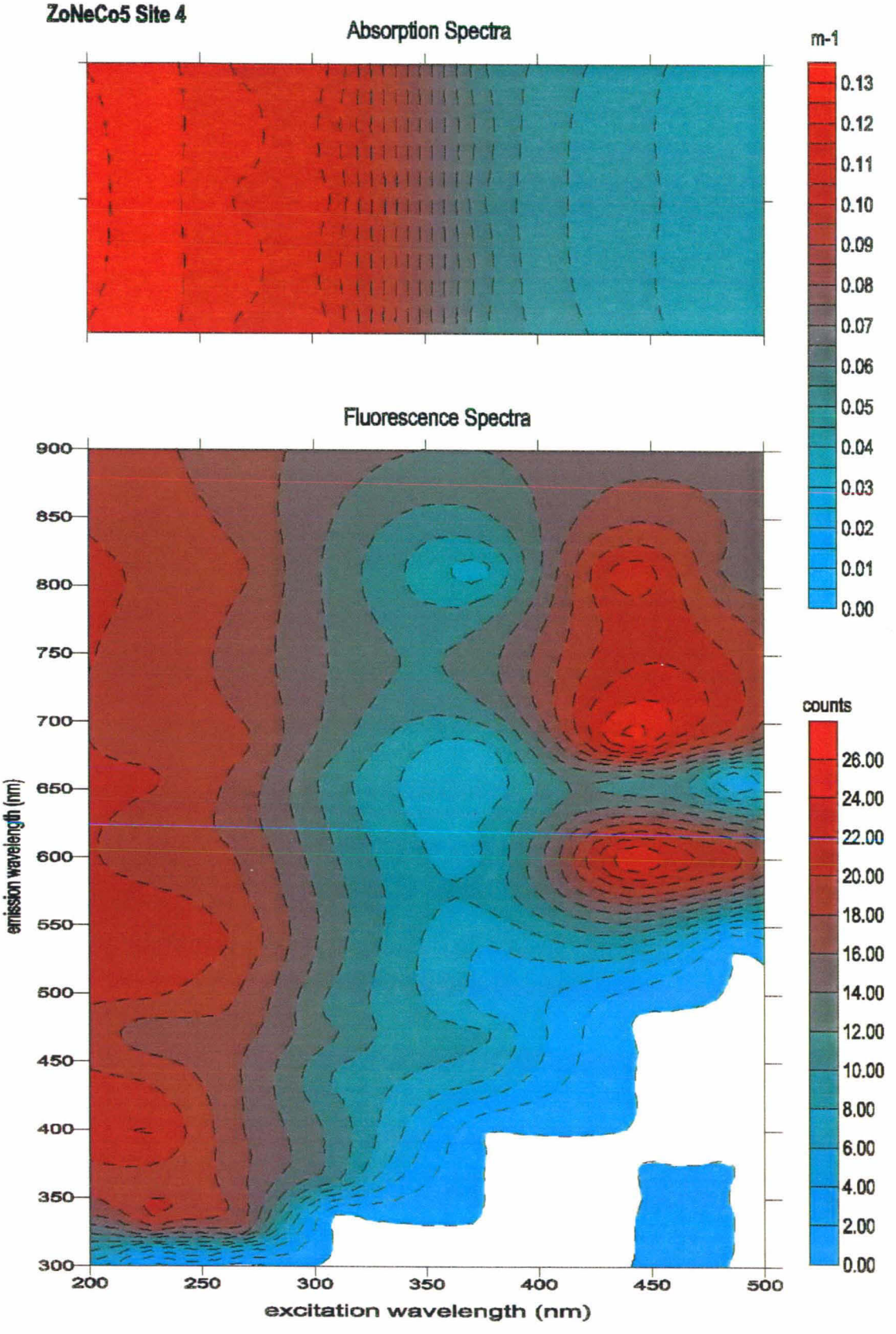

Figure 30. Site 4 - 3D fluorescence and absorption spectra

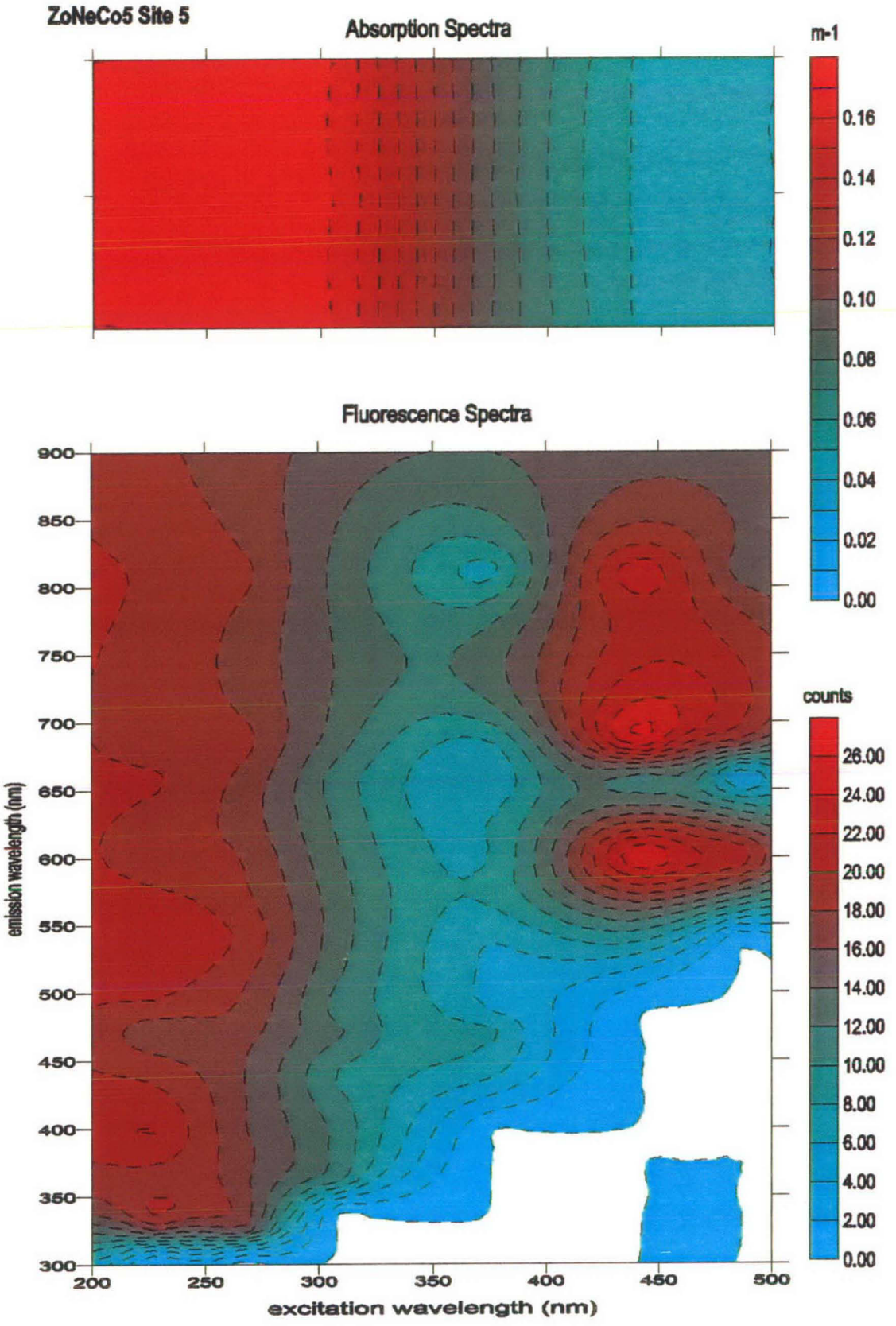

Figure 31. Site 5 - 3D fluorescence and absorption spectra

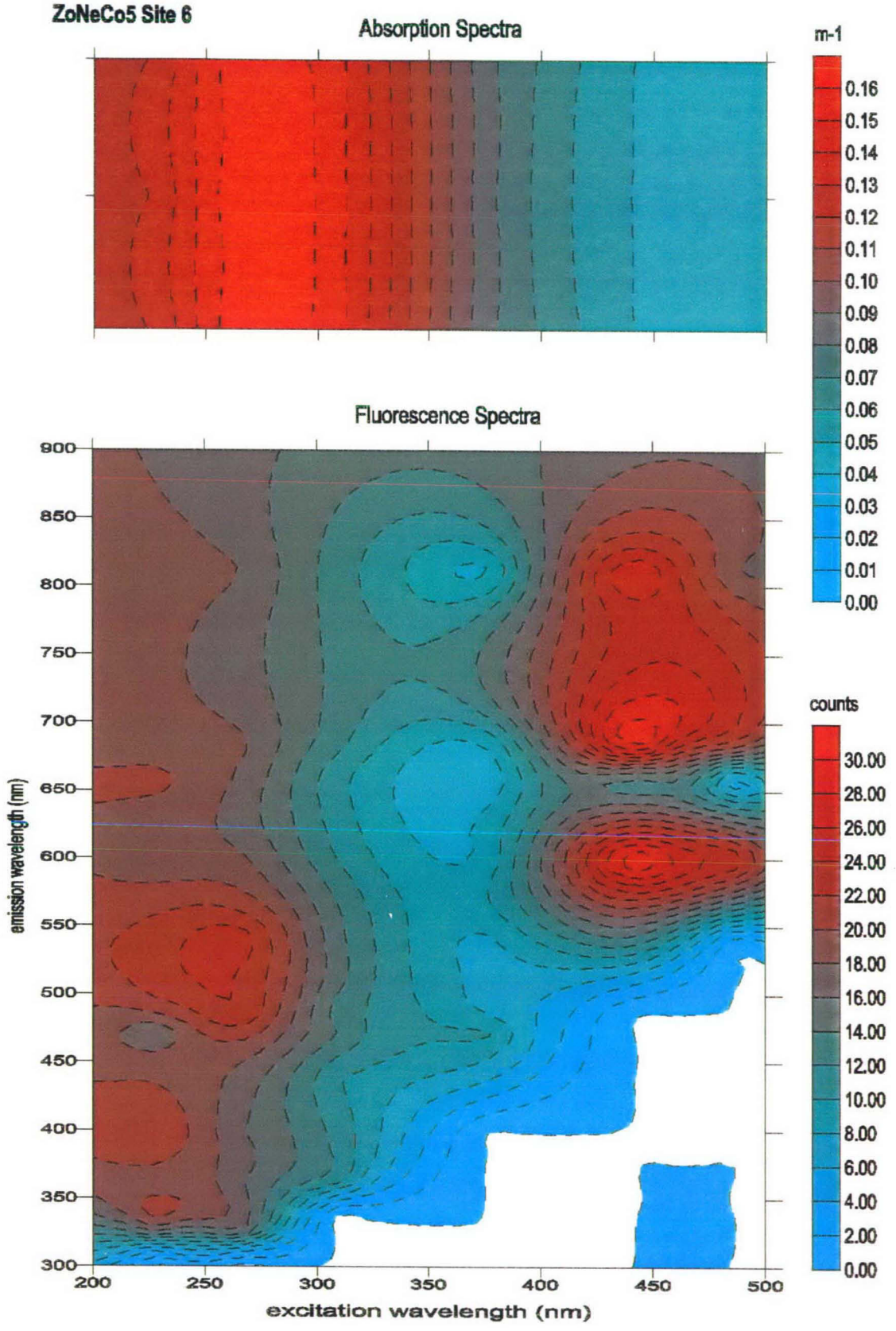

Figure 32. Site 6 - 3D fluorescence and absorption spectra

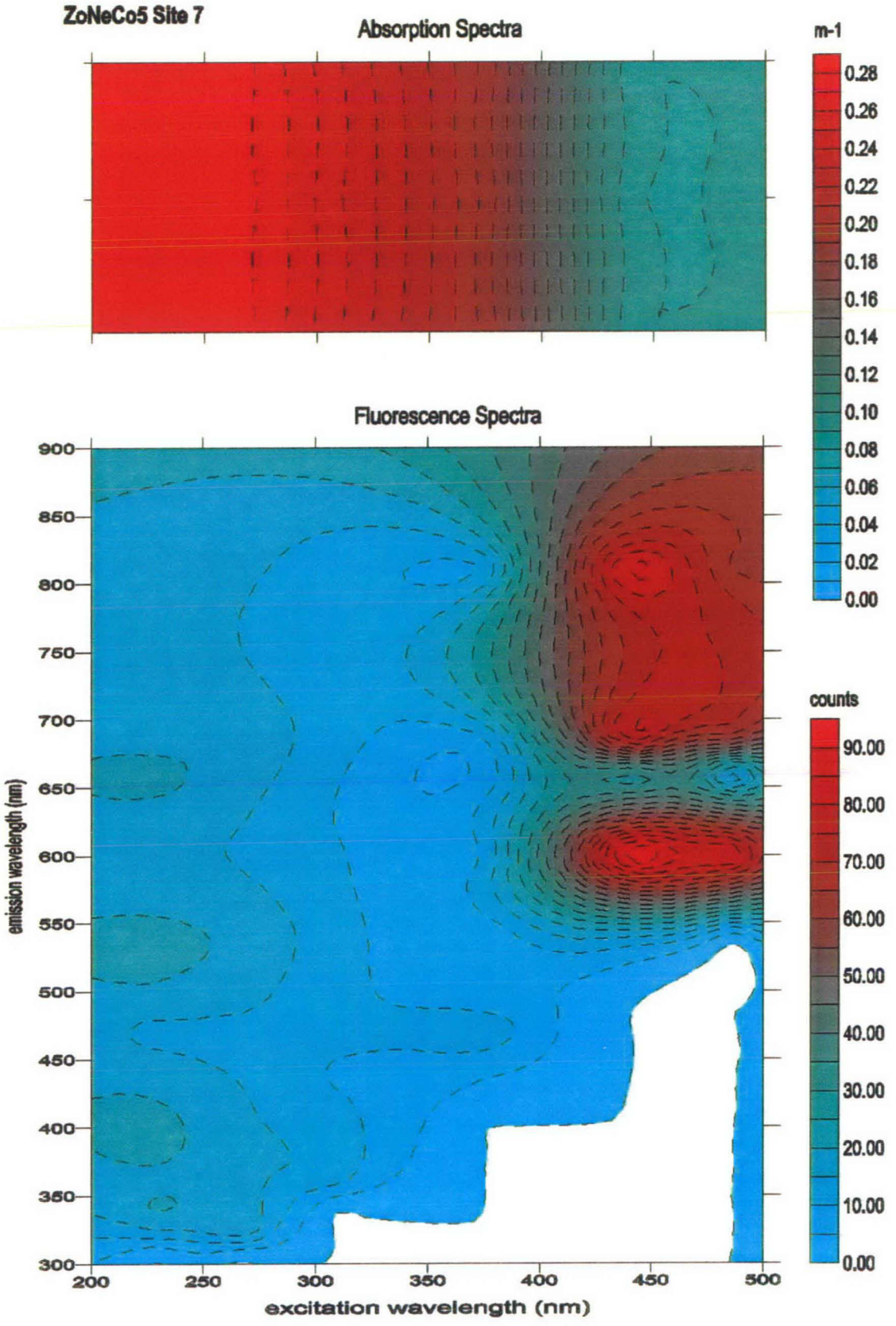

Figure 33. Site 7 - 3D fluorescence and absorption spectra

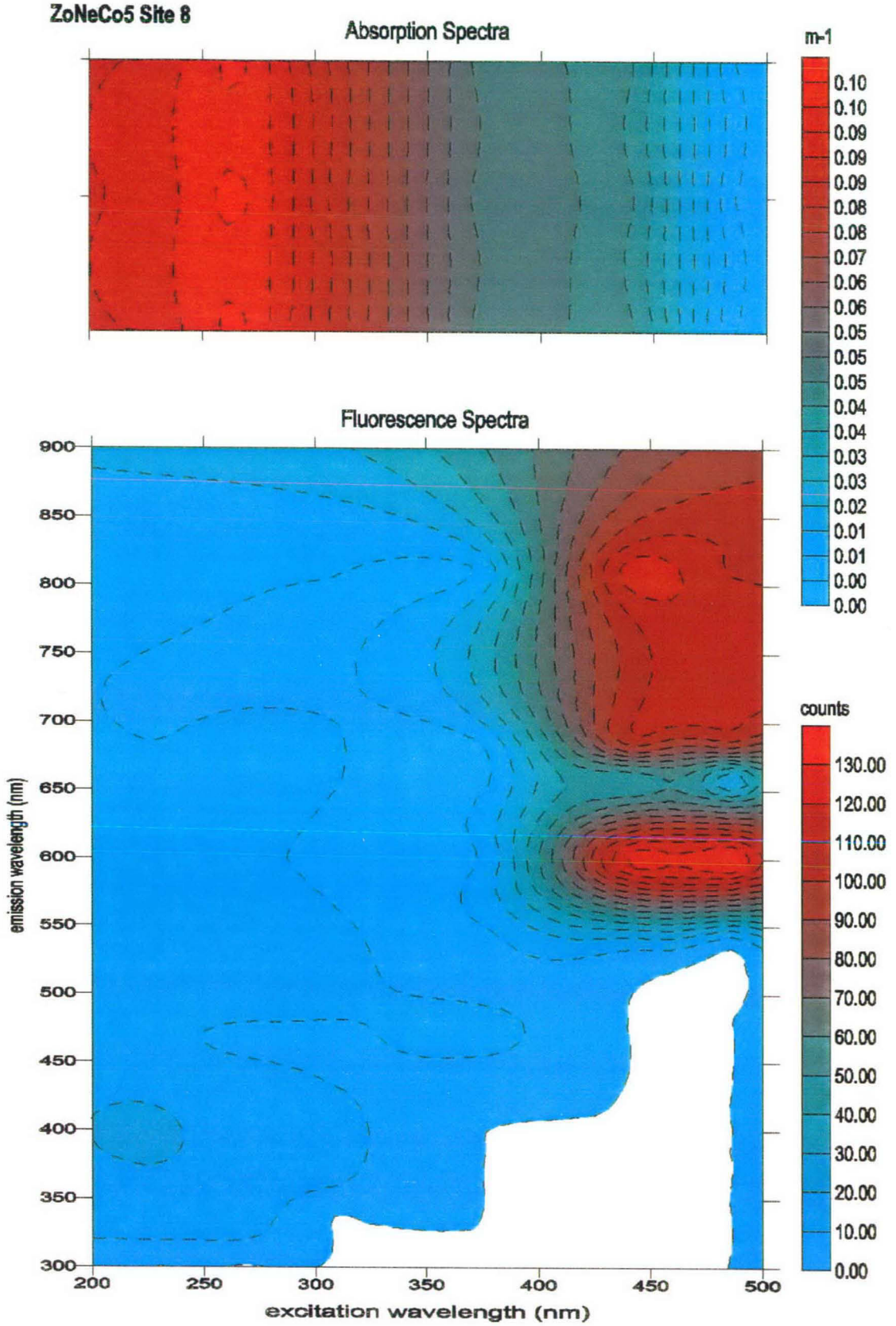

Figure 34. Site 8 - 3D fluorescence and absorption spectra

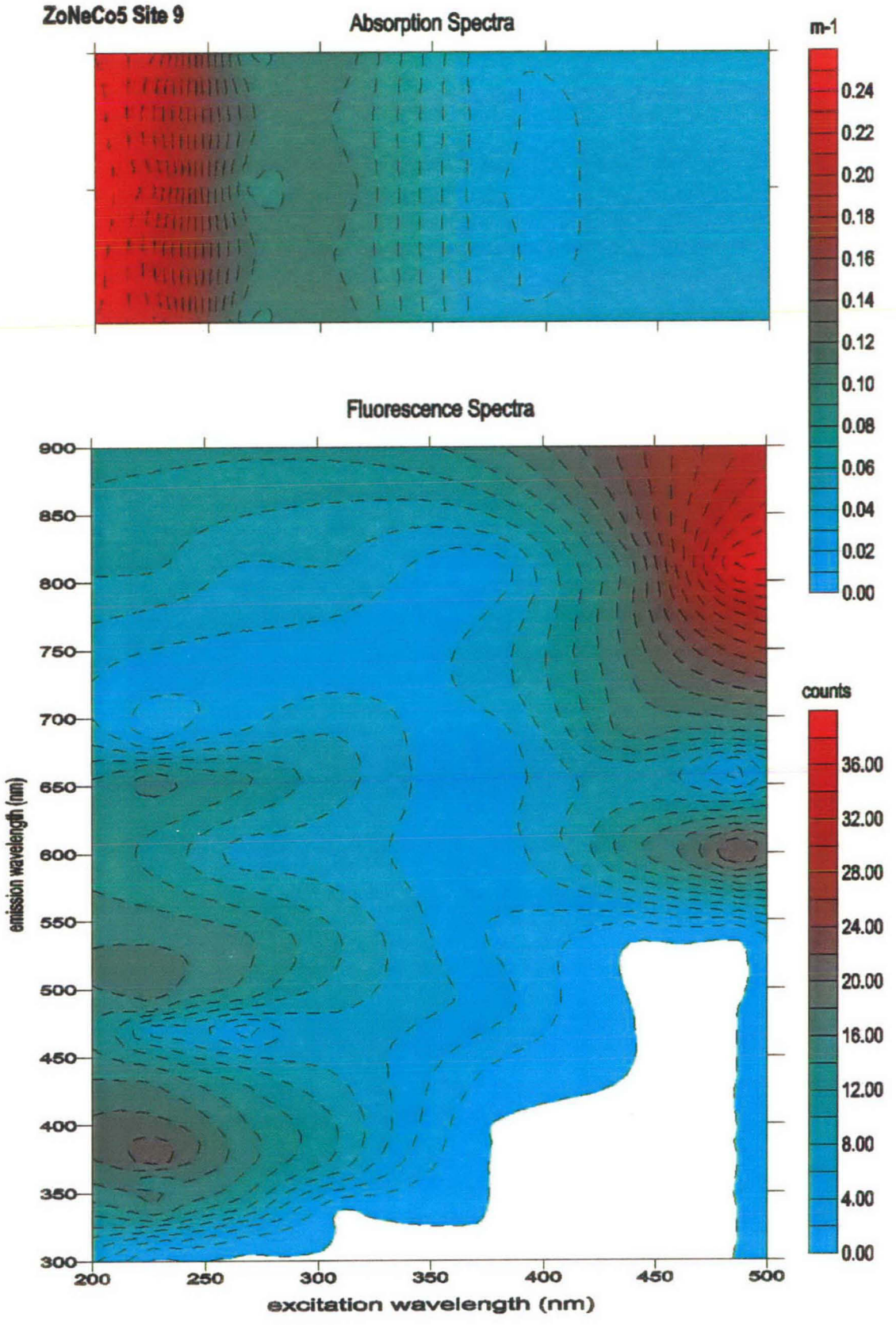

Figure 35. Site 9 - 3D fluorescence and absorption spectra

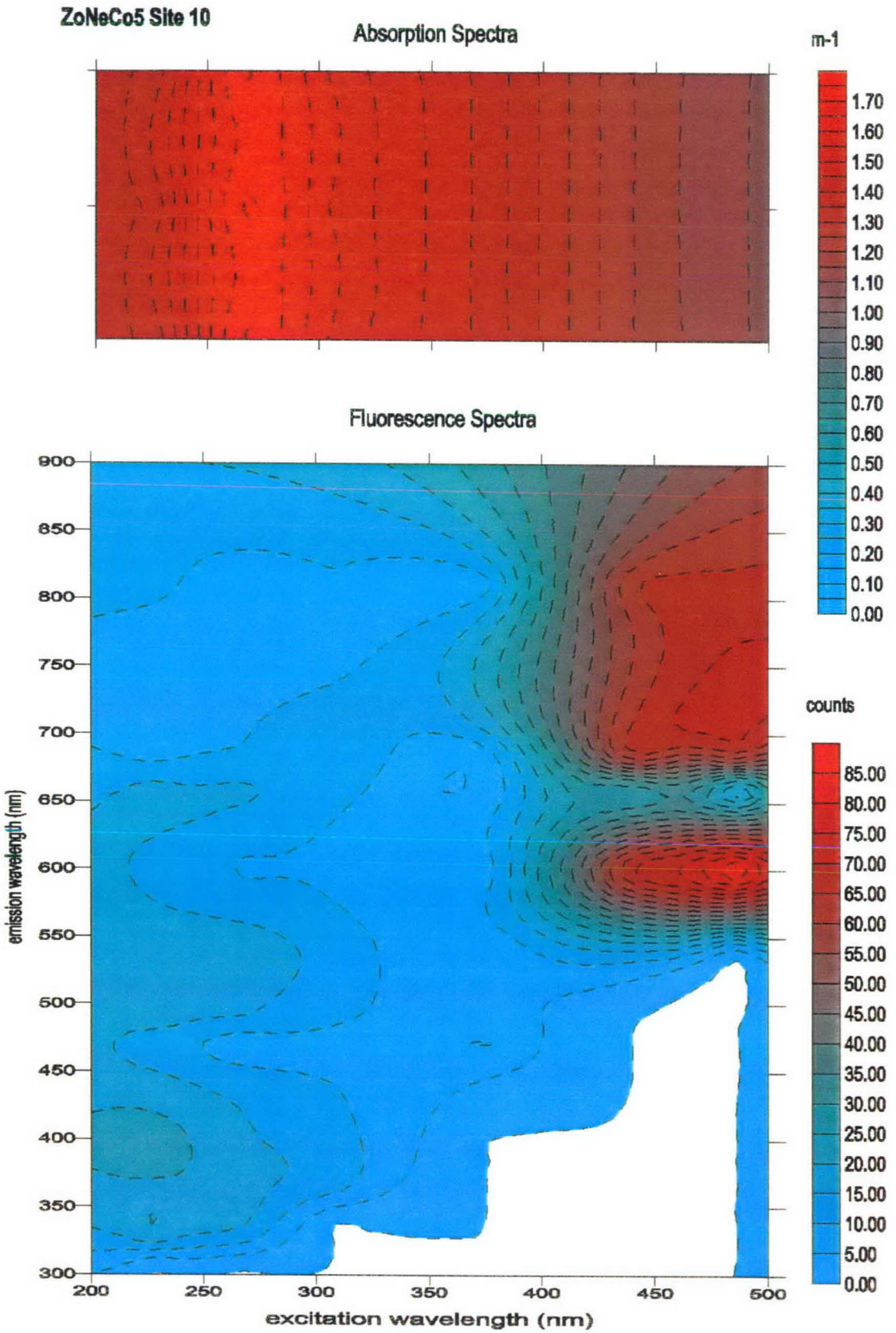

Figure 36. Site 10 - 3D fluorescence and absorption spectra

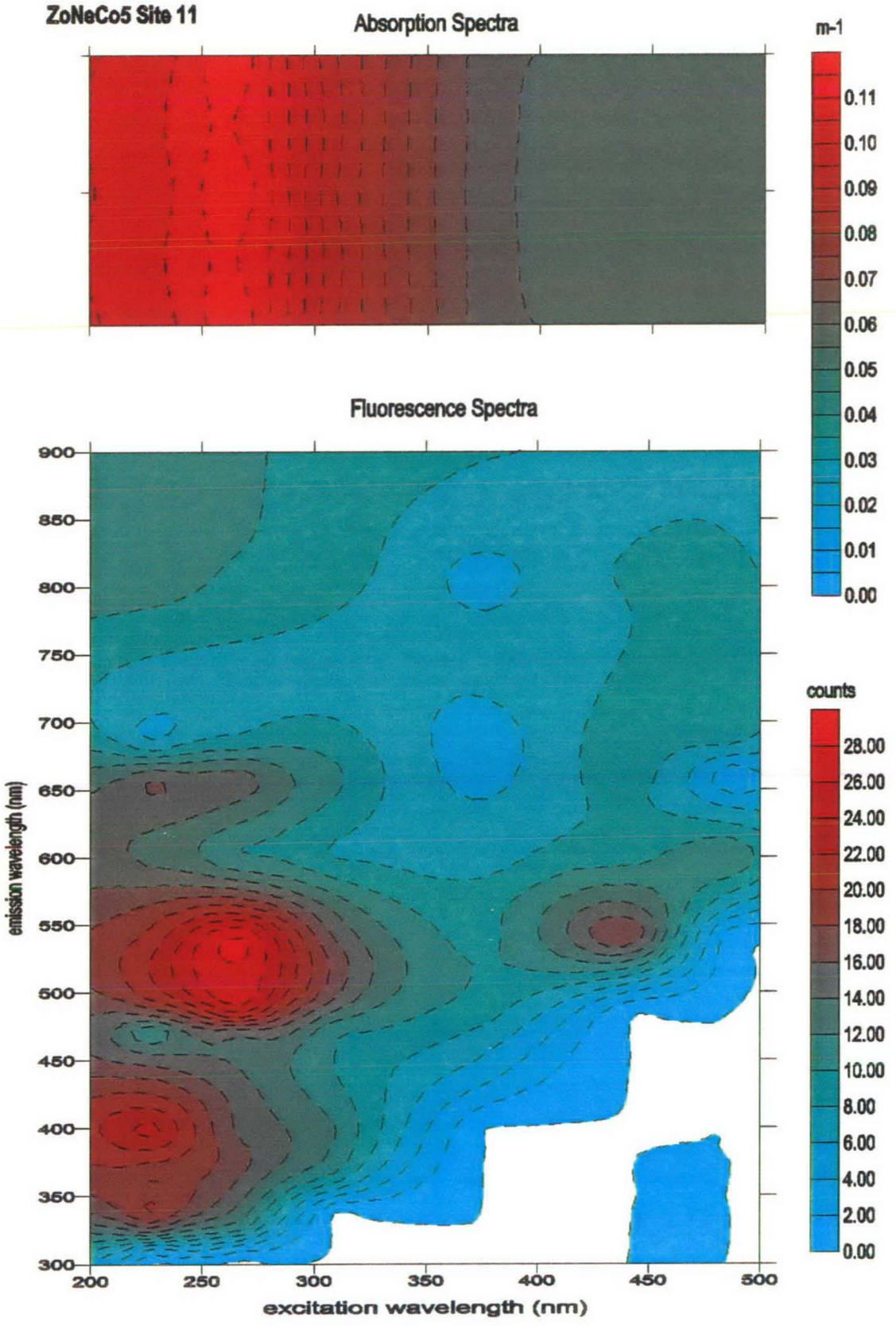

Figure 37. Site 11 - 3D fluorescence and absorption spectra

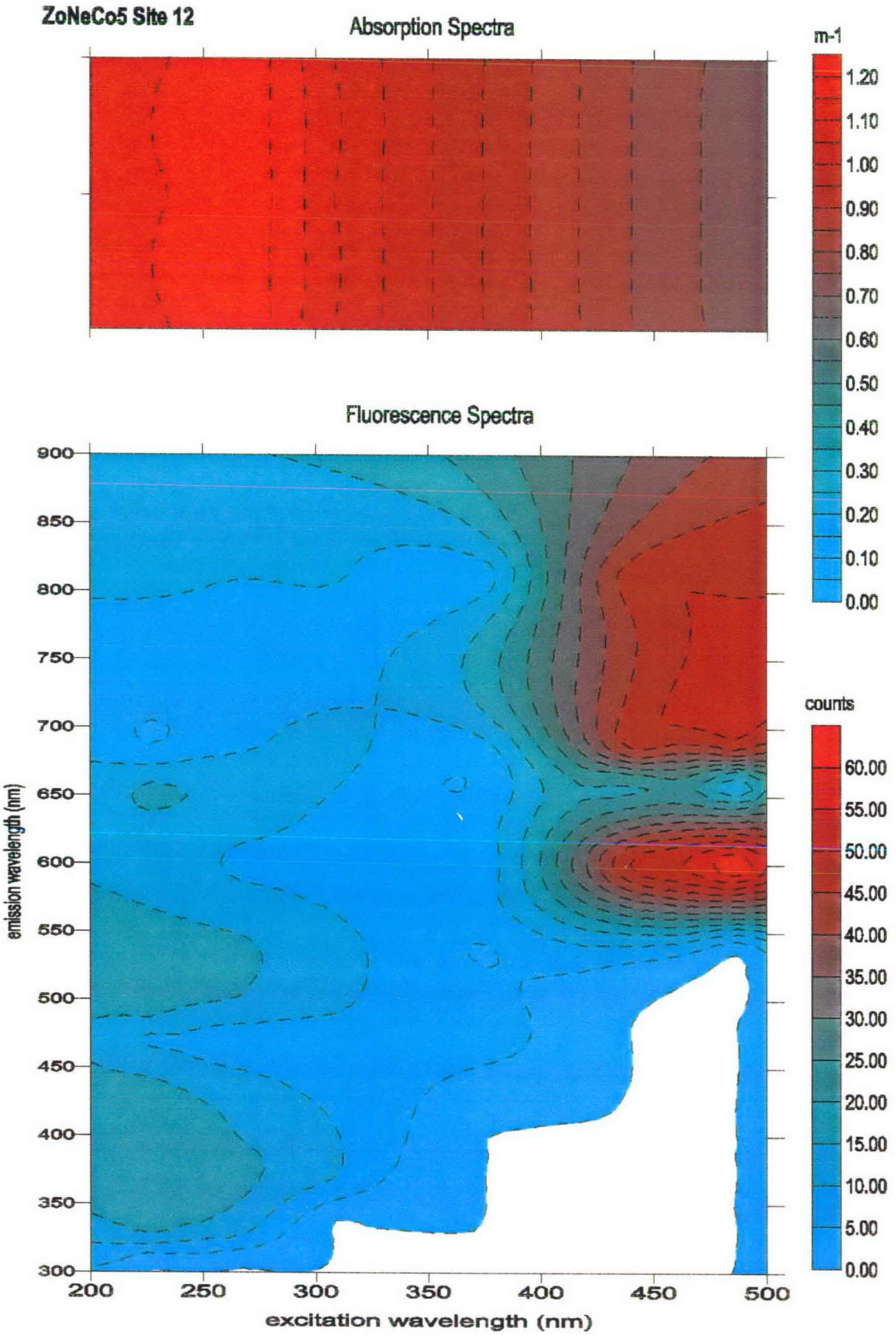

Figure 38. Site 12 - 3D fluorescence and absorption spectra

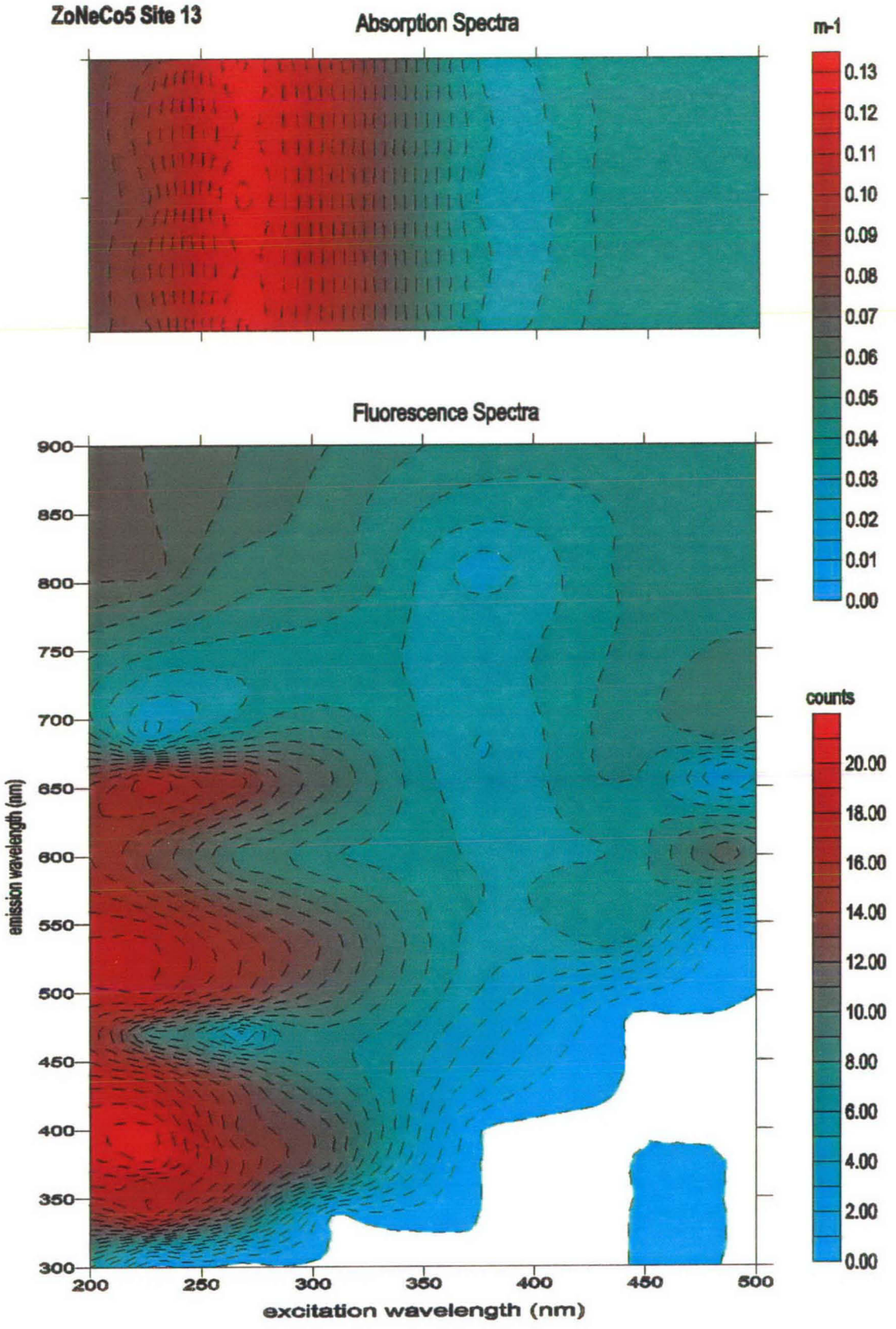

Figure 39. Site 13 - 3D fluorescence and absorption spectra

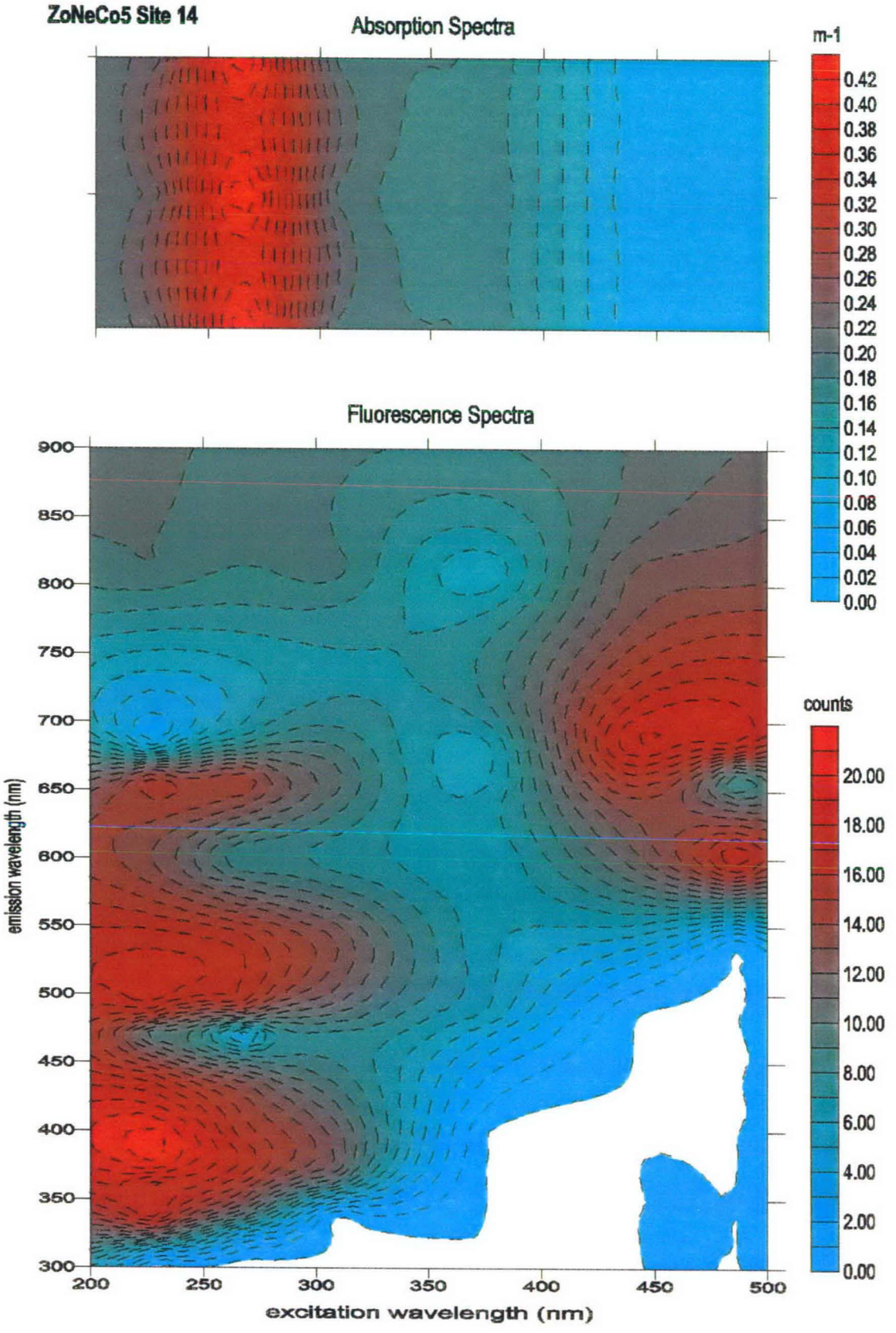

Figure 40. Site 14 - 3D fluorescence and absorption spectra

Appendix A

Calibration procedures and results

This appendix should be read in conjunction with the WET Labs SAFire manual and the AGSO Data Sheets which contain the results of laboratory calibration tests. Some basic calibration data for the SAFire is supplied by the manufacturer in the WET Labs SAFire User's Guide.

In the field, when advice on instrument trouble shooting is required that is not available in the SAFire manual, WET Labs technical help can be obtained on wetlabs@wetlabs.com out of Philomath, Oregon, USA or information on field operation, calibration and data processing from Dave.Holdway@agso.gov.au in Canberra ACT.

Basics

The instrument is initialised using a device file (SAF0116) with workshop calibrated scale factors and offsets. As mentioned in the body of the text, experience has shown that in pristine oceanic conditions it is possible to observe negative values, in both absorption and fluorescence spectra using the SAF0116 offsets. When this happens it indicates that the ocean water is cleaner than the laboratory water blanks used for the calibration. In this situation the raw data need to be adjusted in some manner. This can be done either by re-zeroing the offset (device file) and creating a new master device file or by correcting the offsets in post processing. If new files are generated these must be labelled and their status noted carefully so that field and laboratory results obtained with them can be compared with data from other areas.

In this study, the approach taken to compute the absorption value a (m^{-1}) was to install the standard device file (SAF0116) and use the minimum regional reading from the survey as the baseline, and adjust values in post processing.

Laboratory calibration

WET Labs calibrations

The WET Labs SAFire User's Guide includes a section on instrument characterisation (Section 3.5), dilution series and conversions (regression curves; emission counts to ppb) for quinine sulphate dihydrate and diesel fuel. From these the claimed sensitivity of the instrument can be calculated. Further calibration results have been obtained by AGSO using diesel and North Scott Reef crude in dilution series and comparing the results with those obtained from a Perkin-Elmer laboratory spectro-fluorimeter.

A detailed analysis of SAFire characteristics including advice on quantum and filter corrections has been written by Desiderio & Twardowski, (desi@oce.orst.edu; mtwardo@oce.orst.edu 1999). Twardowski has also produced a manuscript on the WET Labs ac-9 instrument, which has much useful information on absorption corrections. Where comparative results are sufficient (as in this work), quantum and filter corrections need not be applied. The results of WET Labs fluorescence tests at 266 nm excitation are shown attached.

AGSO fluorescence calibration

Tests in the AGSO laboratory included baseline tests with water blanks such as millipore water, deionised water and artificial salt water. Some tests were static and others were continuous. The static test were performed simply by using an inlet and outlet tube on the fluorimeter and pouring in sufficient water to flood the system and agitating until all air bubbles were removed. The continuous tests were either circulatory, where no water was exhaust, or continuous, where water was passed from a tap and through the fluorimeter once in typical survey fashion. The millipore water and salt water tests were either static or circulatory but because the deionised water was available in quanitity for the laboratory, continuous 'field' calibration was possible. The system used for circulatory or continuous flow tests included a debubbler, pump and flow meter with a flow rate around 2 litres per minute. The procedure for all tests, ie. water blanks and petroleum dilution series, was to load the test liquid/solution into the

SAFire, start data acquisition and concurrently, load a subset test solution into a Perkin-Elmer vial (after the routine cleaning procedure - rinsing in methanol, DCM and hexane). The procedure for operating the Perkin-Elmer fluorimeter is included in the SAFire Standard Operating Procedure.

When dilution series calibrations were being performed a micro-litre syringe was used to take a sample, usually 5 ul (diesel or other), and dissolve it in 1 L of de-ionised water while being continuously stirred using a magnetic rod. By diluting this mixture, solutions down to 0.25 ul/L or less were obtained. The most satisfactory test for a dilution series was a static test although circulatory tests were tried. The drawback with the latter is that the test solution was always shown to decrease in dilution over time, presumably because the petroleum dissolved in the water was gradually being absorbed onto the surface of the tubing and being taken out of solution. However if the data subset to be averaged was taken shortly after the SAFire test was started this was not a problem. This problem did not appear to be a serious issue with the static tests. Regardless of the type of test the system was usually run for a half hour or so and then a subset of these results were averaged for the comparison with the P-E results.

A dilution series was typically completed by testing the water blank first and then increasing the concentration incrementally. This minimised the contamination problem for the more dilute solutions. The results of the comparative fluorescence tests - WET Labs versus Perkin-Elmer - are shown attached.

Calibration graphs

Appendix A: Calibration graphs

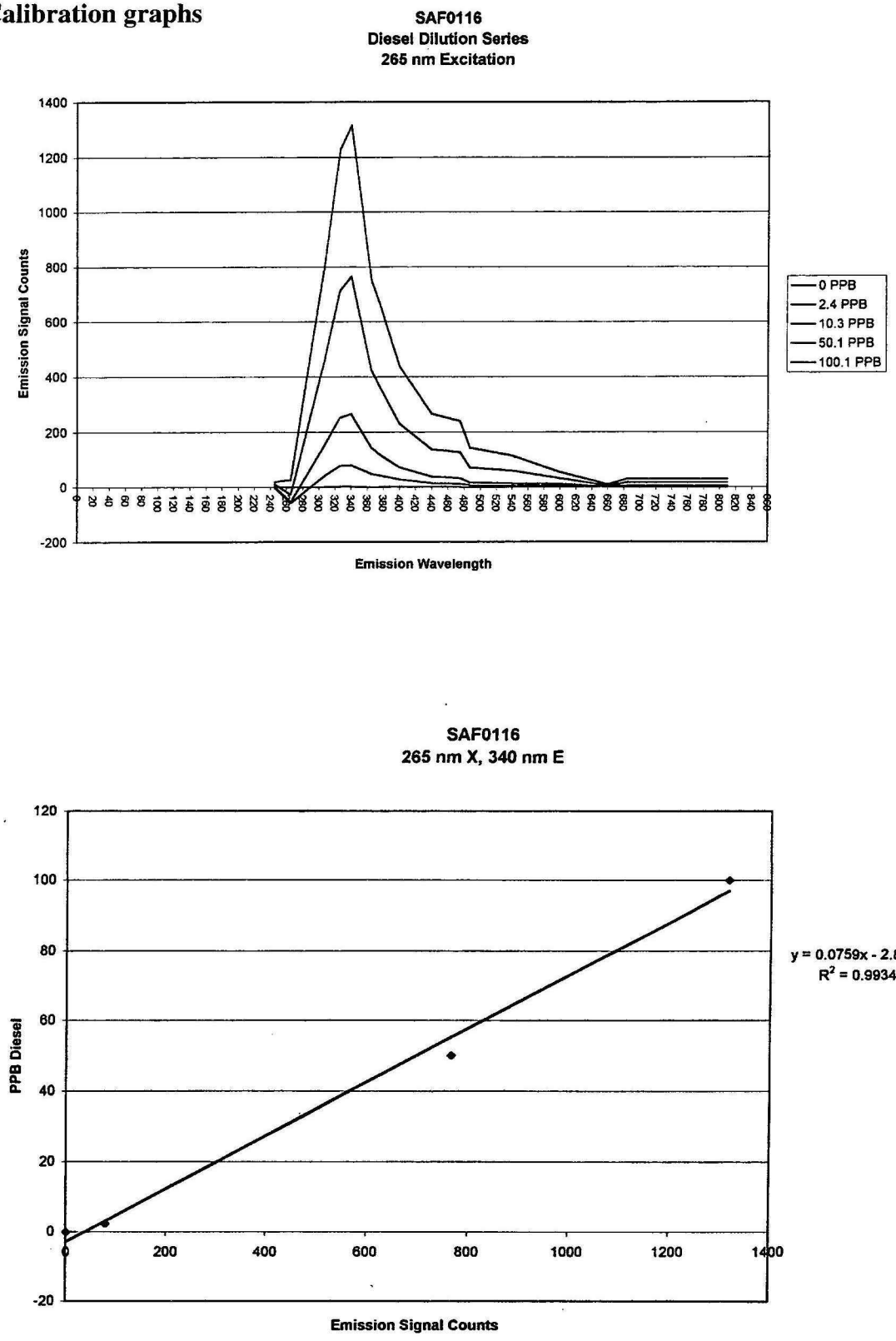

Appendix Figure A. Diesel dilution series and emission counts / concentration (ppb) cross plot, courtesy the WET Labs SAFire Users manual.

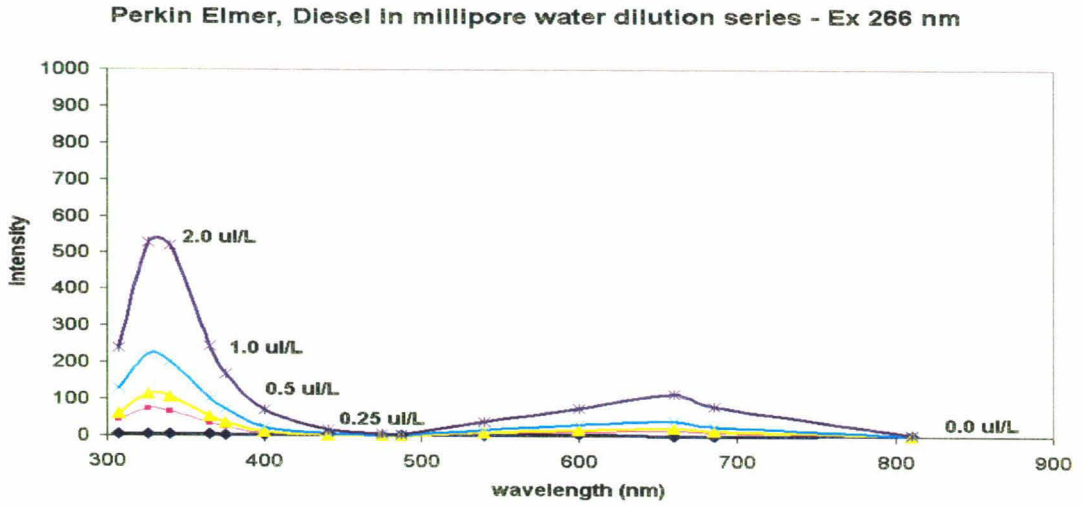

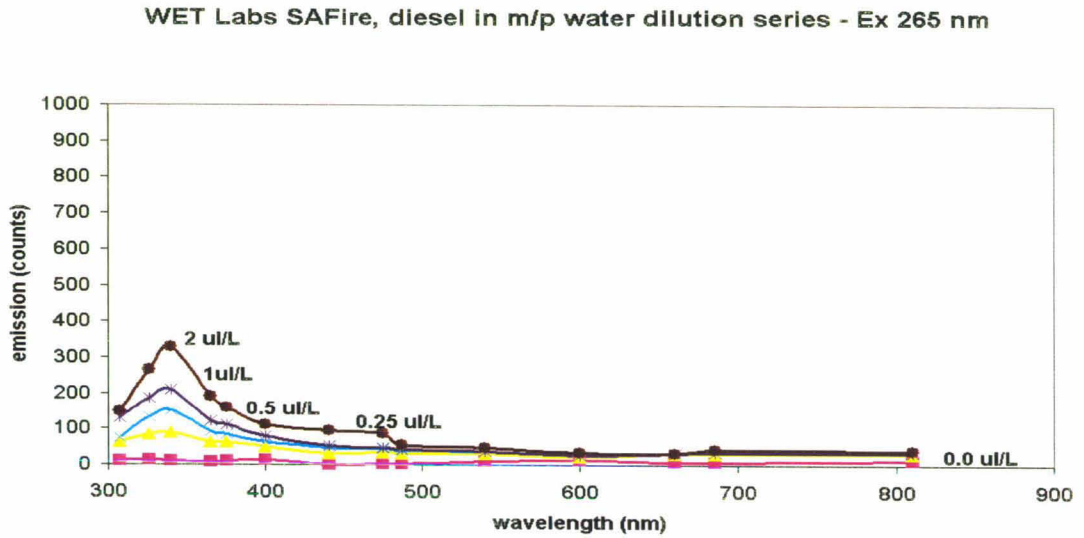

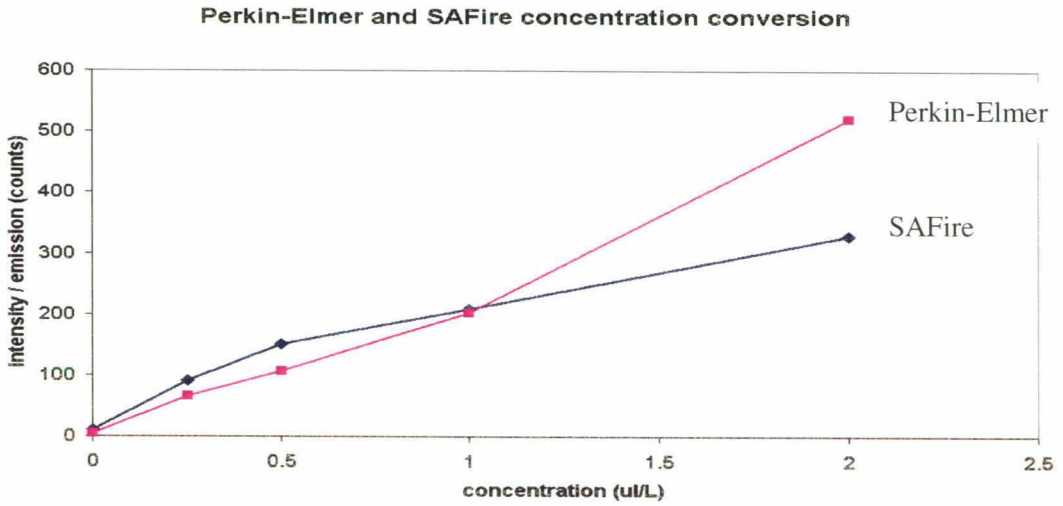

Appendix Figure B. Diesel dilution series and emission counts / concentration (ul/L) plot derived from AGSO laboratory tests.